

Doctoral Dissertation

Molecular cloning and functional
characterization of *Tenebrio PGRP-LE*, *PGRP-
LB* and autophagy-related genes *ATG3*, *5* and *8*
in response to *Listeria monocytogenes* and
Pseudomonas geniculata HT1 infection

Department of Applied Biology
Graduate School, Chonnam National University

Hamisi Juma Tindwa



February 2015

Molecular cloning and functional characterization of *Tenebrio*
PGRP-LE, *PGRP-LB* and autophagy-related genes *ATG3*, *5*
and *8* in response to *Listeria monocytogenes* and
Pseudomonas geniculata HT1 infection

Department of Applied Biology
Graduate School, Chonnam National University

Hamisi Juma Tindwa



Supervised by Prof. HAN, Yeon Soo

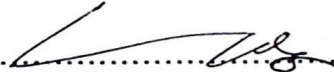
A dissertation submitted in partial fulfilment of the requirements for the Doctor of
Philosophy in **Applied Biology**

Committee in Charge:

Iksoo Kim



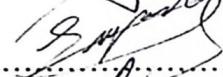
Yasuyuki Arakane



In Seok Bang



Yong Seok Lee



Yeon Soo Han



February, 2015

05 MAY 2016

Table of Contents

Table of contents.....	iii
List of Figures.....	ix
List of Tables.....	xi
Abstract (English).....	xii
Chapter 1. General introduction and review of literature	1
1.1 Introduction.....	1
1.2 Rationale for studying Insect immunity.....	3
1.3 Immune defence system in insects.....	4
1.3.1 Local AMP synthesis and expression.....	6
1.3.2 Production of Reactive Oxygen Species (ROS).....	7
1.4 Cellular and humoral immune responses.....	7
1.4.1 Cellular immune responses.....	7
1.4.2 Humoral immune response.....	9
1.5 Microbial recognition and regulation of AMP synthesis	10
1.5.1 Toll/Toll-like receptors.....	11
1.5.2 Peptidoglycan recognition proteins	13
1.5.3 Gram-negative binding proteins.....	16
1.5.4 Scavenger receptors.....	17
1.5.5 Thiol-Ester proteins and the complement system.....	19

1.6	Innate immune signaling cascades in insects	20
1.6.1	The Toll pathway.....	20
1.6.2	The IMD pathway.....	21
1.6.3	The JAK/STAT pathway	22
1.7	Autophagy as an immune defence mechanism	23
1.8	Overall objective and aims of this thesis.....	25
1.9	References	28
 Chapter 2. Autophagy-related genes, <i>TmATG3</i> and <i>TmATG5</i> are required for survivability against an intracellular pathogen, <i>Listeria monocytogenes</i> in <i>Tenebrio molitor</i>		
2.1	Abstract	41
2.2	Introduction	42
2.3	Materials and methods	45
2.3.1	Insect rearing and maintenance	45
2.3.2	Full-length cDNA cloning and sequencing	45
2.3.3	<i>In silico</i> characterization of <i>TmAtg3</i> and <i>TmAtg5</i>	47
2.3.4	Developmental and tissue-specific expression patterns of <i>TmATG3</i> and <i>TmATG5</i> ..	49
2.3.5	dsRNA synthesis and injection.....	49
2.3.6	Bacterial injections and bioassays	50
2.3.7	Statistical analysis	51
2.4	Results	52
2.4.1	Characterization of full-length cDNA for <i>TmATG3</i> and <i>TmATG5</i>	52

2.4.2	Developmental and tissue-specific expression patterns of <i>TmATG3</i> and <i>TmATG5</i> .	58
2.4.3	Loss of functions of <i>TmATG3</i> and <i>TmATG5</i> by RNAi resulted in high mortality of <i>T. molitor</i> larvae against <i>L. monocytogenes</i> .	60
2.5	Discussion	63
2.6	References	66
Chapter 3. Molecular cloning and characterization of autophagy-related gene <i>ATG8</i> in <i>Listeria</i> -invaded hemocytes of <i>Tenebrio molitor</i> .		
		72
3.1	Abstract	72
3.2	Introduction	73
3.3	Materials and Methods	75
3.3.1	Insect collection and Maintenance	75
3.3.2	Full-length cDNA Cloning and Sequencing	75
3.3.3	<i>In Silico</i> characterization of <i>TmATG8</i>	78
3.3.4	Developmental and Tissue-specific Expression Pattern of <i>TmATG8</i>	80
3.3.5	dsRNA synthesis and injections	80
3.3.6	Bacterial Injections and Bioassay studies	81
3.3.7	Expression of <i>TmATG8</i> in <i>E.coli</i>	82
3.3.8	Sodium dodecyl sulphate-Polyacrylamide gel electrophoresis (SDS-PAGE) and Western blot analysis	83
3.3.9	Immunofluorescence staining and confocal microscopic analysis	84
3.4	Results	86

3.4.1	cDNA characterization and phylogenetic analysis of TmATG8	86
3.4.2	Developmental and tissue-specific expression patterns of TmATG8 mRNAs	91
3.4.3	Characterization of TmAtg8 polyclonal antibody	93
3.4.4	<i>TmATG8</i> gene silencing results in high mortality of <i>Tenebrio</i> larvae against infection by <i>Listeria monocytogenes</i>	96
3.4.5	<i>TmATG8</i> gene silencing causes failure of <i>T. molitor</i> larvae to turn-on autophagic response to invading <i>Listeria</i> in hemocytes	99
3.5	Discussion	102
3.6	Conclusions	104
3.7	References	105
Chapter 4. Cloning, characterization and effect of <i>TmPGRP-LE</i> gene silencing on survival of <i>Tenebrio molitor</i> against <i>Listeria monocytogenes</i> infection		111
4.1	Abstract	111
4.2	Introduction	112
4.3	Materials and methods	115
4.3.1	Insect collection and maintenance	115
4.3.2	Chemicals	115
4.3.3	Bacterial strains and media	115
4.3.4	Construction of full-length enriched cDNA library of <i>T. molitor</i> larvae	115
4.3.5	<i>TmPGRP-LE</i> sequence analysis	117
4.3.6	Phylogenetic analysis	118

4.3.7	Secondary Structure Prediction and Modeling.....	120
4.3.8	Developmental- and Tissue-specific Expression Pattern of <i>TmPGRP-LE</i>	120
4.3.9	RNA interference of <i>TmPGRP-LE</i>	123
4.3.10	Bacterial injections and bioassays.....	124
4.3.11	Statistical Analysis.....	125
4.4	Results and Discussion.....	126
4.4.1	Characterization of <i>TmPGRP-LE</i> full-length cDNA.....	126
4.4.2	Phylogenetic analysis of TmPGRP-LE.....	132
4.4.3	Secondary Structure and Homology Modeling of TmPGRP-LE.....	133
4.4.4	Developmental- and Tissue-specific Expression Patterns of <i>TmPGRP-LE</i>	136
4.4.5	RNAi-mediated knockdown of <i>TmPGRP-LE</i> leads to reduced survival rate of <i>T. molitor</i> larvae infected with <i>L. monocytogenes</i>	138
4.5	Conclusion.....	141
4.6	References.....	142
Chapter 5. Roles and immunological functions of <i>TmPGRP-LB</i> against a soil isolate		
	<i>Pseudomonas geniculata</i> -HT1.....	149
5.1	Abstract.....	149
5.2	Introduction.....	150
5.3	Materials and Methods.....	153
5.3.1	Insect rearing and Maintenance.....	153
5.3.2	Full-length PGRP-LB cDNA Cloning and Sequencing.....	153

5.3.3	<i>In Silico</i> characterization of <i>TmPGRP-LB</i>	155
5.3.4	Developmental Expression Pattern of <i>TmPGRP-LB</i>	157
5.3.5	dsRNA Synthesis and injections	157
5.3.6	Isolation and identification of <i>Pseudomonas geniculata</i> HT1	158
5.3.7	Bacterial Injections and Bioassays	160
5.4	Results and Discussion.....	161
5.4.1	Characterization of full-length <i>TmPGRP-LB</i> cDNA.....	161
5.4.2	Developmental expression pattern of <i>TmPGRP-LB</i>	166
5.4.3	<i>TmPGRP-LB</i> RNAi resulted in increased susceptibility of <i>Tenebrio</i> larvae to infection by a gram negative bacterium <i>P. geniculata</i> HT1.....	167
5.5	References.....	172
	Abstract (Korean).....	173
	Acknowledgements.....	178

List of Figures

Figure 1-1: Schematic representation of DAP-type and Lysine-type PGN building units.	15
Figure 2-1A: Nucleotide and deduced amino acid sequences of <i>TmATG3</i>	54
Figure 3-1: Nucleotide and deduced amino acid sequence for <i>TmATG8</i>	87
Figure 3-2: Multiple alignment of TmAtg8 with orthologs from other insects.	88
Figure 3-3: Molecular phylogenetic analysis of Atg8 sequences by Maximum Likelihood method.....	89
Figure 3-4: Estimates of evolutionary divergence between sequences.....	90
Figure 3-5: Spatial and developmental expression patterns of <i>TmATG8</i> in adults and larvae.....	92
Figure 3-6: Characterization of anti-TmAtg8 polyclonal antibody.	94
Figure 3-7: Induction patterns of autophagy detected by Western blot analysis with anti-TmAtg8 antibody after injection of <i>E. coli</i> and <i>L. monocytogenes</i>	95
Figure 3-8: Knockdown of <i>TmATG8</i> by RNA interference.	97
Figure 3-9: Survival of <i>Tenebrio</i> larvae against <i>L. monocytogenes</i> infection.....	98
Figure 3-10: Time-course autophagy staining in hemocytes.	100
Figure 3-11: Tracking Listeria-induced autophagy using Cyto-ID green detection reagent in hemocytes isolated from ds <i>TmATG8</i> -treated <i>T. molitor</i> larvae.	101
Figure 4-1: Nucleotide and deduced amino acid sequence of a homologue of PGRP-LE from <i>T.</i> <i>molitor</i>	130
Figure 4-2: Characterization and alignment of amino acid sequences of TmPGRP-LE homologues.	131

Figure 4-3: Molecular phylogenetic and percentage identity analysis of TmPGRP-LE.....	134
Figure 4-4: Predicted structural identity and features of TmPGRP-LE.....	135
Figure 4-5: developmental and tissue-specific expression patterns of <i>TmPGRP-LE</i>	137
Figure 4-6: Effect of <i>TmPGRP-LE</i> knockdown on the survivability of <i>T. molitor</i> larvae.....	140
Figure 5-1: Schematic procedure on isolation and effect of <i>P. geniculata</i> on <i>Tenebrio</i> mortality	159
Figure 5-2: Nucleotide and deduced amino acid sequence of a novel homologue of PGRP-LB from <i>T. molitor</i>	162
Figure 5-3: Multiple alignment of amino acid sequences of TmPGRP-LB homologues	163
Figure 5-4: Molecular Phylogenetic analysis of TmPGRP-LB by Maximum Likelihood method	164
Figure 5-5: Percentage identity and distance analysis of TmPGRP-LB with orthologs from other insects.....	165
Figure 5-6: Developmental expression pattern of <i>TmPGRP-LB</i>	166
Figure 5-7: Preliminary pesticidal tests of <i>Pseudomonas geniculata</i> HT1 on <i>T. molitor</i> larva.	169
Figure 5-8: Expression patterns of extracellular IMD-pathway related genes after <i>P. geniculata</i> HT1 inoculation to <i>Tenebrio</i> larvae	170
Figure 5-9: <i>Tenebrio</i> larval survival against DAP- and Lysine-type PGN containing bacteria.	171

List of Tables

Table 2-1: Primers used in this study.....	46
Table 2-2: Accession numbers of Atg3 and Atg5 sequences from various insect species used to generate phylogenetic tree, percentage distance and identity matrices.....	48
Table 3-1: Primers used in this study.....	77
Table 3-2: Accession numbers of Atg8 amino acid sequences from various organisms used to generate the phylogenetic tree, percentage distance and identity matrices.....	79
Table 4-1: Accession numbers of PGRPs from various insect species used to generate the phylogenetic tree, percentage distance and identity matrices	119
Table 4-2: Primers sequences used in the current study.	122
Table 5-1: Primers used in this study.....	154
Table 5-2: Accession numbers of PGRP-LB sequences from various insect species used to generate the phylogenetic tree, percentage distance and identity matrices.....	156

Molecular cloning and functional characterization of *Tenebrio*
PGRP-LE, *PGRP-LB* and autophagy-related genes *ATG3*, *5*
and *8* in response to *Listeria monocytogenes* and
Pseudomonas geniculata HT1 infection

Hamisi Juma Tindwa

Department of Applied Biology
Graduate School, Chonnam National University

(Supervised by Prof. HAN, Yeon Soo)

Abstract

The Current study investigated innate immune responses of the mealworm beetle, *Tenebrio molitor*, against microbial infections. We, therefore, dealt with two major themes, the immune functions of autophagy-related genes *TmATG3*, *TmATG5* and *TmATG8* on the one hand and, roles of *TmPGRP-LE* and *TmPGRP-LB* in immune responses to microbial infections on the other hand. In the first part, the three autophagy-related genes, *TmATG3*, *TmATG5*, and *TmATG8* were identified and characterized for their immunological functions in the beetle against infections by an intracellular pathogen, *Listeria monocytogenes*. *TmATG3*, *TmATG5* genes were identified from *T. molitor* EST and RNAseq databases. The cDNA of *TmATG3* and *TmATG5* comprise of ORF sizes of 963 and 792 bp encoding proteins with 320 and 263 amino acid residues, respectively. *TmATG3* and *TmATG5* transcripts are detected in all developmental stages analyzed, and primarily in fat body and hemocytes of larvae. *TmATG3* and *TmATG5*

showed high amino acid sequence identity (58-95%) with corresponding homologues from various insects and were closer to their orthologs in *T. castaneum*. Loss of function of *TmATG3* and *TmATG5* by RNAi led to a significant reduction in survival ability of *T. molitor* larvae against an intracellular pathogen, *L. monocytogenes*. Six days post-*Listeria* challenge, the survivability in ds*TmATG3*- and ds*TmATG5*-treated larvae was significantly reduced to 3 and 4%, respectively, when compared with ds*EGFP*-injected control larvae. The cDNA of *TmATG8* comprises of an ORF of 363 bp encoding a protein of 120 amino acid residues. *TmATG8* transcripts are detected in all the developmental stages analyzed. TmAtg8 contains a highly conserved C-terminal glycine residue (G116) and shows high amino acid sequence identity (98%) to its *T. castaneum* homologue, TcAtg8. Loss of function of *TmATG8* by RNAi led to a significant increase in mortality of *T. molitor* larvae against *Listeria monocytogenes*. Unlike ds*EGFP*-treated control larvae, *TmATG8*-silenced larvae failed to turn-on autophagy in hemocytes after *L. monocytogenes* injection. Taken together, these data suggest that TmATG3, TmATG5 and TmATG8 play a role in mediating autophagy-based clearance of *Listeria* in *T. molitor*. In the second part, *TmPGRP-LE* and *TmPGRP-LB* were identified and characterised for their immunological functions in *T. molitor*. A *PGRP-LE* homologue, from *T. molitor* was identified and characterized for its functional role in the survival of the insect against infection by a DAP-type PGN containing intracellular pathogen, *L. monocytogenes*. *TmPGRP-LE* cDNA is comprised of an open reading frame (ORF) of 990 bp and encodes a protein of 329 residues. TmPGRP-LE contains one PGRP domain, but lacks critical residues for amidase activity. Quantitative RT-PCR analysis indicated a broad constitutive expression of the *TmPGRP-LE* transcripts at various stages of development spanning from larva to adult. RNAi-mediated knockdown of the *TmPGRP-LE* transcript, followed by a challenge with *L. monocytogenes*, resulted in a significant reduction in survival rate of the larvae, suggesting a putative role of TmPGRP-LE in sensing and control of *L. monocytogenes* infection in *T. molitor*. PGRP-LB, one

of several amidase-capable members of the PGRP family has been demonstrated to specifically recognize DAP-type PGN, thereby preventing over-activation of the IMD pathway upon infections Gram-negative bacteria. We have identified, cloned and partially characterized the immunological functions of a PGRP-LB homologue from *T. molitor* against a newly isolated Gram-negative bacterium *Pseudomonas geniculata* HT1 infection. *TmPGRP-LB* has an ORF of 597 bp encoding a protein with 198 amino acid residues and contains the conserved PGRP domain. *TmPGRP-LB* is closest to its orthologous *TcPGRP-LB1* and *TcPGRP-LB2* isoforms in *T. castaneum* with which it shares the highest (73 %) percentage identity. *TmPGRP-LB* transcripts were detected in all developmental stages examined spanning from the late-instar larva to adult day 1 and 2. *TmPGRP-LB* transcripts were also detected in all tissues examined including the gut, hemocytes, fat body, Malphigian tubules, integuments, ovaries and testes. Infection of *Tenebrio* larvae with HT1 resulted in increased expression of *TmPGRP-LB* but not other IMD pathway-related genes *TmPGRP-LC* and *TmPGRP-LE*. *TmPGRP-LB* loss of function by RNAi resulted in increased susceptibility of larvae to infections by Gram-negative bacteria HT1 and *Escherichia coli* K12 but not Gram-positive bacteria *Staphylococcus aureus* RN4220. Our results suggest that *TmPGRP-LB* plays a role in control of Gram-negative infections in *T. molitor*. Overall, we have demonstrated that both autophagy and peptidoglycan recognition proteins of the IMD pathway are deployed to counter bacterial infections in *T. molitor*.

Chapter 1. General introduction and review of literature

1.1 Introduction

Disease occurs when pathogenic microorganisms invade cells of the host as they seek resources for their growth and survival. This compels the host organism to deploy measures that counter the effects of microbial invasion. The ability of an organism to recognize and defend itself against harmful effects of the non-self is called immunity (Retief and Cilliers, 1998). The immune system in most organisms is organized in at least three lines of defence. The first line of defence is made up of a combination of physical barriers, chemical secretions and mucus linings all of which synergistically prevent the tissues from direct exposure to pathogens as well as retarding the pathogens' entry into the body. The physical barriers include the skin in mammals, the cuticle in insects and the waxy cuticle on plant leaves. Entries into the body which include, the eyes, ears, nose and genital openings in mammals, stomata in plants and gut and spiracles in insects are covered with mucus secretions actively trapping pathogens to deny them entry into the body. Additionally, all these entry routes are lined up with resident microflora, a variety of beneficial microorganisms which protect the host from harmful pathogens. The resident microflora colonise these linings to an extent that the area available for pathogens to attach and become established is minimized. The first line of defence is described to be non-specific as it non-selectively destroys and/or blocks any pathogen from entry into the body (Janeway et al., 2001).

The first line of defence described above may get overwhelmed or evaded and the pathogens get past it into the body interior. When this happens, the body deploys the second and if need be the third lines of defence to fight off the intruders. The second line of defence is, like the first, relatively non-specific and together they constitute what is known as the innate immune

system. The Innate immune system is a fast, generic and maximal response against the presence of non-self entities in the system. Through the second line of defence, the innate immune system recognises the presence of a non-self and initiates the production of a variety of inhibitory substances including interferons, complement cells and antimicrobial peptides in addition to attracting phagocytes to the site of infection (Millichap, 2008). Should the pathogen be able to evade or overwhelm the first two defence lines, the body deploys a third defence line, the adaptive immunity. Unlike innate immunity, the adaptive immunity is made up of a collection of cells with an ability to adapt and specialise for defence against specific pathogens (http://textbookofbacteriology.net/adaptive_3.html).

Adaptive immunity works by the antigen-antibody interaction principle. An antigen is a foreign body such as pathogenic bacteria, virus, fungi or their derivatives like flagellum or cell wall components that provokes an adaptive immune response of the host. Once the adaptive immune system is activated (often times through presentation of the antigen by some parts of the innate immunity), it selects from its reserve of pre-existing cells, one with a receptor that fits the antigen best. The selected cell then proliferates and starts to synthesize and secrete antibodies which would bind to the antigen that provoked the response. This proliferation and mass production of the antibody would go on until the antigen is overcome. Many of such antibody-producing cells will eventually die off but a few will remain to keep the 'memory' of this specific antigen and its best immunological response. This memory will allow the body to respond in a fast and more robust manner next time the body encounters the same kind of infection (Kindt et al., 2007).

Both the innate and adaptive immune systems are divided into the humoral and cellular immune response components. Humoral immunity is the aspect of immune defence which is

mediated by macromolecules found in extracellular fluids and they include secreted antibodies, complement cells and antimicrobial peptides. Cell-mediated immunity, on the other hand, is that aspect of immunity mediated by activation of phagocytic cells, antigen-specific cytotoxic cells and release of various types of cytokines in response to the presence of an antigen (Millichap, 2008; http://en.wikipedia.org/wiki/Cell-mediated_immunity).

1.2 Rationale for studying Insect immunity

Interest and research into insect infection and immunity can be traced to as far back as the 19th century when Agostino Bassi was amongst the first researchers to verify the germ theory of disease by showing that a fungus, *Beauveria bassiana*, was the causative agent of the white muscardine disease in commercial silkworm *Bombyx mori* (Rolff and Reynolds, 2009). Since then research in insect infection and immunity has grown for a number of reasons including:

Firstly, the fact that an estimated 18% of world's annual crop production and up to 20% of world's stored food grains are destroyed by insects pests (Oerke and Dehne, 2004; Bergvinson and Garcia-Lara, 2004). Understanding how insect immunity works and their interactions with pathogens and/or parasites is pivotal in designing ways to manipulate and control them.

Secondly, a wide variety of insects are vectors of plant and animal diseases. The whitefly *Bemisia tabaci*, for example, is both a vector of more than 110 viral species and a pest of an ever increasing number of host plants including cotton, soybean, cassava, potatoes, tomatoes and cucumber. Particularly, the tomato yellow leaf curl virus (TYLCV) and the cucurbit yellow stunting disorder virus (CYSDV) are two of the most serious viruses vectored by this insect (<http://www.fera.defra.gov.uk/plants/publications/documents/factsheets/bemisia.pdf>). Similarly, malaria- a disease that made about 207 million people sick and killed over 0.62 million people from its effects in 2012 worldwide (WHO 2013), is vectored by mosquitoes. These are just two

of an exceptionally huge list of insect vectored diseases of both plants and animals. Again, an understanding of the interactions between these and many other insect vectors and the pathogens/parasites on the one hand, and between the vectors and their host plants and/or animals on the other hand is paramount to effective control of diseases associated with them.

Thirdly, the economic, biological and ecological value of insects as plant pollinators cannot be overemphasized. There has been, however, a recorded decline of pollinator insect populations worldwide. For example, declines on populations of both solitary and social bees (Biesmeijer et al., 2006) is a cause for concern and that research into probable causes of compromised immunity of such insects to their natural parasites and pathogens may be a way to go.

And lastly, insects can be tractable models of vertebrate function such that studies in insect immune systems can potentially lead to discoveries in mechanisms of immune function that can be widely applied in higher eukaryotes including man. A good example in this case is the discovery by Lemaitre et al., (1996) that Toll receptors originally discovered for their role in embryonic development, play an important role in immune signaling in *Drosophila Melanogaster*. This was swiftly followed by the discovery of an immune role of Toll-like receptors (TLRs) in vertebrates (Medzhitov et al., 1997).

1.3 Immune defence system in insects

Insect immunity is heavily dependent on innate immune responses because the adaptive immune system in insects is either rudimentary or absent altogether. While the mechanisms involved to stage an innate immune response are conserved in vertebrates and invertebrates (Hoffman et al., 1999), adaptive immune response mechanisms have, by far and large, been only documented in vertebrates (Agaisse, 2007). Evidence is growing, however, on the existence of

adaptive immune aspects in insects. We will review hereafter, available evidence of learned/adaptive immune response aspects before dealing with the much studied and well-understood innate immune responses in insects.

Immune priming responses is a growing area of research and evidence in *Drosophila melanogaster* shows that priming adults flies by injecting a sub-lethal dose of *Streptococcus pneumoniae* into the hemolymph effectively protects the flies from a lethal second challenge by the same pathogen (Pham et al., 2007). Interestingly, the primed immune response exhibited a specificity aspect, a property of adaptive/learned immunity. It was shown that priming with *S. pneumoniae* only protects the fly from subsequent lethal infection with *S. pneumoniae* but not against infection with other pathogenic microbes such as *Salmonella typhimurium* (Brandt et al., 2004), *Listeria monocytogenes* and *Mycobacterium marinum* (Dionne et al., 2003). The authors showed that priming the flies with other pathogenic microbes like *S. typhimurium* does not give protection against a challenge by *S. pneumoniae* and that the mechanism underlying this protective effect requires phagocytes and the Toll pathway. In another study, Faulhaber and Karp (1992) showed that immunizing the American cockroach, *Periplaneta Americana*, with killed *pseudomonas aeruginosa* prompted the roach to generate a diphasic response when subsequently injected with live bacteria such that it displayed an acute non-specific phase initially, which is then superseded by a long term and relatively specific second response. The authors argued that immunization with any other bacteria such as *Serratia marcescens*, *Enterobacter cloacae*, *Streptococcus lactis* or *Micrococcus lysodeikticus* could provide protection against live *P. aeruginosa* challenge in the first 3 days (acute non-specific response) but only immunization by *P. aeruginosa* was able to provide long term (>14 days) protection against live *P. aeruginosa* challenge. These two examples demonstrate that the concept of

learned immunity in invertebrates may have been grossly overlooked and that this area warrants more research.

An immunological response in an insect body can be either local or systemic. The local immune responses are staged by the epithelial linings of the physical barriers described above well before the systemic response is activated. In *Drosophila*, for example, Epithelia in the alimentary canal, trachea or those beneath the cuticle act as both physical barriers and local defence units by producing antimicrobial peptides and reactive oxygen species against pathogens (Lemaitre and Hoffmann, 2007). Local immune defence in *Drosophila* and other insects can be staged in a number of ways, the most studied of which are briefly presented here.

1.3.1 Local AMP synthesis and expression

Local AMP expression has been reported in a number of insects including *Drosophila* and *Bombyx mori*. Such expressions can be constitutive as is the case with Drosomycin and Cecropin in the *Drosophila*'s female spermatheca and male ejaculatory duct, respectively (Tzou et al., 200), or inducible as is the case with Drosomycin and Dipterucin in the gut and trachea of *D. melanogaster* following local infection by *Erwinia carotovora* (Basset et al., 2000). Constitutive local AMP expression is regulated by factors distinct from the NF- κ B pathways such as the homeobox-containing protein Caudal and mating in virgin *D. melanogaster* females (Labrose et al., 2005). Induced local AMP expression, however, is regulated through the IMD pathway (discussed in detail later in the chapter) mediated through recognition of the pathogen by PGRP-LC (Zaidman-Remy et al., 2006). No involvement of the Toll pathway is known in local expression of AMPs in insects.

1.3.2 Production of Reactive Oxygen Species (ROS)

The production of reactive oxygen species (ROS) is a common defence strategy against infections both in mammals and insects. Natural infections by bacteria, for example, are known to induce ROS production in *D. melanogaster* gut and that *dual oxidase 1* (*Duox*) is a sole gene responsible for epithelial ROS production (Ritsick et al., 2004). Duox proteins are a family of conserved NADPH domain- containing molecules. They in addition contain an N-terminal extracellular peroxidase domain that can regulate the ROS production. It has been demonstrated that hemocytes of the greater wax moth, *Galleria mellonella*, are capable of phagocytosing and killing bacterial and fungal pathogens and that superoxide production and microbial killing were inhibited by diphenyleneiodonium chloride, a known inhibitor of NADPH oxidase (Bergin et al., 2005).

1.4 Cellular and humoral immune responses

1.4.1 Cellular immune responses

The systemic immune response can either be cellular or humoral in nature. The cellular responses refer mainly to the Hemocyte-mediated processes like phagocytosis, nodulation, encapsulation and melanization.

Phagocytosis is a process by which an individual cell (hemocyte) engulfs and destroys entities recognised as foreign. Targets of phagocytosis range from a variety of microbial cells such as bacteria, yeast and viruses to non-living particles like sephadex beads, indian ink particles as well as double-stranded RNA (dsRNA) (Leimatre and Hoffman, 2007). Phagocytosis starts with the attachment of the phagocyte (hemocyte cell specialising in phagocytosis) to its target. This is followed sequentially by cytoskeleton modification, internalization (engulfing) and eventual destruction of the engulfed target within special

structures called phagosomes. The types of hemocytes involved in phagocytosis may differ from insect to insect but the most common types in most insects are the circulating plasmatocytes and granulocytes (Lemaitre and Hoffmann, 2007; Marmaras and Lampropoulou, 2009).

Nodulation is an important albeit poorly understood hemocyte-mediated immune response in insects. It involves multicellular hemocyte aggregation to entrap a large number of bacteria or fungi in the hemolymph. It is a lectin-mediated process whose details are not yet fully understood. Recent research efforts have identified an immune protein called noduler which regulates nodulation in the insect *Antheraea mylitta*. Noduler was shown to be up-regulated after bacterial infection and that RNAi-mediated knockdown of noduler negatively affected the nodulation response (Ganghe et al., 2007).

Encapsulation, unlike nodulation, refers to hemocyte aggregation around a large target such as parasitic wasp eggs or nematodes. During encapsulation, the hemocytes attach to their target followed by formation of a multilayered capsule around the invader. Inside the capsule, which may ultimately be melanized, the target is killed through the production of cytotoxic free radicals including reactive oxygen species (ROS) and reactive nitrogen species (RNS) or through asphyxiation (Nappi et al., 1995; Nappi and Ottaviano 2000). The regulation of encapsulation is not yet clearly understood, but in *D. melanogaster* the encapsulation targets are known to be detected by circulating plasmatocytes in the haemolymph. Once the plasmatocytes attach to the surface of their target (e.g. on the chorion of the wasp egg), a massive proliferation and differentiation of lamellocytes is induced subsequently forming a multi-layered capsule around the target (Lemaitre and Hoffman, 2007).

Melanization, a pathway leading to melanin formation, is an immediate immune response following cuticular injury or parasitic invasion of the hemocoel. It is a blackening

reaction leading to synthesis and deposition of melanin (Marmaras and Lampropoulou, 2009). During melanization, Prophenoloxidase (proPO), an enzyme that plays a central role in melanization, is activated through cleavage by a serine protease called prophenoloxidase activation enzyme (PPAE). PPAE is an inactive zymogen which must be activated through a series of proteolytic reactions by other serine proteases. The activated prophenoloxidase, (PO) then catalyses the oxidation of mono- and diphenols to orthoquinones which in turn, polymerize non-enzymatically to melanin. Since melanization is triggered by either cuticular injury or recognition of a non-self in the hemocoel, it is therefore, an efficient immune defence and non-self recognition mechanism in invertebrates (Lemaitre and Hoffman, 2007).

1.4.2 Humoral immune response

Humoral immunity refers to the aspect of innate immunity carried out mainly by macromolecules found in the extracellular fluids (humours) of the body. The macromolecules involved are of various types ranging from secreted antibodies, certain enzymes which play part in the prophenoloxidase (proPO) cascade and antimicrobial peptides (AMPs). In insects both AMPs and the proPO systems play critical immune defence roles against pathogen invasion.

AMPs are small molecules generally < 10 kDa characterized by an overall cationic charge, hydrophobicity, and amphipathicity. They include two or more positively charged residues provided by arginine, lysine or, in acidic environments, histidine, and a large proportion (generally > 50%) of hydrophobic residues in their sequence composition (Ntwasa et al., 2012). In *Drosophila melanogaster* and many other insects, AMPs and other defence proteins are secreted mainly by the fat body, an organ functionally equivalent to the mammalian liver, into the hemolymph- the insect blood, although expression can also be significant in other tissues such as the hemocytes. At least 20 immune-inducible AMPs are encoded by the *D.*

melanogaster genome and can be grouped in seven major classes namely, Diptericins, Attacins, Drosocins, Cecropins, Defensins, Drosomycins and Metchnikowins (Lemaitre and Hoffmann, 2007). Many of these AMPs have also been reported in other insects but a few AMPs such as Drosomycin and Metchnikowins appear to be specific to *Drosophilidae* (Imler and Bulet, 2005). AMPs have also been studied in a number of coleopteran beetles such as *Tribolium castaneum* (Zou et al., 2007), *Allomyrina dichotoma* (Sagisaka et al., 2001) and *Tenebrio molitor* (Moon et al., 1994).

1.5 Microbial recognition and regulation of AMP synthesis

The expression and synthesis of insect AMPs is regulated at a transcriptional level. Studies in *D.melanogaster* revealed a number of DNA motifs required for inducibility of immune responses in insects. These include the NF- κ B binding sites, GATA binding sites which are specifically recognised by the transcription factor Serpent, and a poorly understood motif R1 (Lemaitre and Hoffman, 2007). NF- κ B is the most characterized DNA motif required for induction of immune responses. The NF- κ B together with another protein Rel constitutes a family of the Rel/NF- κ B transcription factors. They are structurally related eukaryotic transcription factors conserved from insects such as *D. melanogaster* to larger eukaryotic mammals such as humans. They are related through a highly conserved DNA-binding/dimerization domain called the Rel homology (RH) domain. Based on the C-terminal sequence of the RH domain members of the family of Rel/ NF- κ B transcription factors can be divided into two classes. Class 1 is comprised of the NF- κ B proteins including the mammalian p105, p100, and *Drosophila* Relish which have long C-terminal domains that contain multiple copies of ankyrin repeat-containing inhibitory domains, which can be removed by proteasome-mediated proteolysis. The proteins in this class become shorter active DNA-binding proteins (p105 to p50, p100 to p52) by either limited proteolysis or arrested translation

(<http://www.bu.edu/nf-kb/>). Members of class 1 cannot activate transcription unless they form dimers with members of class 2. Class 2 is made up of Rel proteins which include c-Rel, v-Rel, RelA (p65), RelB and the *Drosophila* Dorsal and Dif proteins. These have transcriptional activation domains on their C-terminal sequences. As indicated above, three NF- κ B/Rel-like proteins namely Relish, Dorsal and Dif are encoded in the *Drosophila* genome. These proteins have been shown to bind to the κ B sites and transactivate certain AMP genes regulated through two distinct immune signaling pathways, the Toll and the IMD immune transduction pathways.

The interaction between the invading pathogen and the host's immune defence system starts with the action of pattern recognition proteins/receptors (PRP/PRR). PRRs are families of host-based proteins that recognise conserved microbial determinants collectively referred to as pathogen-associated molecular patterns (PAMPs) such as lipopolysaccharides (LPS), peptidoglycan (PGN), and fungal β -1, 3 glucans. In recognition of PAMPs, some PRRs act singly while others act in congruency before the signal is channeled downstream to initiate a signaling cascade that will lead to eventual production of immune effectors such as AMPs and cytokines and, trigger the activation of phagocytosis and proteolytic cascades (Pal and Wu, 2009). Some of the most studied families of PRRs in insects include the Toll/Toll-like receptors, Peptidoglycan recognition proteins (PGRPs), Gram-negative binding proteins (GNBPs), Thiol-Ester proteins (TEPs) and Scavenger receptors.

1.5.1 Toll/Toll-like receptors

The Toll receptor was initially discovered during genetic screening studies to identify genes involved in dorsal-ventral patterning in *D. melanogaster*. Toll along with 11 other genes named here in the order they appear in the signaling cascade: pipe, nudel, windbeutel, gastrulation defective, snake, easter, spatzle, toll, tube, pelle, cactus and dorsal (Belvin and

underson, 1996) were discovered mainly because maternal mutations in most of them caused dorsalisation of the embryo, an abnormally altered phenotype in which the embryo consists of an elongate tube covered with a dorsal cuticle (Irish and Gilbert, 1987). As indicated above, the discovery of this cascade of genes involved in dorsal-ventral patterning was swiftly followed by a discovery (Lemaitre et al., (1996) that a sizable number of these genes played a critical role in immune defence signaling in *D. melanogaster*. However, although the original *D. melanogaster* Toll receptor does not act as a pattern recognition molecule (but plays a central role in mediating responses to a multitude of infection types as discussed later in this chapter), tractable research has revealed that Toll-like receptors indeed act as PRRs in vertebrates (Medzhitov et al., 1997). Up to 11 TLRs have been characterised in mammals and shown to be specialised in recognition of different types of PAMPs. Some of such mammalian TLRs do so by the help of associated proteins while others perform their duties singly, without help from other proteins. TLR3, TLR5 and TLR9 are examples of mammalian TLRs that act singly, executing their recognition functions without need of helper proteins. TLR3 has been shown to bind to and recognise double-stranded RNA thus implicating this receptor to recognition and immune responses against viral infection in mammals (Alexopoulou et al., 2001). Similarly, TLR5 has been shown to recognize flagellin, the constituent protein of the bacterial flagella, by a direct physical interaction to a highly conserved structure that is particular to bacterial flagellin (Smith et al., 2003). TLR9 recognizes un-methylated CpG DNA which is typical of bacterial genomes thus implicating TLR9 for an immunological distinction between resident usually heavily methylated and invading un-methylated CpG bacterial DNA (Hemmi et al., 2000). On the other hand, examples of TLRs that cooperate with helper proteins to recognise specific PAMPs include TLR2 and and TLR4. TLR2 is known to show a range of ligand specificities mainly by forming dimers with other TLRs receptors. The dimerization of TLR2/TLR1 is important in the binding to and recognition of triacylated lipopeptides, whereas the dimer between TLR 2/TLR6 is

specific for diacylated lipopeptides (Ozinsky, et al., 2000). Similarly, a complex of TLR4 and helper proteins CD4 and MD2 is required for the recognition of bacterial lipopolysaccharide (LPS) (Akashi et al., 2000).

1.5.2 Peptidoglycan recognition proteins

Peptidoglycan recognition proteins (PGRPs) constitute a class of PRR found in invertebrates such as insects, echinoderms and mollusks and most vertebrates but not in plants and nematodes (Dziarski and Gupta, 2006). They are characterised by at least one to three PGRP domains (approximately 165 amino acid residues) located in the C-terminus end of the sequence that is homologous to bacteriophage and bacterial type 2 amidases. However, the PGRP domain is distinct from typical type 2 amidase domain because they are relatively longer at their amino terminus end and contain a PGRP-specific segment not present in type 2 amidases (Kim et al., 2003). Up to 19 PGRP proteins have been characterised in insects generally grouped into two, the short (S) and long (L) forms. The short PGRPs are about 18-20 kDa invariably characterised by a signal peptide suggesting that they are mainly secreted proteins. The intermediate and long PGRPs, on the other hand, characterised by in addition to the carboxyl terminal PGRP domain, a highly variable amino-terminal sequence that is not conserved and unique for a given PGRP. The intermediate and long forms of PGRPs can be secreted, transmembrane or intracellular proteins (Dziarki and Gupta, 2006).

Insect PGRPs have recognition and effector functions. Recognition of peptidoglycan (PGN), a fundamental component of the bacterial cell wall, is achieved by specific types of PGRPs depending on the type of PGN. PGN is a polymer of alternating residues of β -(1, 4) linked N-acetylglucosamine and N-acetylmuramic acid with all the actly groups of the N-acetylmuramic acid residues having been replaced by a stem peptide of four to five alternating L

and D- amino acids (Royet and Dziarki, 2007). The composition of a third amino acid of the stem peptide distinguishes PGN into two types namely those containing a *meso*-diaminopimelic acid residue thus called diaminopimelic acid (DAP)-type PGN and those containing a lysine residue thus named lysine-type PGN (Fig. 1-1). Adjacent chains of the DAP-type PGN are usually directly cross-linked while those of the lysine-type PGN are cross-linked through an inter-peptide bridge that varies widely in length and composition among bacterial species (Royet and Dziarki, 2007).

All gram negative-bacteria and gram-positive bacilli such as *Listeria monocytogenes* have DAP-type PGN while most gram positive bacteria have lysine-type PGN in their cell walls. As indicated above some PGRPs have a preferentially high affinity to DAP-type PGN while others are specific to lysine-type PGN and a few others can recognise both types of PGN. Insect PGRPs which preferentially bind to DAP type PGN include PGRP-LB, PGRP-LC and PGRP-LE while PGRP-SA and PGRP-SD are examples of those that recognise lysine-type PGN (Aggrawal and Silverman, 2007). The discrimination of DAP from Lysine-type PGN by PGRPs is explained by the chemistry of the PGN-binding groove of all PGRPs. In all known DAP-type recognizing PGRPs, the PGN-binding cleft has a conserved arginine residue (e.g. Arg²⁵⁴ in PGRP-LE) that provides critical DAP-interactions. The arginine residue is almost invariably flanked by a glycine and a tryptophan residue which play other DAP-specific interactions (Chang et al., 2006; Lim et al., 2006; Swaminathan et al., 2006). All lysine-specific PGRPs encode a threonine instead of an arginine as a critical lysine-interacting residue. Studies in *Drosophila* have shown that replacing the Arg²⁵⁴ with threonine in the DAP-recognizing PGRP-LE dramatically reduces its affinity to a monomeric DAP-type PGN, the tracheal cytotoxin (TCT) (Lim et al., 2006). Similarly, replacing the Gly³⁹³ and Trp³⁹⁴ of PGRP-LCx with asparagine and phenylalanine (as

found in the lysine-type PGN- recognizing PGRP-SA) was found to allow the PGRP-LCx to bind to a lysine-containing muropeptide (Swaminathan et al., 2006).

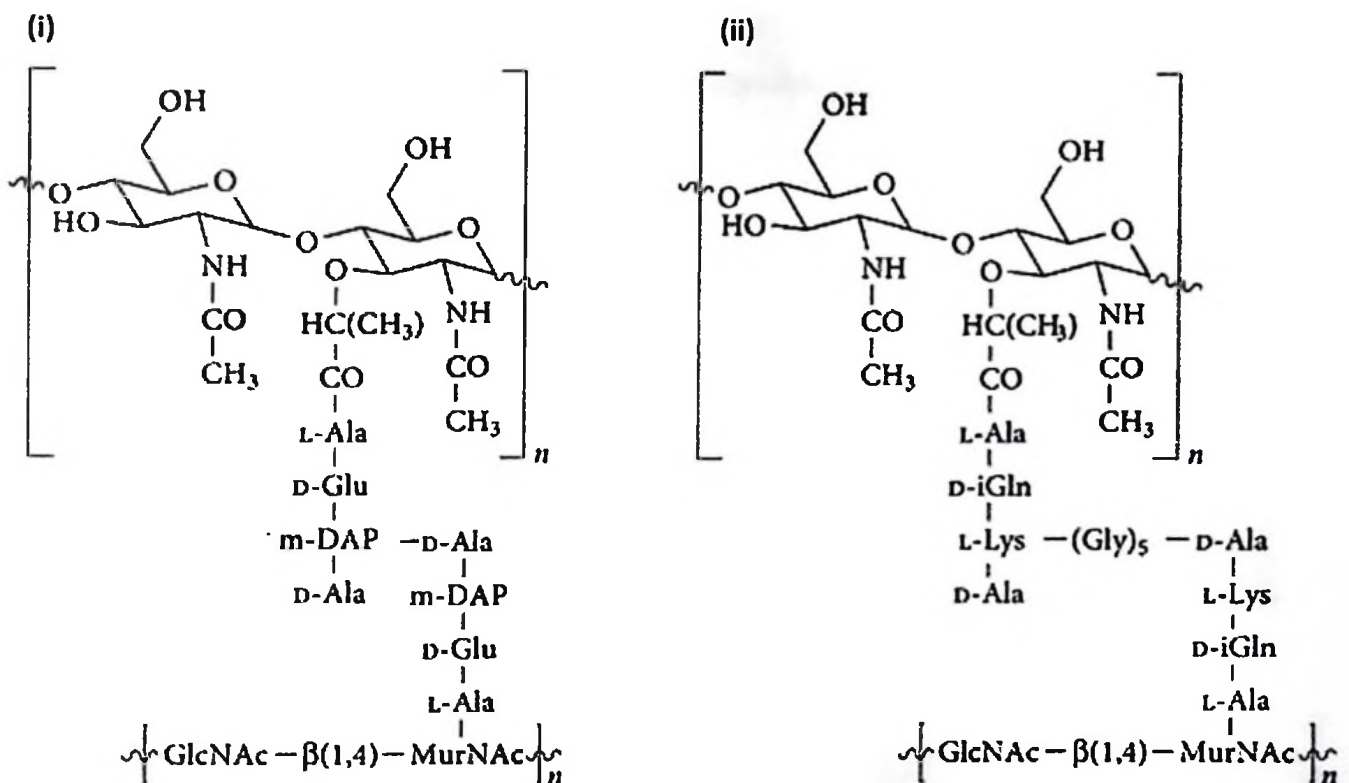


Figure 1-1: Schematic representation of DAP-type and Lysine-type PGN building units.

(i) Dap-type PGN building unit showing the position and linkage of the *meso*-diaminopimelic acid (m-DAP) residue on the side chain. (ii) Lysine-type PGN-building unit with a Lysine residue occupying the position of the m-DAP residue. (Adapted from: Royet and Dziarki, 2007).

The direct effector function of some insect PGRPs is defined by presence or absence of amidase activity of individual PGRPs. PGRPs with the ability to cleave the bound PGN are referred to as catalytic PGRPs and they are distinguished from the non-catalytic PGRPs by a zinc-dependent ability of the former to cleave the amide bond between the N-acetylmuramic acid residue and L-alanine of the stem peptide. The catalytic (also known as amidase) activity of PGRPs is ascribed to the presence of a key cysteine residue required for zinc binding into the PGN-binding cleft. This zinc ion acts as an electrophilic catalyst which accepts an electron pair from the carbonyl atom of the N-acetylmuramic acid thereby polarizing the bond and making it more susceptible to nucleophilic attack by the catalytic water molecule coordinated to the bound Zn^{2+} (Guan et al., 2004). Some of the most studied insect catalytic PGRPs include PGRP-LB, PGRP-SC1a and -C1b. By scavenging and cleaving PGN, catalytic PGRPs act as negative regulators of the immune systems that would have otherwise been stimulated by the presence of the invading pathogens.

1.5.3 Gram-negative binding proteins

Gram-negative bacteria-binding proteins (GNBPs) are a class of PPRs found only in invertebrates although they contain a protein domain that is similar to bacterial glucanases. They are so named because they were initially isolated from immune challenged *Bombyx mori*, as molecules with ability to bind to Gram-negative bacterial surface, but not significantly to Gram-positive bacteria (Lee et al., 1996). Subsequent studies showed that the drosophila genome encodes three GGBP genes namely GGBP1, 2 and 3. Of these, the GGBP1 is the most characterised member of the class and it has been shown to have a high affinity to microbial immune elicitors including lipopolysaccharide (LPS) and beta-1,3-glucan but does not bind to peptidoglycan, beta-1,4-glucan, or chitin (Kim et al., 2000). A complex of GGBP1 and PGRPSA has been shown to be responsible for activation of the Toll signaling cascade possibly because

GNBP1 facilitates the cleavage of PGN from Gram positive-bacteria thereby generating products that are recognised by its complex partner, PGRP-SA (Philippe et al., 2005). Disruption of the GNBP1 gene has been shown to lead to compromised ability of mutant flies to survive Gram-positive bacterial infections, but not fungal or Gram-negative bacterial infections (Gobert et al, 2003).

1.5.4 Scavenger receptors

These constitute a class of membrane-based PPRs originally discovered for their ability to recognize and remove modified lipoproteins. They are now appreciated for their role in pathogen clearance, lipid transport, the transport of cargo within the cell and functioning as taste receptors. Based on sequence alignment, protein domain architecture and functional considerations, scavenger receptors (SRs) have been grouped into several classes namely SR-A to SR-H (Canton et al., 2013). Since SR proteins are structurally highly heterogeneous, their grouping into one superfamily is mainly a result of shared functional properties rather than structural similarities. Their overall functional resemblance is based around the fact that SRs perform their duties either through identification and removal of modified self entities such as apoptotic cells and damaged proteins or through the recognition of non-self entities such as invading pathogens. By recognizing and removing modified self entities, SRs act as receptors for recognition and removal of *danger associated molecular patterns* (DAMPs). On the other hand, the ability of SR proteins to recognise and remove exogenous non-self entities (such as PAMPs) makes them a subset of PPRs.

A shared feature of SRs involved in innate immunity is that a single SR can interact with and recognise different types of ligands. In mammals, for example, it has been shown that SR-A1 can bind to (i) the lipid A moiety of LPS, an integral component of Gram-negative

bacterial cell walls, (ii) Lipoteichoic acid (LTA), a major constituent of Gram-positive bacterial cell wall, and (iii) bacterial CpG DNA (Hampton et al., 1991; Greenberg et al., 1996; Zhu et al., 2001; Mukhopadhyay, S. and Gordon, S., 2004). The ability to of SR-A1 recognise LPS, LTA and bacteria CpG is shared by MARCO a structurally similar (though a product of distant gene) scavenger receptor suggesting that the two SRs may be functionally redundant (Canton et al., 2013). Additionally, several SRs share the ability to interact with and influence signaling through other PRRs of the innate immune system. SR-A1, for example, has been shown to interact with TLR4 thereby promoting phagocytosis of a Gram-negative bacterium *Escherichia coli*, whereas its interaction with TLR2 enhanced phagocytosis of a Gram-positive bacterium *S. aureus* (Amiel et al. 2009). Similarly, functional complexes can be formed between the mammalian CD36 and TLR2 and TLR6 to augment the cytokine response to LTA derived from *S. aureus* (Canton et al., 2013).

From an insect perspective, the *D. melanogaster* genome is known to encode four class C scavenger receptors namely DScr-CI, DScr-CII, DScr-CIII and DScr-CIV. Of these, the DScr-CI is the most characterised member of the family and is known to be expressed in embryonic hemocytes and is important for phagocytosis of both Gram-positive and Gram-negative bacteria but is not involved in phagocytosis of yeast (Pearson et al., 1995; Ramet et al., 2001). The *D. melanogaster* scavenger receptor Croquemort is a homologue of the mammalian CD36. Croquemort plays a role in identification of apoptotic markers and phagocytosis of dying cells (Pal and Wu, 2009). Unlike CD36, the involvement of Croquemort in phagocytosis of pathogens and the activation of Toll pathways remains to be established.

1.5.5 Thiol-Ester proteins and the complement system

The complement is an integral component of the innate immune system which functions by recognizing and opsonizing particulate materials including invading microorganisms and altered (dying or damaged) host cells. The complement system is well characterised in mammals and its machinery includes a collection of up to 35-40 proteins found in various body fluids such as blood plasma and on cell surfaces (Mayilyan et al., 2008). The target is usually recognised by large polymeric complement proteins such as clq and MBL leading to activation of proteases which in turn cleave the thioester-containing protein, C3. The cleaved C3 protein binds to the target thus promoting interaction with phagocytic cells which express complement receptors leading to opsonization of the target.

Although much of what is known about the complement system originates from research in mammals, evidence on the existence of the system in invertebrates is emerging and expanding. The first report of the presence of a thiol-ester protein related to the mammalian C3 protein in an invertebrate was from work on α_2 -macroglobulin proteinase-inhibitor homologue present in the plasma of the American horseshoe crab *Limulus Polyphemus* (Armstrong and Quigley, 1987). A search for C3- α -macroglobulin like molecules in *Drosophila* led to identification of four proteins of this family named thioester containing proteins (TEP1-4) (Lagueux et al., 2000). They all contain a signal peptide suggesting that they are secreted proteins. TEP1, 2 and 4 are upregulated in the fat body upon immune challenge by bacteria and their induction is linked to the JAK/STAT pathway and the Toll receptor as gain of function of JAK components or Toll mutants lead to induction of TEP factors (Lagueux et al., 2000). RNAi experiments have provided evidence that TEP3 may be specifically required for efficient phagocytosis of *S. aureus* (Pal and Wu, 2009; Peltan et al., 2006) while TEP2 is required for efficient phagocytosis of *E. coli* (Peltan et al., 2006).

1.6 Innate immune signaling cascades in insects

Signaling activities leading to production of antimicrobial peptides and most other innate immune responses in insects are controlled by two major pathways; the Toll and IMD signal transduction pathways. By far, AMPs are the most common effector molecules whose production is regulated through these two pathways in insect innate immunity. Genetic studies have revealed that the Toll pathway is activated upon recognition of Gram-positive bacteria, especially of the lysine-type PGN and fungi while the IMD pathway responds mainly to Gram-negative bacteria and a few Gram-positive bacilli carrying the DAP-type PGN on their cell walls (Gregorio et al., 2002). However, depending on the type of infection, and selective adaptation of the host to repeated exposure to the aggressor pathogen, the production of most AMP genes in *D. melanogaster* and other insects can be regulated by either pathway.

1.6.1 The Toll pathway

In *D. melanogaster* - the most extensively studied insect innate immunity model, major Toll signaling pathway components are well established. As indicated above, the activation of the Toll signaling pathway is preceded by recognition of mainly lysine-type PGN or β -glucan. Depending on the type of invading/ immune elicitor, a proteolytic cascade is mounted through the modular Serine Protease (modSP) which integrates signals from the upstream recognition molecules (i.e. GGBP3 or GGBP1/PGRPSA complex or PGRPSD) to another serine protease called Gram-positive- specific serine protease (Grass). The activated Grass interacts with either of the next serine proteases namely spirit, spheroid or sphinx1/2 to activate Spatzle-processing enzyme (SPE) which in turn activates the Toll receptor ligand, spatzle. Spatzle is a cytokine produced in an inactive precursor form where its prodomain masks its predominantly hydrophobic C-terminal (also known as C-106) region. This proteolytic activation of spatzle induces conformational changes leading to exposure of determinants that are critical for the

binding spatzle to its receptor, Toll (Arnot et al., 2010; Valanne et al., 2011). Following the binding of processed spatzle to the extracellular domain of Toll, the activated Toll receptor binds to an adaptor protein, MyD88 via its intracellular TIR (Toll/interleukin-1 receptor) domain (Horng and Medzhitov, 2001; Valanne et al., 2011). The interaction of Toll and MyD88 recruits an adaptor protein, Tube and a kinase, Pelle leading to the formation of MyD88-Tube-Pelle heterotrimeric complex through death domain (DD)-mediated interactions such that two distinct DD domains of the adaptor protein Tube separately bind to MyD88 and Pelle (Xiao et al., 1999; Sun et al., 2002). By yet a less understood interaction, the signal from the MyD88-Tube-Pelle heterotrimeric complex proceeds to cause phosphorylation and subsequent degradation of Cactus. The phosphorylation-dependent degradation of Cactus frees its complex partner(s), the NF- κ B transcription factor(s) Dif and/or Dorsal which, in turn, translocate to the nucleus to activate transcription of specific AMP genes (Wu et al., 1998).

1.6.2 The IMD pathway

D. melanogaster IMD signal transduction pathway is involved in the expression of AMPs through NF- κ B-like transcription factors distinct from those of the Toll pathway and appears to share no Toll pathway intermediate components (Gregorio et al., 2002). After the initial recognition of DAP-type PGN by PGRPLC or synergistic action of PGRPLC and PGRPLE as detailed above, the signal is propagated from the extracellular domain of PGRPLC to IMD, a cytoplasmic protein containing a death domain (DD) homologous to the mammalian RIP1 (Georgel et al. 2001). Through its DD, IMD interacts with (dFADD) a *D. melanogaster* homologue of the mammalian Fas-associated death domain (FADD), which in turn, interacts with and recruits the caspase-8 homologue DREDD to the signaling complex through its homotypic Death-effector domain (DED) (Hu and Yang, 2000). DREDD has been proposed to play dual roles in the activation of IMD pathway. It has been shown to cleave IMD (Paquette et



al. 2010) thus contributing to its activation but it has also been proposed to be required for the cleavage of Relish, a transcription factor further downstream the IMD pathway (Leulier et al. 2000, Stöven et al. 2003). As indicated under section 1.5 above, Relish consists of both the N-terminal Rel homology domain (RHD) and a C-terminal inhibitory I κ B part the latter of which must be removed by endo-proteolytic cleavage to release the NF- κ B part. The cleaved NF- κ B part translocates to the nucleus and initiates the transcription of its target genes, such as the AMPs, while the inhibitory C-terminal part remains in the cytoplasm (Stöven et al. 2000, Stöven et al. 2003). In addition to the DREDD-mediated cleavage, the activation of Relish is promoted by its phosphorylation by the I κ B kinase (IKK) complex, a core component of the NF- κ B signaling cascade (Krappmann et al., 2000; Silverman et al., 2000). It has been reported that Ird5, the *D. melanogaster* IKK β , phosphorylates two serine residues (serines 528 and 529) in the N-terminal part of Relish, and that this phosphorylation is necessary for Relish cleavage, translocation to the nucleus, or binding to the DNA target sequence (Ertürk-Hasdemir et al. 2009).

1.6.3 The JAK/STAT pathway

The JAK-STAT pathway is an evolutionarily conserved signal transduction pathway comprising of two major player components, the Janus kinases (JAK) and the signal transducers and activators of transcription (STAT) in addition to receptors. Depending on the tissue and cellular context involved, JAK-STAT signaling may lead to proliferation, differentiation, migration, apoptosis, or cell survival (Harrison, 2009; Ghoreschi et al. 2009). JAKs are a unique class of tyrosine kinases that contain both a catalytic domain and a second kinase-like domain that has an auto-regulatory function (Harrison, 2012). Following an external stimuli, the JAKs bind to cell surface cytokine receptors leading to the activation of JAKs. The increased kinase activity of receptor-bound JAKs leads to phosphorylation of tyrosine residues on the receptor

which in turn creates sites for the interaction of the receptors with proteins that contain phosphotyrosine-binding SH2 domains. STATs which are proteins possessing these SH2 domains are then recruited to the receptors prompting the bound JAKs to further phosphorylate the tyrosine residues on them. The phosphorylated tyrosine residues on activated STATs act as binding sites for SH2 domains of other STATs leading to dimerization of STATs. The activated STAT dimers translocate to the nucleus where they bind as dimers or as more complex oligomers to specific enhancer sequences in target genes, thus regulating their transcription (Harrison, 2012). Members of the JAK/STAT signaling cascades vary among eukaryotes. While most mammals have four members of the JAK family and seven STATs which are recruited based on their tissue-specificity and the receptors engaged in a particular signaling event (Schindler and Plumlee 2008), insects like *D. melanogaster* appear to have only one JAK and one STAT (Arbouzova and Zeidler 2006).

1.7 Autophagy as an immune defence mechanism

Autophagy is a cellular mechanism that mediates bulk degradation of cytoplasmic components of in eukaryotic cells. During autophagic processes, a portion of the cytoplasm, which often times includes the targeted cargo, is sequestered in an isolation membrane which matures into a double-membrane structure called the autophagosome, a structure distinct from the single-membrane phagosome (Yano and Kurata, 2011) and the former fuses with the lysosome to form an autolysosome in which the cargo is degraded. Under non-infectious conditions autophagy is used to perform well-documented housekeeping functions of (i) degrading unused long-lived proteins and faulty cellular organelles (ii) recycling nutrients in response to starvation and (iii) tissue remodeling process during developmental changes (Yang, and Klionsky, 2010). In addition to the housekeeping roles, autophagy has been linked to intracellular clearance of invading pathogens. The recognition PAMPS by host-based PRRs is,

again, central to innate immune signaling that leads to autophagy. In mammals, Toll-like receptors (TLRs) and Nod-like receptors (NLR) are two of the relatively well-known PRRs. TLRs are transmembrane proteins that contain Leucine-rich repeats (LRR) in their ectodomains for PAMP recognition and they mediate defense responses to fungal, bacterial and viral pathogens. Stimulation of TLR4, for example, is reported to promote the co-localization of mycobacterial phagosomes with autophagosomes (Xu Y. et al., 2007). Studies have shown that several other TLRs are capable of inducing autophagy. Induction of autophagy by TLR7 was shown to be capable of eliminating *Mycobacterium tuberculosis* var. *bovis* infection in macrophages (Delgado et al., 2008). It has been shown further that phagocytosis of TLR agonist-coated beads promotes the maturation of phagosomes by recruiting some elements of the autophagy pathway to the phagosome (Sanjuan et al., 2007).

NLRs on the other hand are cytoplasmic surveillance proteins that contain the Nucleotide-binding oligomerization domain (NOD). The bacterial peptidoglycan receptors (Nod1 and Nod2) are two of the most studied mammalian NLRs. Upon activation, the nods can process the signals in two downstream channels. In the first scenario, nods (Nod1 or Nod2) can recruit an adaptor protein RIP2, prompting a series of downstream events leading to the activation of NF- κ B and an inflammatory response to help the elimination of invading microbes (Travassos et al., 2010). Alternatively, the nods can directly interact with and recruit essential components of the autophagy pathway such as the Atg12-Atg5-Atg16 complex to the bacterial entry site effectively promoting the formation of the autolysosome for eventual degradation of sequestered pathogens. Studies in mice have shown that cells expressing mutations in Nod2 fail not only to signal the NF- κ B but also to recruit the Atg12-Atg5-Atg16 complex to the bacterial entry site and therefore, they become unable to initiate the formation of the autophagosome around the invading pathogens (Travassos et al., 2010).

Cytoplasmic sensors that link microbial recognition to their autophagic clearance in insects are poorly understood. Research in this area is in its infancy and only one molecule, the Peptidoglycan Recognition Protein-LE (PGRP-LE) has been identified as an intracellular sensor of invading pathogens that induces their eventual autophagic clearance from the cytosol (Yano et al., 2008). Originally identified as an extracellular pattern recognition molecule that senses DAP-type Peptidoglycan in cooperation with PGRP-LC and subsequent activation of the IMD signaling pathway, PGRP-LE was later shown to play a role in intracellular recognition of DAP-type peptidoglycan containing pathogens without the requirement for PGRP-LC. In their report, Yano et al., 2008 produced evidence that PGRP-LE is critical in the ability of *D. melanogaster* to resist infections by *L. monocytogenes*, an intracellular gram positive bacterium with DAP-type peptidoglycan mainly through the induction of targeted autophagic clearance of the pathogen. PGRP-LE-dependent induction of autophagy following intracellular pathogen recognition does not require the involvement of factors of the signal transduction pathways of toll or Imd, but does require the canonical autophagy molecules such as Atg5 and Atg1 (Yano et al., 2008; Yano and Kurata, 2011) indicating that PGRP-LE may play an important role of linking intracellular bacterial recognition and autophagy induction. Although it is clear that PGRP-LE is required for the autophagic clearance of *L. monocytogenes* in drosophila, the mechanism by which PGRP-LE accomplishes this task together with other key players of the pathway remains to be elucidated.

1.8 Overall objective and aims of this thesis

Tenebrio molitor is an economically important insect causing significant loss in quantity and quality of stored agricultural products, mainly because the larvae not only feed on the stored produce but also contaminates it with exuviate, excrements and dead insect bodies (Siemianowska et al., 2013). On the other hand, its large-sized larval stages have been explored as potential sources of food for both humans (Ghaly and Alkoaik, 2009; Ravzanaadii et al.,

2012; Siemianowska et al., 2013) and livestock (Klasing et al., 2000; Ramos-Elorduy et al., 2002). Devising and implementing effective control strategies against *T. molitor* as a pest of stored agricultural products and/or maximizing the exploitation of *T. molitor* larvae as a source of food, cannot be stepped up to its full potential without sufficient knowledge on how the insect thrives against odds to resist infections from its surroundings either naturally as a pest of stored produce or in captivity.

There is need, therefore, to explore and understand important aspects of *Tenebrio* immunity. However, unlike *Drosophila*- an established model of insect immunity, many aspects of coleopteran immune system in general and *Tenebrio* immunity in particular are in their infancy. Furthermore, there is evidence in literature that mode of response against a common immune elicitor may differ among insects. There exists biochemical evidence, for example, on the biological diversity of innate immune responses in molecular recognition mechanism for polymeric DAP-type peptidoglycan between *Tenebrio* larvae and *Drosophila* adults (Yu et al., 2010). With reference to *Tenebrio* immune systems, while individual components of the extracellular segment of the *Tenebrio* Toll pathway have been identified, largely through biochemical approaches (Kim et al., 2008; Roh et al., 2009; Yu et al., 2010), components and makeup of the intracellular segment of the toll pathway as well as the IMD and autophagy are yet to be fully characterised. The current work was, therefore, designed to make a contribution in bridging this gap by realizing the following specific objectives

- (i) Identify, clone and functionally characterise three genes of the *Tenebrio* autophagy pathway (*TmATG3*, *TmATG5* and *TmATG8*) in response to infection by an intracellular pathogen, *Listeria monocytogenes*.

- (ii) Using *Listeria monocytogenes* as a pathogen, identify, clone and functionally characterise, TmPGRP-LE, as a potential cytoplasmic sensor of DAP-type PGN in the *Tenebrio* IMD signal transduction pathway and;
- (iii) Identify, clone and functionally characterise the role TmPGRP-LB, in recognition and control of non-conventional soil-isolated entomopathogen. *Pseudomonas geniculata* HT1

1.9 References

- Agaisse, H. (2007). An Adaptive Immune Response in *Drosophila*? *Host cell & microbe*. 1(2): 91-93.
- Akashi, S., Ogata, H., Kirikae, F. et al. (2000). Regulatory roles for CD14 and phosphatidylinositol in the signaling via toll-like receptor 4-MD-2. *Biochem Biophys Res Commun* 268(1):172-177.
- Alexopoulou, L., Holt, A.C., Medzhitov, R. et al. (2001). Recognition of double-stranded RNA and activation of NF-kappaB by Toll-like receptor 3. *Nature* . 413(6857):732-738.
- Amiel, E. (2009). Pivotal advance: Toll-like receptor regulation of scavenger receptor-A-mediated phagocytosis. *J. Leukoc. Biol.* 85, 595–605.
- Arbouzova, N.I., Zeidler, M.P. (2006). JAK/STAT signalling in *Drosophila*: Insights into conserved regulatory and cellular functions. *Development* 133: 2605–2616.
- Armstrong, P.B. and Quigley, J.P. (1987). Limulus α_2 -macroglobulin: First evidence in an invertebrate for a protein containing an internal thiol ester bond. *Biochem. J.* 248, 703-707.
- Arnot, C. J., Gay, N. J. and Gangloff, M. (2010). Molecular mechanism that induces activation of Spatzle, the ligand for the *Drosophila* Toll receptor. *J. Biol.Chem.* 285: 19502–19509.
- Beismejier, J.C., Roberts, S.P., Reemer, M., Ohlemüller, R., Edwards, M., Peeters, T., Schaffers, A.P., Potts, S.G., Kleukers, R., Thomas, C.D., Settele, J. and Kunin, W.E

- (2006). Parallel declines of pollinators and insect-pollinated plants in Britain and the Netherlands. *Science*, 303: 531-354.
- Bergvinson, D., and Garcia-Lara, S. (2004). Genetic approaches to reducing losses to stored grains to insects and diseases. *Current opinion in plant biology*, 7: 480-485.
- Brandt, S.M., Dionne, M.S., Khush, R.S., Pham, L.N., Vigdal, T.J. and Schneider D.S. (2004). Secreted Bacterial Effectors and Host-Produced Eiger/TNF Drive Death in a *Salmonella*-Infected Fruit Fly *PLoS Biol.*, 2 DOI: 10.1371/journal.pbio.0020418.
- Chang, C.I., Chelliah, Y., Borek, D., Mengin-Lecreulx, D. and Deisenhofer, J. (2006). Structure of tracheal cytotoxin in complex with a heterodimeric pattern-recognition receptor. *Science*. 311(5768):1761-4.
- Cheong, H., Nair, U., Geng, J. and Klionsky D.J. (2008). The Atg1 kinase complex is involved in the regulation of protein recruitment to initiate sequestering vesicle formation for nonspecific autophagy in *Saccharomyces cerevisiae*. *Mol Biol Cell*. 19:668–81.
- Chiang, H., Terlecky, S.R., Plant, C. and Dice, J. (1989). "A role for a 70-kilodalton heat shock protein in lysosomal degradation of intracellular proteins". *Science* 246 (4928): 382–5.
- Lamb, C.A, Dooley H.C. and Tooze S, A. (2012). Endocytosis and autophagy: Shared machinery for degradation.
- Delgado, M.A., Elmaoued, R.A., Davis, A.S., Kyei, G. and Deretic, V. (2008) Toll-like receptors control autophagy. *EMBO J*. 27:1110–1121.

- Dionne, M.S., Ghorri, N. and Schneider, D.S. (2003). *Drosophila melanogaster* is a genetically tractable model host for *Mycobacterium marinum*. *Infect. Immun.*, 71: 3540–3550.
- Ertürk-Hasdemir, D., Broemer, M., Leulier, F., Lane, W.S., Paquette, N., Hwang, D., Kim, C.H., Stöven, S., Meier, P. and Silverman, N. (2009). Two roles for the *Drosophila* IKK complex in the activation of Relish and the induction of antimicrobial peptide genes. *Proc Natl Acad Sci USA*. 106:9779-9784.
- Faulhaber, L.M. and Karp, R.D. (1992). A diphasic immune response against bacteria in the American cockroach. *Immunology*, 75: 378-381.
- Filipe, S.R., Tomasz, A. and Ligoxygakis, P. (2005). Requirements of peptidoglycan structure that allow detection by the *Drosophila* Toll pathway. *EMBO Rep*. 6(4):327-333.
- Georgel, P., Naitza, S., Kappler, C., Ferrandon, D., Zachary, D., Swimmer, C., Kopczynski, C., Duyk, G., Reichhart, J.M. and Hoffmann, J.A. (2001). *Drosophila* immune deficiency (IMD) is a death domain protein that activates antibacterial defense and can promote apoptosis. *Dev Cell*. 1:503-514.
- Ghaly, A.E. and Alkoaik, F.N. (2009). The Yellow Mealworm as a Novel Source of Protein. *American Journal of Agricultural and Biological Sciences* 4 (4): 319-331.
- Ghoreschi, K., Laurence, A. and O’Shea, J.J. (2009). Janus kinases in immune cell signaling. *Immunol Rev* 228: 273–287.

- Gobert, V., Gottar, M., Matskevich, A.A., Rutschmann, S., Royet, J., Belvin, M., Hoffmann, J.A. and Ferrandon, D. (2003). Dual Activation of the *Drosophila* Toll Pathway by Two Pattern Recognition Receptors *Science* 302 2126-30.
- Gregorio, E. D., Spellman, P.T., Zhou, P., Rubin, G.M. and Lemaitre, B. (2002). The Toll and Imd pathways are major regulators of immune response in *Drosophila*. *EMBO* 21(11):2568-2579.
- Guan, R., Roychowdhury, A., Ember, B., Kumar, S., Boons, G-J., and Mariuzza, R.A. (2004). Structural basis for peptidoglycan binding by peptidoglycan recognition proteins. *Proc. Natl. Acad. Sci. U.S.A.* 101(49): 17168–17173.
- Hampton, R.Y., Golenbock, D.T., Penman, M., Krieger, M. and Raetz, C.R. (1991). Recognition and plasma clearance of endotoxin by scavenger receptors. *Nature.* 352, 342–344.
- Harrison, D. (2012). The JAK/STAT pathway. *Cold Spring Harb Perspect Biol* . doi: 10.1101/cshperspect.a011205.
- Hemmi, H., Takeuchi, O., Kawai, T. et al. (2000). A Toll-like receptor recognizes bacterial DNA. *Nature* 2000; 408(6813):740-745.
- Hoffmann, J.A., Kafatos, F.C., Janeway, C.A., and Ezekowitz, R.A. (1999). *Science*, 284:1313–1318.
- Horng, T. and Medzhitov, R. (2001). *Drosophila* MyD88 is an adapter in the Toll signaling pathway. *Proc Natl Acad Sci USA* 98(22):12654–12658.

<http://www.bu.edu/nf-kb/> NF- κ B Transcription Factors. The Rel/NF- κ B Signal Transduction Pathway (accessed on 13 September 2014).

<http://www.slideshare.net/fullscreen/acoleman2/insect-infection-and-immunity-evolution-ecology-and-mechanisms-oxford-biology/14>.

Hu, S. and Yang, X., (2000). DFADD, a novel death domain-containing adapter protein for the *Drosophila* caspase DREDD. *J. Biol. Chem.* 275, 30761–30764.

Imler, J.L., and Bulet, P. (2005). Antimicrobial peptides in *Drosophila*: structures, activities and gene regulation. *Chem. Immunol. Allergy* 86:1–21.

Kim, M-S, Byun, M. and Oh, B-H: (2003). Crystal structure of peptidoglycan recognition protein LB from *Drosophila melanogaster*. *Nat Immunol.* 4:787-793.

Kim, C.H., Kim, S.J., Kan, H., Kwon, H.M., Roh, K.B., Jiang, R., Yang, Y., Park, J.W., Lee, H.H., Ha, N.C., Kang, H.J., Nonaka, M., Söderhäll, K. and Lee, B.L (2008). A three-step proteolytic cascade mediates the activation of the peptidoglycan-induced toll pathway in an insect. *J Biol Chem.* 283(12):7599-607.

Kim, Y-S., Ryu, J-H., Hani, S-J., Choi K-H., Ki-Bum Nam, K-B., Jang, I-H., Lemaitre, B., Breyi, P.T. and Lee, W-J (2000). Gram-negative Bacteria-binding Protein, a Pattern Recognition Receptor for Lipopolysaccharide and β -1,3-Glucan That Mediates the Signaling for the Induction of Innate Immune Genes in *Drosophila melanogaster* Cells. *J Biol Chem* 275(42): 32721–32727.

- Kindt, T.J., Goldsby, R.A. and Osbourne, B.A. (2007). *Kuby - Immunology*. New York, Freeman.
- Klasing, K. C., Thacker, P., Lopez, M. A. and Calvert, C. C. (2000). Increasing the calcium content of mealworms (*Tenebrio molitor*) to improve their nutritional value for bone mineralization of growing chicks. *J. Zoo Wildlife Med.*, 31 (4): 512-517.
- Krappmann, D., Hatada, E. N., Tegethoff, S., Li, J., Klippeli, A., Giese, K., Baeuerle, P. A. and Scheidereit, C. (2000). The I κ B Kinase (IKK) Complex Is Tripartite and Contains IKK γ but Not IKAP as a Regular Component. *J Biol Chem* . 275 (38): 29779–29787.
- Lagueux, M., Perrodou, E., Levashina, E.A. , Capovilla, M., and Hoffmann, J.A. (2000). Constitutive expression of a complement-like protein in toll and JAK gain-of-function mutants of *Drosophila*. *Proc Natl Acad Sci USA* 97(21):11427-11432.
- Laplante and Lambatini (2009). mTOR signaling at a glance. *Journal of cell science*. 122, 3589-3594.
- Lee, W.J., Lee, J.D., Kravchenko, V.V. et al (1996). Purification and molecular cloning of an inducible Gram-negative bacteria-binding protein from the silkworm, *Bombyx mori*. *Proc Natl Acad Sci USA* 93(15):7888-7893.
- Lemaitre, B., Nicolas, E., Michaut, L., Reichhart, J-M., and Hoffmann. J.A. (1996). The Dorsoventral Regulatory Gene Cassette *spatzle/Toll/cactus* Controls the Potent Antifungal Response in *Drosophila* Adults. *Cell*. 86: 973–983.

- Leulier, F., Rodriguez, A., Khush, R.S., Abrams, J.M. and Lemaitre, B. (2000). The *Drosophila* caspase Dredd is required to resist Gram-negative bacterial infection. *EMBO Rep.* 1: 353-358.
- Shanga L., Chenb, S., Dua, F., Lib, S., Zhao A.B., and Xiaodong W.B. (2011). Nutrient starvation elicits an acute autophagic response mediated by Ulk1 dephosphorylation and its subsequent dissociation from AMPK.
- Lim, J.H., Kim, M.S., Kim, H.E., Yano, T., Oshima, Y., Aggarwal, K., Goldman, W.E., Silverman, N., Kurata, S., Oh, B.H. (2006). Structural basis for preferential recognition of diaminopimelic acid-type peptidoglycan by a subset of peptidoglycan recognition proteins. *J Biol Chem.* 281(12):8286-95.
- Mayilyan, K.R., Kang, Y.H., Dodds, A.W. and Sim, R.B. (2008). The complement system in innate immunity. *Nucl aci Mol Biol* (21): 219-236.
- Medzhitov, R., Preston-Hurlburt, P. and Janeway, C.A. (1997). A human homolog of *Drosophila* toll protein signals activation of adaptive immunity. *Nature.* 388: 394-397.
- Moon, H.J., Lee, S.Y., Kurata, S., Natori S. and Lee, B.L. (1994). Purification and Molecular Cloning of cDNA for an Inducible Antibacterial Protein from Larvae of the Coleopteran, *Tenebrio molitor*. *J Biochem.* 116 (1): 53-58.
- Mukhopadhyay, S. and Gordon, S (2004). The role of scavenger receptors in pathogen recognition and innate immunity. *Immunobiology* 209, 39–49 (2004).
- Nappi, A.J. and Ottaviani, E. (2000). Cytotoxicity and cytotoxic molecules in invertebrates. *Bioassays.* 22(5):469-80.

- Nappi, A.J., Vass, E., Frey, F. and Carton, Y. (1995). Superoxide anion generation in *Drosophila* during melanotic encapsulation of parasites. *Eur J Cell Biol.* 68(4):450-6.
- Oerke, E-C. and Dehne, H-W. (2004). Safeguarding production-losses in major crops and the role of crop protection. *Crop protection.* 23: 275-285.
- Ozinsky, A., Underhill, D.M., Fontenot, J.D. et al. (2000). The repertoire for pattern recognition of pathogens by the innate immune system is defined by cooperation between toll-like receptors. *Proc Natl Acad Sci USA* 97(25):13766-13771.
- Pal, S. and Wu, L.P. (2009). Lessons from the Fly: Pattern Recognition in *Drosophila melanogaster*. *Adv Exp Med Biol.* 653:162-74.
- Paquette, N., Broemer, M., Aggarwal, K., Chen, L., Husson, M., Ertürk-Hasdemir, D., Reichhart, J.M., Meier, P., and Silverman, N. (2010). Caspase-mediated cleavage, IAP binding, and ubiquitination: linking three mechanisms crucial for *Drosophila* NF-kappaB signaling. *Mol Cell.* 37:172-82.
- Pearson, A., Lux, A. and Krieger, M. (1995). Expression cloning of dSR-CI, a class C macrophage-specific scavenger receptor from *Drosophila melanogaster*. *Proc Natl Acad Sci USA* 92(9):4056-4060.
- Peltan, A., Briggs, L., Matthew, G., Sweeney, S.T. and Smith, D.F (2006). Identification of *Drosophila* gene products required for phagocytosis of *Candida albicans*. *PLoS Biol* 4(1):84-99.

- Pham, L.N., Dionne, M.S., Shirasu-Hiza, M. and Schneider D.S. (2007). A Specific Primed Immune Response in *Drosophila* Is Dependent on Phagocytes. *PLoS Pathog.* 3(3): e26. doi:10.1371/journal.ppat.0030026.
- Ramet, M., Pearson, A., Manfrulli, P. et al. (2001). *Drosophila* scavenger receptor CI is a pattern recognition receptor for bacteria. *Immunity.* 15(6):1027-1038.
- Ramos-Elorduy, J., Avila G. E., Rocha, H.A., and Pino, J. M., 2002. Use of *Tenebrio molitor* (Coleoptera: Tenebrionidae) to recycle organic wastes and as feed for broiler chickens. *J. Econ. Entomol.*, 95 (1): 214-220.
- Ravzanaadii, N., Kim, S-H., Choi, W.H., Hong, S-J. and Kim, N.J.(2012). Nutritional Value of Mealworm, *Tenebrio molitor* as Food Source. *Int J Indust Entomol.* Vol. 25(1): 93-98.
- Retief, F.P. and cilliers, L. (1998). The epidemic of Athens, 430-426 BC. *S Afr Med J*, 88, 50-3.
- Ritsick, D.R., Edens, W.A., McCoy, J.W., Lambeth, J.D. (2004). The use of model systems to study biological functions of Nox/Duox enzymes. *Biochem. Soc. Symp.* :85–96.
- Roh, K.B., Kim, C.H., Lee, H., Kwon, H.M., Park, J.W., Ryu, J.H., Kurokawa, K, Ha N.C., Lee, W.J., Lemaitre, B., Söderhäll, K and Lee, B.L. Proteolytic cascade for the activation of the insect toll pathway induced by the fungal cell wall component. *J Biol Chem.* 284(29):19474-81.
- Rolff, J. and Reynolds, S.E. (2009). Introducing insect infection and immunity. In *Insect infection and immunity: Evolution, ecology and mechanisms.* Rolff and Reynolds (editors). Oxford University Press, Oxford, UK. 267pp.

- Sagisaka, A., Miyanoshita, A., Ishibashi, J., and Yamakawa, M. (2001). Purification, characterization and gene expression of a glycine and proline-rich antibacterial protein family from larvae of a beetle, *Allomyrina dichotoma*,” *Insect Molecular Biology*. 10(4):293–302.
- Sanjuan, M.A, (2007). Toll-like receptor signalling in macrophages links the autophagy pathway to phagocytosis. *Nature*. 450:1253–1257.
- Sanjuan, M.A., Dillon, C.P., Tait, S.W., Moshiah, S., Dorsey, F., Connell, S., Komatsu, M., Tanaka, K., Cleveland, J.L., Withoff, S., Green, D.R. (2007). Toll-like receptor signalling in macrophages links the autophagy pathway to hagocytosis. *Nature* 450:1253–1257.
- Schindler, C. and Plumlee, C. (2008). Inteférons pen the JAK-STAT pathway. *Semin Cell Dev Biol* 19: 311–318.
- Siemianowska, E., Kosewska A., Aljewicz, M., Skibniewska, K.A., Polak-Juszczak, L., Jarocki, A. Jędras, M. (2013). Larvae of mealworm (*Tenebrio molitor L.*) as European novel food. *Agric. Sciences* 4 (2013) 287-291.
- Silverman, N., Zhou, R., Stöven, S., Pandey, N., Hultmark, D., Maniatis, T. (2000). A *Drosophila* IκB kinase complex required for Relish cleavage and antibacterial immunity. *Genes Dev*. 14:2461-2471.
- Smith, K.D., Andersen-Nissen, E., Hayashi, F. et al. (2003). Toll-like receptor 5 recognizes a conserved site on flagellin required for protofilament formation and bacterial motility. *Nat Immunol* 4(12):1247-1253.

- Stöven, S., Ando, I., Kadalayil, L., Engström, Y. and Hultmark, D. (2000). Activation of the *Drosophila* NF- κ B factor Relish by rapid endoproteolytic cleavage. *EMBO Rep.* 1: 347-352.
- Stöven, S., Silverman, N., Junell, A., Hedengren-Olcott, M., Erturk, D., Engström, Y., Maniatis, T., and Hultmark D. (2003). Caspase-mediated processing of the *Drosophila* NF- κ B factor Relish. *Proc Natl Acad Sci USA.* 100:5991-5996.
- Sun, H., Bristow, B. N., Qu, G. and Wasserman, S. A. (2002). A heterotrimeric death domain complex in Toll signaling. *Proc. Natl. Acad. Sci. USA* 99: 12871–12876.
- Suzuki, K., Kubota, Y., Sekito, T., Ohsumi, Y. (2007). Hierarchy of Atg proteins in pre-autophagosomal structure organization. *Genes Cells* 12: 209–18.
- Swaminathan, C.P., Brown, P.H., Roychowdhury, A., Wang, Q., Guan, R., Silverman, N., Goldman, W.E., Boons, G.J. and Mariuzza, R.A. (2006). Dual strategies for peptidoglycan discrimination by peptidoglycan recognition proteins (PGRPs). *Proc Natl Acad Sci U S A.* 103(3):684-9.
- Swaminathan, C.P., Brown, P.H., Roychowdhury, A., Wang, Q., Guan, R., Silverman, N., Goldman, W.E., Boons, G.J. and Mariuzza, R.A. (2006). Dual strategies for peptidoglycan discrimination by peptidoglycan recognition proteins (PGRPs). *Proc. Natl. Acad. Sci. U.S.A.* 103, 684–689.
- Takeshige, K., Baba, M., Tsuboi, S., Noda, T., Ohsumi, Y. (1992) Autophagy in yeast demonstrated with proteinase-deficient mutants and conditions for its induction. *J. Cell Biol.* 119:301–311.

- Travassos, L.H., Carneiro, L.A.M., Ramjeet, M., Hussey, S., Kim, Y-G., Magalhães, J.G., Yuan, L., Soares, F., Chea, E., Le Bourhis, L., Boneca, I.G., Allaoui, A., Jones, N.L., Nuñez, G., Girardin, S.E. and Philpott, D.J. (2010). Nod1 and Nod2 direct autophagy by recruiting ATG16L1 to the plasma membrane at the site of bacterial entry. *Nat Immunol.* 11(1):55-62.
- Valanne, S., Wang, J-H. and Ramet, M. (2011). The drosophila Toll signaling pathway. *J Immunol.* 186:649-656.
- World Health organization, (2013). World Malaria report 2013. http://www.who.int/malaria/publications/world_malaria_report_2013/report/en/ (Accessed 25th August 2014).
- Wu, L. P., and Anderson. K. V. (1998). Regulated nuclear import of Rel proteins in the *Drosophila* immune response. *Nature* 392: 93–97.
- Wullschleger, S., Loewith, R. and Hall MN (2006). TOR signaling in growth and metabolism. *Cell.* 124:471–484.
- Xiao, T., P. Towb, S. A. Wasserman, and Sprang, S. R. (1999). Three-dimensional structure of a complex between the death domains of Pelle and Tube. *Cell* 99: 545–555.
- Xu, Y., Jagannath, C., Xian-De Liu, X-D., Sharafkhaneh, A., Kolodziejska, K. E., and Eissa, N. T. (2007). Toll-like receptor 4 is a sensor for autophagy associated with innate immunity. *Immunity* 27(1): 135–144.

- Yang, Z. and Klionsky, D. (2010). Eaten alive: a history of macroautophagy. *Nat. Cell Biol.* 12, 814-822.
- Yano, T. and Kurata S. (2011). Intracellular recognition of pathogens and autophagy as an innate immune host defence. *J Biochem.* 150(2):143–149.
- Yano, T.; Mita, S.; Ohmori, H.; Oshima, Y.; Fujimoto, Y.; Ueda, R.; Takada, H.; Goldman, W.E.; Fukase, K.; Silverman, N.; et al. (2008). Autophagic control of *Listeria* through intracellular innate immune recognition in *Drosophila*. *Nat. Immunol.* 9, 908–916.
- Yu, Y., Park, J.W. Kwon, H.M. Hwang, H.K., Jang, I.H., Masuda, A., Kurokawa, K., Nakayama, H., Lee, W.J., Dohmae, N., Zhang J. and Lee, B.L. (2010). Diversity of Innate Immune Recognition Mechanism for Bacterial Polymeric *meso*-Diaminopimelic Acid-type Peptidoglycan in Insects. *J Biol Chem.* 285(43): 32937–32945.
- Zhu, F.G., Reich, C.F. and Pisetsky, D.S., (2001). The role of the macrophage scavenger receptor in immune stimulation by bacterial DNA and synthetic oligonucleotides. *Immunology* 103,226–234.

Chapter 2. Autophagy-related genes, *TmATG3* and *TmATG5* are required for survivability against an intracellular pathogen, *Listeria monocytogenes* in *Tenebrio molitor*

2.1 Abstract

Macroautophagy (hereinafter called autophagy) is an evolutionarily conserved catabolic process involved in physiological and developmental processes including cell survival, death, and innate immunity. Homologues of most of 36 autophagy-related genes (ATG) originally discovered in yeast have been characterized in higher eukaryotes including insects. In this study, the homologues of *ATG3* (*TmATG3*) and *ATG5* (*TmATG5*) genes were identified from the order coleoptera, the mealworm, *Tenebrio molitor* by EST and RNAseq approaches. The cDNA of *TmATG3* and *TmATG5* comprise of ORF sizes of 963 and 792 bp encoding proteins with 320 and 263 amino acid residues, respectively. *TmATG3* and *TmATG5* transcripts are detected in all developmental stages analyzed, and primarily in fat body and hemocytes of larvae. *TmATG3* and *TmATG5* showed high amino acid sequence identity (58-95%) with corresponding homologues from various insects and were closer to their orthologs in *Tribolium castaneum*. Loss of function of *TmATG3* and *TmATG5* by RNAi led to a significant reduction in survival ability of *T. molitor* larvae against an intracellular pathogen, *Listeria monocytogenes*. Six days post-*Listeria* challenge, the survivability in ds*TmATG3*- and ds*TmATG5*-treated larvae was significantly reduced to 3 and 4%, respectively, when compared with ds*EGFP*-injected control larvae. These data suggested that *TmATG3* and *TmATG5* may play a role in mediating autophagy-based clearance of *Listeria* in *T. molitor* model.

2.2 Introduction

Cell homeostasis is a cellular mechanism that is precisely regulated to achieve a balance between synthesis and degradation of cellular components. In eukaryotic cells, homeostasis is achieved through two hydrolytic mechanisms namely the proteasome and lysosome/vacuole systems. While most of the intracellular short-lived proteins are selectively degraded by the ubiquitin-proteasome pathway (Hershko and Ciechanover, 1998), most long-lived proteins are degraded by lysosome/vacuole mechanism (Ahlberg et al., 1985; Hoffman and Chiang, 1996). The lysosome/vacuole mechanism can occur in three different pathways: the cytosol to vacuole targeting (Cvt) pathway (Scott et al., 1996; Scott et al., 2001), the vacuole import and degradation (Vid) pathway (Shieh et al., 1998) and autophagy (Scott et al. 1996; Wang and Klionsky, 2003).

Autophagy is an evolutionarily conserved catabolic process involved in many physiological and developmental processes including cell survival, cell death, and innate immunity (Yang et al, 2005; Bryant and Raikhel, 2011). The autophagic process involves a controlled rearrangement of subcellular membranes that sequester a portion of the cytoplasm and/or organelles, thereby forming the autophagosome, subsequently delivering the contents sequestered thereof to the lysosome (Chang and Neufeld, 2010). The fusion of the autophagosome with the lysosome forms the autolysosome within which the sequestered cargo is degraded to small molecules that can be recycled for macromolecular synthesis and/or energy generation. The autophagosome formation is a tightly regulated mechanism involving a series of autophagy-related (Atg) proteins encoded by *ATG* genes. The proteins are organized into complexes such as ULK1/Atg1/Atg13 protein kinase complex responsible for autophagosome initiation, the BECN1/Atg6-PIK3C3/Vps34 complex regulating the autophagosome nucleation

and the two ubiquitin-like conjugation systems: Atg12-Atg5-Atg16L1 and Atg8 conjugation systems that regulate autophagosome expansion and completion (Tian et al., 2013).

ATG genes were originally discovered in the yeast *Saccharomyces cerevisiae*, and to date 36 *ATG* genes have been characterised, 17 of which form the 'core' autophagy machinery as they are directly involved in the formation of autophagosome, (Motley et al., 2012; Cao and Klionsky, 2007). Homologues of *ATG* genes have since been identified and characterized in higher eukaryotes including mammals and insects including *Drosophila melanogaster* (Juhasz et al., 2003), *Bombyx mori* (Zhang et al., 2009; Casati et al., 2012; Tian et al., 2013), *Helicoverpa armigera* (Gai et al., 2013) and *Galleria mellonella* (Khoa and Takeda, 2012).

The induction of autophagy in insects has been studied in response to starvation and during the developmental processes such as metamorphosis. Autophagy prevents insect cells from undergoing apoptosis and necrosis under nutrient depletion conditions (Wu et al., 2010). A shift from autophagy to apoptosis was necessary for *Spodoptera litura* cells to resist infection by a baculovirus, *Autographa californica* nucleopolyhedrovirus (AcMNPV) (Wei et al., 2012). Liu et al. (2007) have also reported that autophagy precedes apoptosis in *S. litura* cells undergoing glucose starvation. An up-regulation of *ATG* genes by the steroid hormone 20-hydroxyecdysone during the molting and pupation stages has been reported in *Bombyx mori* fat body cells (Tian et al., 2013). In *Aedes aegypti*, depletion of ecdysone receptor (*EcR*) results in autophagy-incompetent female mosquitoes that fail to complete their second reproductive cycle characterized by retardation and abnormalities in egg maturation (Bryant and Raikhel 2011). Similarly, loss of function of *ATG6* homologue from *Haemaphysalis longicornis* (HIATG6) by RNAi resulted in incompetent females who lay poorly developed eggs (Kawano et al., 2011).

The role of autophagy in innate immunity of insects has received considerable attention. In *Drosophila*, the control of intracellular bacteria such as *Listeria monocytogenes* is triggered by autophagic reactions (Yano et al., 2008). Similarly, the replication of vesicular stomatitis virus (VSV) in *Drosophila* S2 cells was inhibited by autophagy. Down-regulation of *ATG* genes including *ATG1*, *ATG2*, *ATG4*, *ATG6*, *ATG7*, *ATG8*, and *ATG9* led to an increase in viral titre with time (Shelly et al. 2009). The invasion of endoparasitoid such as *Exorista bombycis* was also reported to induce autophagy in *B. mori* (Pradeep et al., 2013).

ATG3 and *ATG5* have direct role in autophagosome formation and their cellular depletion hinders the autophagic process. In *Toxoplasma gondii*, the depletion of *TgATG3* led to impaired *TgAtg8* lipidation, and subsequent autophagosome association (Besteiro, 2012). In *S. cerevisiae*, site-directed mutations in *Atg3* have been shown to severely impair *Atg8*-PE conjugation both *in vivo* and *in vitro* (Hanada et al., 2009). Similarly, cellular depletion of *ATG5* has been shown to interfere with the autophagic process. *Atg5*-dependent conversion of the mammalian homologue *Atg8-I* to *Atg8-II* inhibited the lens of 15-month-old *Atg5^{fllox/fllox}*; MLR10-Cre mutant mice leading to age-related cataract (Morishita et al., 2013). The inhibition of autolysosome formation induced by starvation has also been reported in *ATG5*-deficient mouse embryonic stem cells (Mizushima et al., 2001).

In light of the above reports, there exists no information on the role of *TmATG3* and *TmATG5* in conjunction with the survivability of *Tenebrio molitor* against bacterial infections. We isolated and characterized *ATG3* and *ATG5* homologues from the coleopteran beetle, *T. molitor*, and show that silencing of *TmATG3* and *TmATG5* by RNAi leads to reduced survivability of *T. molitor* larvae against an intracellular pathogen, *L. monocytogenes*. This is the first report on the characterization and functional relevance of *TmATG3* and *TmATG5* in *T. molitor*.

2.3 Materials and methods

2.3.1 Insect rearing and maintenance

T. molitor larvae were procured from College of Pharmacy, Pusan National University, Busan, South Korea and maintained on wheat bran meal in an environmental chamber at $26 \pm 1^\circ\text{C}$ with $60 \pm 5\%$ relative humidity and a 16:8 hrs light and dark cycle. Late-instar larvae were used for all experiments.

2.3.2 Full-length cDNA cloning and sequencing

Partial cDNA sequences of *TmATG3* and *TmATG5* were obtained from *T. molitor* expressed sequence tags (EST) and RNAseq databases previously annotated for identification and characterization of immunity-related genes (unpublished data). To obtain the full-length cDNA sequences corresponding to *TmATG3* and *TmATG5*, we performed the 5'- and 3'-rapid amplification of cDNA end (RACE) PCR. Total RNAs isolated from late instar larvae were used as templates to synthesize RACE-ready cDNA using SMARTer™ RACE cDNA amplification kit (Clontech laboratories, CA, USA) according to manufacturer's instructions. Gene-specific primers for *TmATG3* and *TmATG5* (Table 2-1) were designed based on the corresponding ESTs to clone the full-length cDNAs of both genes. Both the first and nested PCR reactions were carried out under the following conditions: initial denaturation at 94°C for 3 min. followed by 28 cycles of denaturation at 94°C for 30 s, annealing at 53°C for 30 s, extension at 72°C for 1 min and a final extension at 72°C for 10 min. The nested PCR products were resolved on 1% agarose gel at 100 V for 20 min., extracted and gel-purified by using AccuPrep Gel purification kit (Bioneer Company, Daejeon, Korea). The gene products were subsequently cloned into TOPO TA cloning vector (Invitrogen Corporation, Carlsbad, CA) and transformed into the competent *E. coli* DH5 α . Transformed DH5 α cells were sub-cultured overnight and plasmids carrying the target gene products were recovered and sequenced.

Table 2-1: Primers used in this study

Primer name	Direction	Sequence (5'-3')*
Oligo (dT) adaptor	R	GGCCACGCGTCGACTAGTACT17
M13-F	F	GTAAAACGACGGCCAG
M13-R	R	CAGGAAACAGCTATGAC
<i>TmL27a</i> sq	F	TCATCCTGAAGGCAAAGCTCCAGT
<i>TmL27a</i> sqPCR	R	AGGTTGGTTAGGCAGGCACCTTTA
<i>TmL27a</i> qPCR	F	TCATCCTGAAGGCAAAGCTCCAGT
<i>TmL27a</i> qPCR	R	GGTTGGTTAGGCAGGCACCTTTA
<i>TmATG3</i> dsRNA	F	TAATACGACTCACTATAGGGAGAGAATTTGTAGCTGCTGGAGACC
<i>TmATG3</i> dsRNA	R	TAATACGACTCACTATAGGGAGAGATGTGGGCTGAATCACTGTAG
<i>TmATG3</i> sqPCR	F	ATGCAGAACGTGATTAATAGCGTA
<i>TmATG3</i> sqPCR	R	CTAATTACTGTTAATAGTAAAATTTTGGGT
<i>TmATG3</i> qPCR	F	CAATGAGCACCACAAACCAC
<i>TmATG3</i> qPCR	R	GCATGTCTGCATGGATGAAC
<i>TmATG5</i> dsRNA	F	TAATACGACTCACTATAGGGAGACAAGACAGAGAGATGTGGTTGG
<i>TmATG5</i> dsRNA	R	TAATACGACTCACTATAGGGAGAGGTGTCCATCTTCAGAAACAGG
<i>TmATG5</i> sqPCR	F	ATGGCTAACGACAGGGAAGTTTTA
<i>TmATG5</i> sq PCR	R	TCACATCTGCACACACAAATGC
<i>TmATG5</i> qPCR	F	GGGCTGTGAATCGAAAGTTG
<i>TmATG5</i> qPCR	R	GTTTTGCGGTGTCCATCTTC

T7 Polymerase recognition sequences are indicated in bold.

F = Forward, R = Reverse.

* Sequences are read from 5' to 3' end.

2.3.3 *In silico* characterization of TmAtg3 and TmAtg5

The cDNA and deduced amino acid sequences of TmAtg3 and TmAtg5 were analyzed using InterProScan at EBI (<http://www.ebi.ac.uk/Tools/pfa/iprscan/>) and BLAST algorithm at NCBI (<http://blast.ncbi.nlm.nih.gov/>). Specific protein domains for each gene were highlighted by the InterProScan during the analysis. Amino acid sequences of TmAtg3 and TmAtg5 orthologs were obtained by performing the tBLASTn search on GenBank (<http://www.ncbi.nlm.nih.gov>) and have been summarized in Table 2-2.

Multiple sequence alignment and percentage identity analysis were performed using ClustalX2 program (Larkin et al., 2007). MEGA5 (Tamura et al., 2011) program was used to calculate corresponding percentage distances with *Atg3* and/or *Atg5* homologues from other insects. The maximum likelihood (ML) method based on the JTT matrix-based model (Jones et al., 1992) was used to generate the phylogenetic trees for *Atg3* and *Atg5* homologues using MEGA5 software.

Table 2-2: Accession numbers of Atg3 and Atg5 sequences from various insect species used to generate phylogenetic tree, percentage distance and identity matrices

Species name	Atg3		Atg5	
	abbreviation	Accession number	abbreviation	Accession Number
<i>Tribolium castaneum</i>	TcAtg3	EFA03061.1	TcATG5	XP_973840.1
<i>Drosophila melanogaster</i>	DmAtg3	XP_003695500.1	DmATG5	NP_572390.1
<i>Apis florea</i>	AfAtg3	XP_003695500.1	AfATG5	XP_003698645.1
<i>Bombus terrestris</i>	BtAtg3	XP_003392860.1	BtATG5	XP_003394334.1
<i>Bombyx mori</i>	BmAtg3	NP_001135961.1	BmATG5	NP_001135959.1
<i>Culex quinquefasciatus</i>	CqAtg3	XP_001842904.1	CqATG5	XP_001866028.1
<i>Acromyrmex echinator</i>	AeAtg3	EGI67628.1	AeATG5	EGI57478.1
<i>Aedes aegypti</i>	AaAtg3	XP_001657463.1	AaATG5	XP_001661241.1
<i>Caenorhabditis elegans</i>	CeAtg3	Y55F3AM.4a	CeATG5	WP:CE43967

2.3.4 Developmental and tissue-specific expression patterns of *TmATG3* and *TmATG5*

Total RNA was extracted from various developmental stages of *T. molitor*, including the late instar larvae (LIL), pupal day 1-7 (P1-P7) and adult day 1 and 2 (A1 and A2). For analysis of spatial expression patterns, Total RNA was extracted from various tissues including gut (whole gut), hemocytes, integument, Malphigian tubules, fat body of the late instar larvae, and ovaries and testes of the adult stage using SV Total RNA isolation system (Promega Corporation, Madison, WI) according to manufacturer's protocol. First-strand cDNA corresponding to each stage of development and/or each tissue sampled was synthesized using AccuPowerR RT PreMix kit (Bioneer, Daejeon, Korea). cDNAs were used as templates for quantitative PCR (qPCR) reactions performed on an Exicycler™ 96 real-time quantitative thermal block (Bioneer, Korea) with gene specific primers (Table 2-1) at an initial denaturation of 95°C for 20 s, followed by 45 cycles of denaturation at 95°C for 5 s and annealing at 60°C for 20 s. The $2^{-\Delta\Delta C_t}$ method was employed to analyze the expression levels of *TmATG3* and *TmATG5*. *TmL27a* was used as an internal control to normalize differences in concentration of templates.

2.3.5 dsRNA synthesis and injection

TmATG3 and *TmATG5* DNA fragments were amplified by PCR from cloned cDNA using gene-specific primers tailed with a T7 promoter sequence (Table 2-1). The PCR products were purified using the AccuPrep PCR purification kit (Bioneer, Daejeon, South Korea) and used to synthesize the double-stranded RNA (dsRNA) with an Ampliscribe™ T7-Flash™ transcription kit (Epicentre Biotechnologies, Madison, WI, USA). dsRNA was purified and precipitated using 5M ammonium acetate. The integrity of the purified dsRNA was confirmed by running 1% agarose gel and quantified using NanoDrop spectrophotometer (Thermo

Scientific, Wilmington, DE, USA). dsRNAs were stored at -20°C until injected into *T. molitor* larvae. dsRNA for *EGFP* (ds*EGFP*) was synthesized and injected to serve as negative control.

ds*TmATG3*, ds*TmATG5* or ds*EGFP* (1 µg/larva) were dissolved in injection buffer (0.1 mM sodium phosphate, 2.5 mM potassium chloride, pH 7.2) (Fabrick et al., 2009) and injected into the hemocoel of the larvae (n = 55) at the 2nd or 3rd visible sternite. The injections were carried out using disposable needles mounted onto a micro-applicator (Picospirtizer III micro dispense system, Parker Hannifin, Hollis, NH, USA). Animals treated with dsRNAs were maintained on wheat bran meal under standard rearing conditions until the extraction of total RNA.

To analyze knockdown levels of *TmATG3* and *TmATG5*, total RNA was isolated from larvae 5 days after dsRNA injection. Subsequent cDNA synthesis was conducted as described above. cDNA was used as a template for semi-quantitative PCR with the gene-specific primers (Table 2-1). The PCR cycles were performed as follows: initial denaturation at 94°C for 3 min. followed by 28 cycles of denaturation at 94°C for 30 s, annealing at 55°C for 30 s, extension at 72°C for 60 s and a final extension at 72°C for 10 min. in a PTC-200 thermal cycler (MJ Research, GMI, Minnesota, USA). Ribosomal protein-L27A (*TmRPL27a*) was used as a positive control and amplified using RPL27a primers (Table 3-1). Quantitative real-time PCR was performed on Exicycler™ 96 real-time quantitative thermal block (Bioneer, Korea).

2.3.6 Bacterial injections and bioassays

Listeria monocytogenes strain ATCC 7644 used in this study was directly procured from the American Type Culture Collection (ATCC). Brain-heart infusion (BHI) medium was used to grow the bacterium used for the multiplication and colony forming unit (CFU) determination studies.

To obtain the *L. monocytogenes* culture for infection studies, a single colony was picked from a BHI agar plate using a sterile wire loop and inoculated into 5 ml of fresh BHI broth in 10 ml round-bottomed culture tube. The tube was incubated overnight under aerobic conditions in an orbital shaker at 200 revolutions per minute (rpm) and 37°C. The overnight cultures were washed thrice, re-suspended and serially diluted in 0.9% saline (NaCl) to achieve desired concentrations determined by measurements at OD₆₀₀. The OD₆₀₀ values were confirmed by aseptically spread-plating the serially diluted samples on BHI agar plates. The plates were incubated at 37°C for 16 h prior to colony counting.

For survival studies, dsRNA (1 µg/larva) of *TmATG3* or *TmATG5* was injected into the hemocoel of the larvae (n = 55) at the 2nd or 3rd visible sternite as described above. Five days post-injection of dsRNA, 30 larvae in each group were challenged with 2 µl (~10⁶ cells/larva) of the diluted cultures of *L. monocytogenes*. The injected larvae were maintained at 26°C and the number of dead larvae was recorded on a daily basis for 6 days post injection. Rates of survival were compared between the ds*TmATG3* or ds*TmATG5* and ds*EGFP* (control) groups.

2.3.7 Statistical analysis

Data from insect survival study was analyzed by the Wilcoxon-Mann Whitney test (Yano et al., 2008) of the cumulative survival rates (%) and a *p-value* < 0.05 was considered significant.

2.4 Results

2.4.1 Characterization of full-length cDNA for *TmATG3* and *TmATG5*

The partial cDNA sequences of *TmATG3* and *TmATG5* were identified from *T. molitor* EST library and RNAseq data. The full-length cDNA sequences of *TmATG3* and *TmATG5* genes were obtained by RACE PCR. The deduced amino acid sequences were designated as TmAtg3 and TmAtg5 for *TmATG3* and *TmATG5* genes, respectively.

The full length cDNA of *TmATG3* is comprised of an open reading frame (ORF) of 963 bp that encodes a protein of 320 amino acid residues (Fig. 2-1A) with a predicted molecular weight of 36.4 kDa and a theoretical pI of 4.57. The 5'- and 3'- untranslated region (UTR) of *TmATG3* comprise of 93 and 213 bp, respectively. The polyadenylation signal (AATAA) was located 108 bp downstream of the termination codon. *TmATG3* cDNA sequence has been deposited in the GenBank under accession number KF670693. Analysis of *TmATG3* deduced amino acid sequence indicates that it has three characteristic domains namely, the N-terminal domain, the catalytic (autophagy-related protein 3) domain and the C-terminal domain (Fig. 2-1A). The N-terminal domain comprises of 149 amino acid residues and extends from amino acids at the 8 - 156 positions. The catalytic domain of TmAtg3 comprises of 63 amino acid residues that spans amino acids at the 205 - 268 positions. A cysteine residue within the conserved 'HPC' motif is the putative active-site residue for recognition of the Apg5 subunit of the autophagosome complex. The C-terminal domain of TmAtg3 consists of 45 amino acid residues and extends from amino acids at 269 - 313 positions. The highly conserved 'FLKF' sequence motif characteristic of Atg3 C-terminal domain was also found.

The full length cDNA of *TmATG5* includes an ORF of 792 bp that encodes a protein of 263 amino acids (Fig.2-2) with a predicted molecular weight of 31.6 kDa and a theoretical pI of 5.58. The 5'and 3'-UTR for *TmATG5* are composed of 47 and 357 bp, respectively. The

polyadenylation signal is located 336 bp downstream of the termination codon (Fig.2-1B). The *TmATG5* cDNA sequence has been deposited in the GenBank under accession number KF670694. An analysis of TmAtg5 deduced amino acid sequence reveals an autophagy-related protein-5 domain that is made up of 183 amino acid residues at 41 -223 positions (Fig.1B).

TmATG3 shares highest sequence identity of 95% with *TcATG3* (Fig. 2-2) followed with those of a dipteran *Aedes aegypti* (74%) and hymenopteran insects *Apis florea* (73%) and *Bombus terrestris* (72%). These observations were further validated by performing the distance matrix analysis. *TmATG3* was placed at a distance of 4% from *TcATG3*.

TmATG5 shared high sequence identity with *T. castaneum ATG5* (93%) followed by the orthologs from *A. florea* (70%) and *B. terrestris* (69%). The percentage distances were recorded to be 7, 36 and 30% from *T. castaneum*, *A. florea* and *B. terrestris*, respectively, (Fig. 2-2). The percentage identity and distance analyses indicated that *TmATG3* and *TmATG5* genes were phylogenetically closest to orthologs from another coleopteran beetle, *T. castaneum*.

To determine the evolutionary position of TmAtg3 and TmAtg5 within their respective orthologous groups, Maximum Likelihood phylogenetic trees were reconstructed. Amino acid sequences of ScAtg3 and ScAtg5 from the fungus, *Saccharomyces cerevisiae*, were used as outgroup for the Atg3 and Atg5 phylogenetic trees, respectively. Consequently, TmAtg3 and TmAtg5 were grouped with counterparts from *T. castaneum* namely, TcAtg3 and TcAtg5, respectively (Fig.2- 3).

TA TGA CAG AGT AGT TGT TAA TGT TTT GTG TTA GAA TTA ATG TAA AAT	
ATG GCT AAC GAC AGG GAA GTT TTA CGA GAG GTT TGG GAG GGT AAA CTA CCC ATT TCG TTT	60
M A N D R E V L R E V W E G K L P I S F	20
CAC CTG GAT TCA GAT GAA GTT GTC GAA TTA CAA CAA CCA GAT CCA TTT TAT TTA ATG GTA	120
H L D S D E V V E L Q Q P D P F Y L M V	40
CCC CGT TTA AGT TAT TTT CCT TTG GTT ACT GAT AAA GTT CGT AAG CAT TTC TTG CGC TAT	180
P R L S Y F P L V T D K V R K H F L R Y	60
GTC ACT AAT GAT AAA CAA GAC AGA GAG ATG TGG TTG GAA TAT GAT GGT CAG CCC ATT AAA	240
V T N D K Q D R E M W L E Y D G Q P I K	80
TGG CAT TAT CCC ATA GGT GTT CTT TTC GAT TTA CTC ATT ACT TCT GAT GAT CAA CTG CCA	300
W H Y P I G V L F D L L I T S D D Q L P	100
TGG AAT ATT ACC GTG CAT TTT GAT AAG TTT CCA GAA AAT CAA ATC TAC AAG TTT AAT AAT	360
W N I T V H F D R F P E N Q I Y K F N H	120
AAA GAA ACA GTT GAG TCC TAT TTC ATG GCA TGT TTG AAG GAA GCA GAT GTG TTA AAA CAT	420
K E T V E S Y F M A C L K E A D V L K H	140
AGA GGG CAA ATT GCT AGT AAC ATG CAG AAA AAA GAC CAG AAT CAG TTG TGG TTA GGT TTG	480
R G Q I A S N M Q K K D E N Q L W L G L	160
CAA AAT GAC AAA TTT GAA CAA TTT TGG GCT GTG AAT CGA AAG TTG ATG GAA GTC TCA TCA	540
Q N D K F E Q F W A V N R K L M E V S S	180
GAA CAA GAA TAC TTC AAA TAC AAT CCT TTT AGA TGT TAC ATA GAT GAT GGT TAC AGA CAG	600
E Q E Y F K Y I P F R C Y I D D G Y R Q	200
AAA TTA ATT AAG CCT GGT TCT GAA CAT GGA CAG CGC AAA ACT TTA CAA GAC TTA ATA AAT	660
K L I K P V S E D G H R K T L Q D L I N	220
GAA ATG TTT CCT GGG AAA GAG AAT AGC ATT AAA ACA CAT GGA ATG ATT CCT CCC TTA GAG	720
E M F P G K D I S E K T H G M I P P L K	240
ACA CCT CTT CAA TGG ATG TCT GAG CAT CTC AGT TAT CCT GAT AAC TTC CTG CAT TTG TGT	780
T P L Q W M S E H L S Y P D N F L H L C	260
GTG CAG ATG TGA	792
V Q N *	263
TGA AGC TTT TGT GTG ATA ATG TAA AAG GAC TCT ATA TTT ATT GCC TTC ATT TAA TGT GAA	
ACT CTT ATA AAT AGG TGC CCA ATT TAA AAG CAA TTT TTT TTT ATC TTG TAG GTA TCA ATA	
ATT TCA AAT GAT CAA ATA TAA ATA TGG AGA TGT ACT GTC ATA TTG ACT TTG TCA TAA AAT	
GTA TTT TCT TTA ATT GTA ATA GAA TTC TTC AGT CTG AAG TGT TTG CTA AAA GAC GTG AAT	
TTC AGT GGA CTT AAT TTG TAA TCT ATA GTA ATA TGA TGC AAT GTT TTA TTA AAA TTC ATA	
TAC TTA TAA TTT TAT ATT CAA TGT AGA TGC TAT AAA AAT AAA ACT ACT ATT TAA TGC AAA	
AAA AAA AAA AAA AAA AAA AAA A	

Figure 2-1B: Nucleotide and deduced amino acid sequences of *TmATG5*.

Full-length *TmATG5* cDNA and deduced amino acid sequence. Gray-highlighted sequence represents the autophagy-related protein 5 domain. Underline indicates polyadenylation signal sequence (AATAAA).

		Atg3								Atg5										
		Tm	Tc	Dm	Af	Bt	Bm	Cq	Ae	Aa	Tm	Tc	Dm	Af	Bt	Bm	Cq	Ae	Aa	
Atg3	Tm	95	65	73	72	69	68	74	68	10	10	10	9	10	12	13	10	12	% Identity	
	Tc	0.04	66	74	73	69	69	74	69	10	10	11	9	10	12	12	11	12		
	Dm	0.41	0.39	66	67	69	77	68	79	10	10	11	9	9	11	11	10	11		
	Af	0.28	0.24	0.37	96	70	72	86	69	11	10	11	9	10	11	11	10	10		
	Bt	0.29	0.26	0.36	0.04	70	71	86	69	11	10	11	9	10	11	11	10	10		
	Bm	0.32	0.32	0.31	0.31	0.31	70	69	72	12	10	11	10	10	13	12	11	11		
	Cq	0.36	0.34	0.19	0.31	0.31	0.31	71	88	11	11	12	9	10	12	12	11	13		
	Ae	0.28	0.28	0.38	0.15	0.15	0.34	0.33	70	11	10	11	9	10	12	11	10	11		
	Aa	0.35	0.33	0.18	0.32	0.31	0.29	0.10	0.32	12	11	12	10	10	12	13	11	12		
Atg5	Tm	2.29	2.34	2.25	2.17	2.17	2.13	2.10	2.21	2.06	0.07	60	70	69	64	58	68	64		
	Tc	2.34	2.38	2.34	2.34	2.34	2.25	2.17	2.38	2.13	0.54	0.54	60	69	65	59	68	64		
	Dm	2.25	2.25	2.29	2.25	2.25	2.21	2.10	2.29	2.06	0.36	0.37	0.60	56	55	59	56	63		
	Af	2.38	2.43	2.54	2.38	2.38	2.34	2.34	2.43	2.29	0.37	0.38	0.62	0.03	97	63	56	88		62
	Bt	2.34	2.38	2.54	2.34	2.34	2.29	2.29	2.38	2.25	0.47	0.46	0.53	0.47	0.47	63	56	88		61
	Bm	2.13	2.17	2.21	2.13	2.13	2.06	2.03	2.13	2.03	0.57	0.56	0.59	0.62	0.61	0.55	58	63		66
	Cq	2.06	2.13	2.25	2.13	2.13	2.06	2.03	2.17	2.00	0.39	0.39	0.59	0.12	0.13	0.45	0.60	57		85
	Ae	2.29	2.29	2.48	2.34	2.34	2.25	2.25	2.38	2.21	0.47	0.46	0.48	0.50	0.52	0.42	0.17	0.50		62
	Aa	2.10	2.17	2.25	2.25	2.25	2.13	2.03	2.21	2.00										

Figure 2-2: Percentage distance and identity matrix of Atg3 and Atg5 from *Tenebrio molitor*.

Sequences of all insect species used in the analysis are presented in Table 2-2. *TmAtg3* and *TmAtg5* shared the highest percentage (%) identity with their orthologs in *T. castaneum*, *TcAtg3* and *TcAtg5*, respectively. The % identity results are highly supported by the % distance results which put *TmAtg3* and *TmAtg5* at 4 and 7% from their *T. castaneum* counterparts, *TcAtg3* and *TcAtg5*, respectively. The % identity between *Atg3*s and *Atg5*s are very low ranging from 9 to 13%.

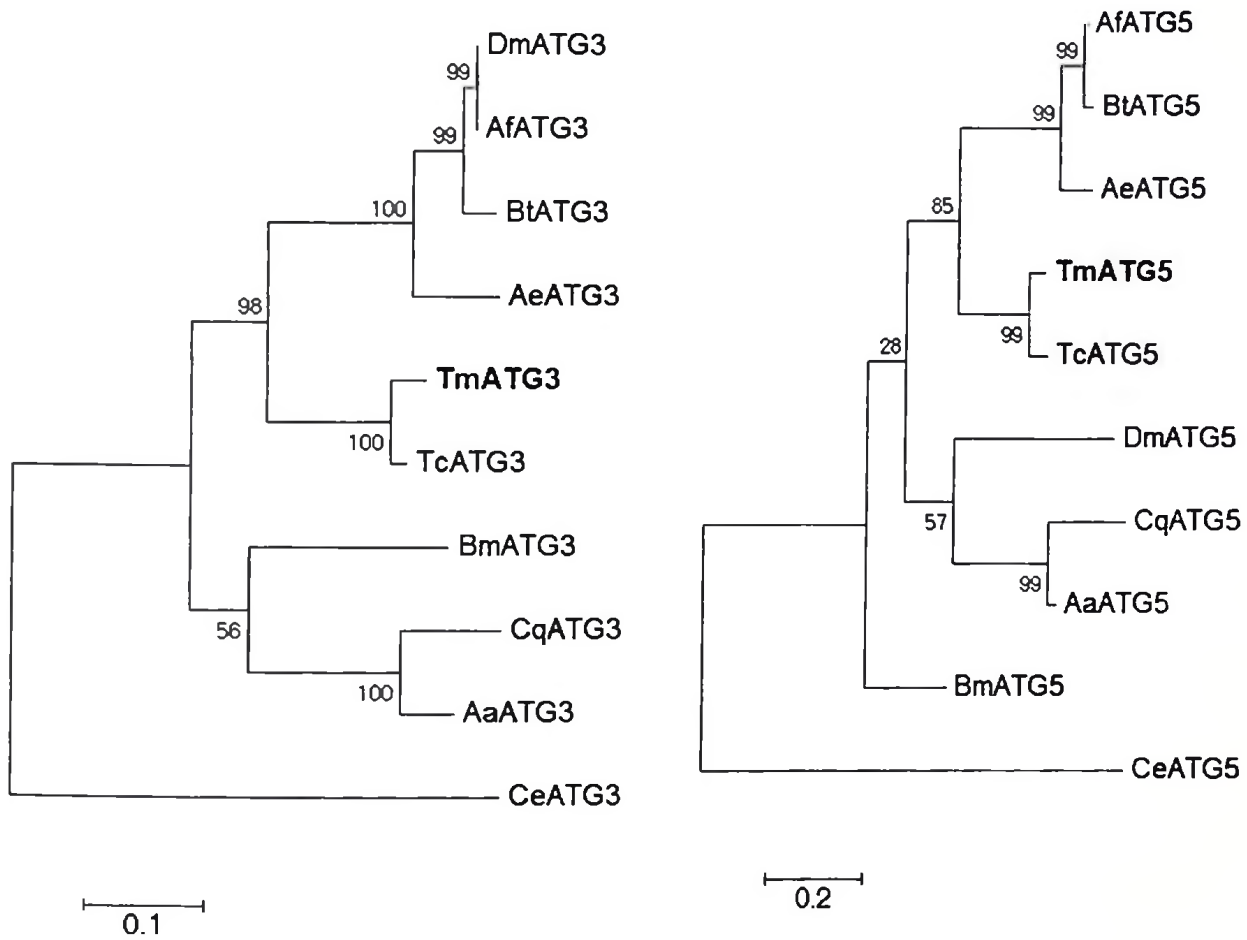


Figure 2-3: Molecular phylogenetic analysis of *ATG3* and *ATG5* from *Tenebrio molitor*.

Phylogenetic trees for *Atg3* (left) and *Atg5* (right) were generated using MEGA5 program. The evolutionary history of each tree was inferred using the maximum likelihood method based on the Jones Taylor Thornton (JTT) matrix-based model. *TcAtg3* and *TcAtg5* presented the phylogenetically closest counterparts of *TmAtg3* and *TmAtg5*, respectively. The accession numbers of all sequences of insect species used to create the trees are enlisted in Table 2-2.

2.4.2 Developmental and tissue-specific expression patterns of *TmATG3* and *TmATG5*

In order to understand the biological role of *TmATG3* and *TmATG5* genes in *T. molitor*, the mRNA expressions in late developmental stages and different tissues were investigated by real-time PCR. *TmATG3* transcripts were detected in all developmental stages examined (Fig. 2-4A). The transcripts of *TmATG3* were also detected in all tissues examined including Malphigian tubules, integument, gut, fat body, hemocytes, ovaries and testes with slightly elevated transcript levels in fat body and hemocytes (Fig.2-4B).

Similarly, *TmATG5* transcripts were detected in all developmental stages examined (Fig. 2-4C.) *TmATG5* transcripts were also detected in all tissues examined with slightly higher transcript levels in the fat body and hemocytes (Fig. 2-4D).

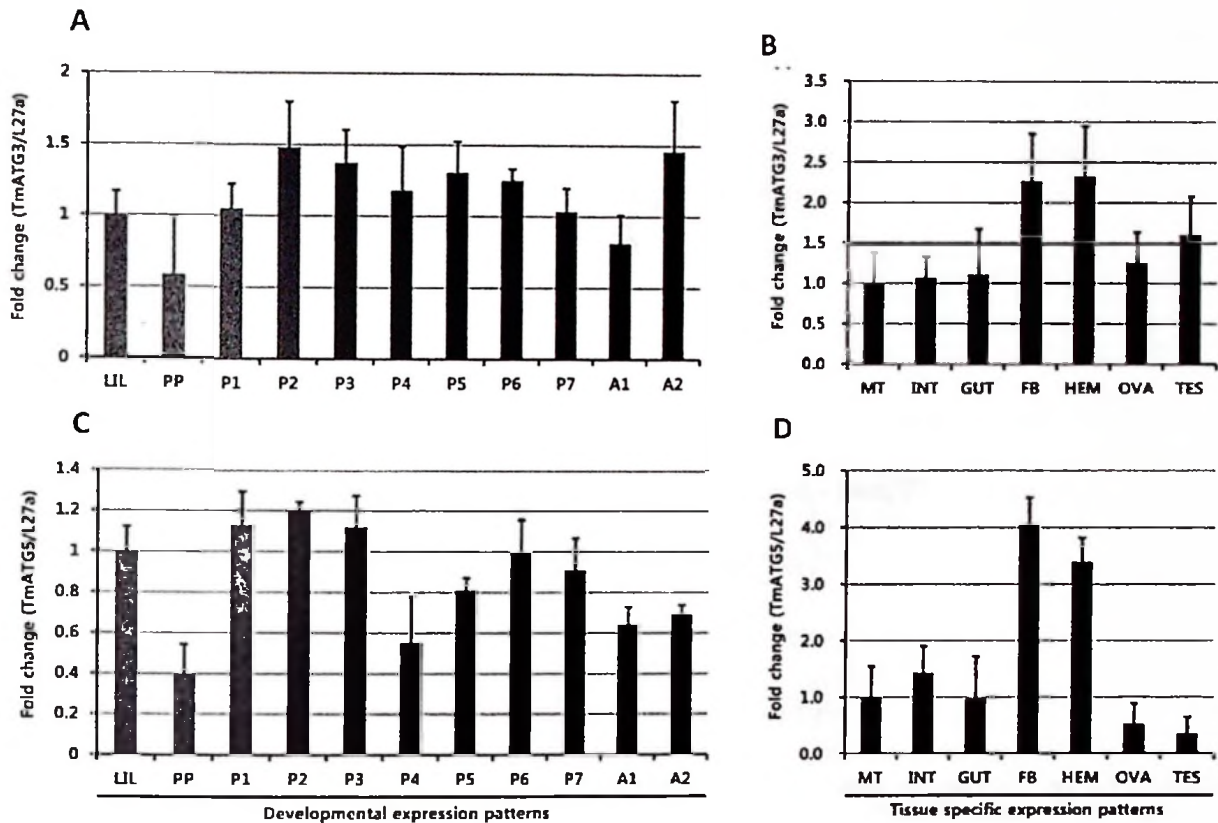


Figure 2-4: Developmental and tissue-specific expression patterns of *TmATG3* and *TmATG5*.

Transcripts at all developmental stages and tissues examined were amplified and quantified by the real-time PCR. Top: Developmental and tissue-specific expression patterns of *TmATG3* respectively are shown (A and B). Bottom: Developmental and tissue-specific expression patterns *TmATG5*, respectively are also shown (C and D). MT, INT, FB, HEM, OVA and TES represent Malphigian tubules, integument, fat body, hemocytes, ovaries and testes, respectively. LIL, PP, P1-P7 and A1 and A2 represent late-instar larvae, pharate pupa, pupa day 1-7 and adult day 1 and day 2, respectively. Data are shown as the mean \pm standard deviation (n = 3).

2.4.3 Loss of functions of *TmATG3* and *TmATG5* by RNAi resulted in high mortality of *T. molitor* larvae against *L. monocytogenes*.

Insects are known to deploy autophagy in response to infections by intracellular pathogens including *L. monocytogenes*. We have used *L. monocytogenes* as an infection agent to challenge the *T. molitor* larvae. This is partly because it is known to be a convenient model bacterium used in studying intracellular pathogen-host interactions, especially in autophagic reactions of the host including mammals (Birmingham; Lam et al., 2012) and insects (Yano et al., 2008; Joyce and Gahan, 2010; Cheng, and Portnoy, 2003). We hypothesized that depletion of the mRNAs of *TmATG3* or *TmATG5* by RNAi would lead to compromised ability of *T. molitor* larvae in combating the infection. This could have an impact on the overall survivability of the larvae. Using RNAi, *TmATG3* and *TmATG5* transcripts levels were decreased by 70 and 60%, respectively, in the late-instar larvae of *T. molitor* (Fig. 2-5A). Subsequently, the larvae were challenged with a lethal dose (10^6 CFU/larva) of *L. monocytogenes*. We observed a significant ($p < 0.05$) reduction in the survival rates of *T. molitor* larvae relative to the control (dsEGFP) (Fig. 2-5B). At the end of the observation period (six days post infection), the survival rate in control set of larvae were found to be significantly higher (55%) as compared with 4% and 3% for ds*TmATG3*- and ds*TmATG5* -injected larvae, respectively. The observations were found to be similar for three separate sets of experiments.

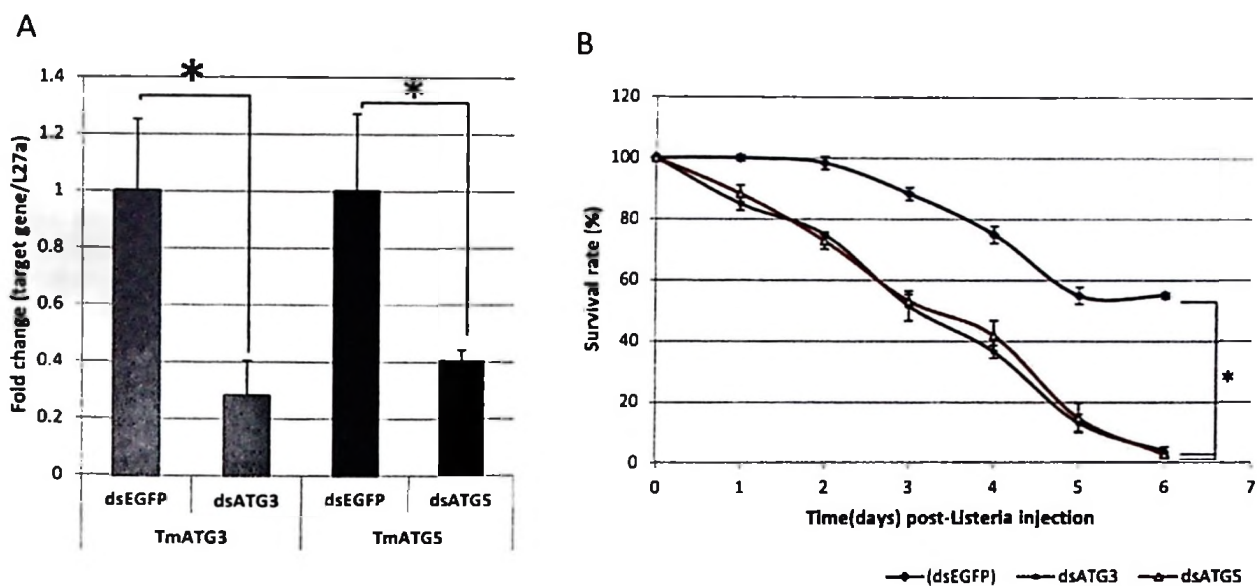


Figure 2-5: Effect of *TmATG3* and *TmATG5* gene silencing on survivability of *T. molitor* larvae.

(A) Down-regulation of *TmATG3* and *TmATG5* transcripts by the RNA interference. Transcript levels were reduced by 70 and 60% for *TmATG3* and *TmATG5*, respectively prior to challenge by *L. monocytogenes* (B). Survival curves of *T. molitor* larvae infected with *L. monocytogenes* following down-regulation of *TmATG3* or *TmATG5* mRNA transcripts. At the end of the experimental period (6 days post-infection), the survival rates of larvae were 3% and 4%, respectively, in *TmATG3* and *TmATG5*-depleted larvae compared to 55% in the dsEGFP control group. “*” shows significant ($p < 0.05$) difference. Data are shown as the mean \pm standard deviation ($n = 3$).

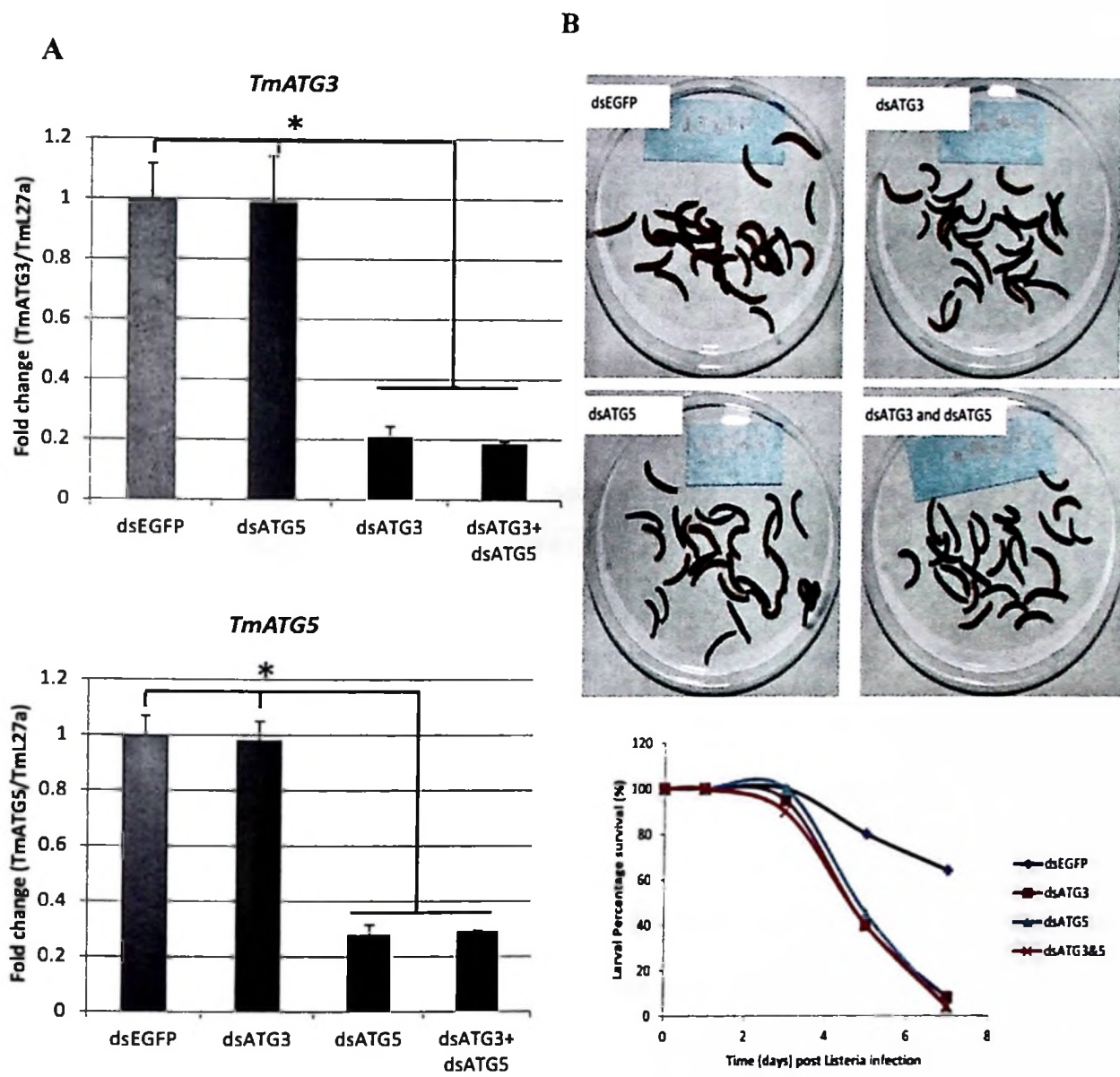


Figure 2-6: Effect of double knockdown of *TmATG3* and *TmATG5* genes on survival of *Tenebrio* larvae.

(A) Real-time PCR results showing double knockdown of *TmATG3* and *TmATG5* by co-injection of ds*TmATG3* and ds*TmATG5* to *Tenebrio* larvae. (B) Upper: photos showing status of larval survival at day 7 post-*Listeria* infection. Lower: Curves quantifying the survival of larvae at the same period of time. Notably, double *TmATG3* and *TmATG5* RNAi did not result in additive effects on survival. “*” indicate significant ($p < 0.05$) difference between means. Statistical bars indicate mean \pm standard deviation three independent experiments.

2.5 Discussion

Atg3 and Atg5 have been reported to perform distinct yet interconnected functions in the eukaryotic autophagy pathway. While the E-2 ubiquitin-like enzyme Atg3 is responsible for the covalent binding of phosphatidylethanolamine to the C-terminal Gly of Atg8, the Atg12-Atg5 conjugate is known to act as an E-3 enzyme, primarily by stimulating the conjugating activity of Atg3 (Hanada et al., 2007). In the current study *Tenebrio* homologues of the two genes have been identified, their corresponding cDNAs cloned and partially characterized.

The catalytic domain of TmAtg3 contains a conserved cysteine residue within the 'HPC' motif. Conservation of this residue is a characteristic feature of autophagic E2-like enzymes including Atg3 and Atg10 homologues from various eukaryotic hosts (Flanagan et al., 2013). Conserved cysteine residue has been identified in amino acid sequences of homologues in *Homo sapiens*, *Arabidopsis thaliana* and *S. cerevisiae* (Yamada et al., 2007). Cysteine is the only active site residue that is universally conserved in the wider spectrum of E-2 and E-2-like enzymes in eukaryotes (Burroughs et al., 2008; Flanagan et al., 2013).

The wide-spread tissue-specific expression of *TmATG3* and *TmATG5* observed in the current study may indicate that the two genes are probably involved in various cellular processes such as autophagy-mediated nutrient recycling, disposal of damaged cellular organelles and clearance of infectious agents (Yang et al, 2005; Bryant and Raikhel, 2011). Earlier reports have shown roles of *ATG3* and *ATG5* in development in *Haemaphysalis longicornis* (Kawano et al., 2010; Hu et al., 2011), starvation stress response in *Spodoptera litura* SL-ZSU-1 cells (Wu et al., 2010; Liu et al., 2007) and defense against pathogenic infections in *Drosophila melanogaster* (Shelly et al., 2009). In addition, RNAi for the gene encoding 20-hydroxyecdysone receptor partner (USP) in *Bombyx mori*, resulted in reduced autophagy stemming from down-regulation

in expression of several *ATG* genes including *ATG3* and *ATG5* during pupation, thus, confirming the involvement of *ATG3* and *ATG5* in insect development (Tian et al., 2013).

The reduced survivability of *T. molitor* larvae against *L. monocytogenes* infection following down-regulation of *TmATG3* and *TmATG5* indicate that the two genes may be directly deployed to counter *Listeria* infections in the beetle probably through their roles in the autophagy pathway. In general, these results are consistent with previous reports that RNAi-based down-regulation of autophagy-related genes compromises the ability of the host to resist the infection (Yano et al., 2008; Shelly et al. 2009). Autophagic reaction against intracellular infections are induced or regulated through the action of specific pathogen-recognition receptors (PRR) such as *PGRP-LE*, *Toll-7* and/or *TLRs*. Blocking or interfering the activity of these upstream PRRs produce effects similar to those observed when canonical autophagy-related genes like *ATG5* are interfered by techniques such as RNAi. In *Drosophila*, intracellular *PGRP-LE* was responsible for the induction of autophagic control of *L. monocytogenes* (Yano et al., 2008). Down-regulation of hemocyte-specific *DmPGRP-LE* by RNAi in adult flies exhibited a significant reduction in survival rate against *L. monocytogenes* in a manner similar to flies whose autophagy gene *ATG5* expression was depleted by RNAi. While working with *Toll-7*, one of the many members of the *Drosophila* Toll family, Nakamoto et al. (2012) demonstrated that infection of *Drosophila* cultured cells by vesicular stomatitis virus (VSV) provoked an antiviral autophagic response regulated by *Toll-7*. The authors demonstrated further that loss of function of *ATG5* in *Drosophila* adult flies led to a blockage of the characteristic puncta formation effectively arresting the autophagic response of the fly against the infection.

In conclusion, we have in the present study, isolated homologues of *ATG3* and *ATG5* from the coleopteran *T. molitor*, designated as *TmATG3* and *TmATG5*, respectively, from

Tenebrio EST and RNAseq databases. We subsequently characterized the full-length cDNA sequences of *TmATG3* and *TmATG5*. The expression profiles of *TmATG3* and *TmATG5* transcripts in different developmental stages and tissues examined indicate that the genes are ubiquitously expressed, suggesting their roles in growth, development and innate immunity. Reduction in survival ability of the larvae following depletion of transcripts of *TmATG3* and *TmATG5* underscored the general role of autophagy as a reaction mechanism of the host against infection by *L. monocytogenes*. Currently, our on-going studies have been focused on the experimental insights that would link intracellular microbial pathogen titer values to autophagosome formation and the signaling cascades that lead to autophagic control of the pathogen in *T. molitor*.

2.6 References

- Ahlberg J, Berkenstrafm A, Hennell F, Glaumann H. 1985. Degradation of short and long-lived proteins in isolated rat liver lysosomes, effects of pH, temperature and proteolytic inhibitor. *J. Biol. Chem.* 260: 5847-5854.
- Besteiro S. 2012. Role of ATG3 in the parasite *Toxoplasma gondii*. Autophagy in an early branching eukaryote. *Autophagy*, 8 (3): 435–437.
- Birmingham CL, Canadien V, Gouin E, Troy EB, Yoshimori T, Cossart P, Higgins DE, Brumell JH. 2007. *Listeria monocytogenes* evades killing by autophagy during colonization of host cells. *Autophagy*. 3(5): 442-51.
- Bryant B, Raikhel AS. 2011. Programmed autophagy in the fat body of *Aedes aegypti* is required to maintain egg maturation cycles. *PLoS ONE* 6(11):e25502.
- Burroughs AM, Jaffee M, Iyer LM, Aravind L. 2008. Anatomy of the E2 ligase fold: implications for enzymology and evolution of ubiquitin/Ub-like protein conjugation. *J. Struct Biol.* 162(2): 205–218.
- Casati B, Terova G, CattaneoAG, Rimoldi S, Franzetti E, Eguileor MD, Tettamant G. 2012. Molecular cloning, characterization and expression analysis of ATG1 in the silkworm, *Bombyx mori*. *Gene*. 511: 326–337.
- Chang YY, Neufeld T.P. 2010. Autophagy takes flight in *Drosophila* *FEBS Lett.* 584: 1342-1349.

- Cheng L W, Portnoy DA. 2003. *Drosophila* S2 cells: an alternative infection model for *Listeria monocytogenes*. *Cell Microbiol.* 5: 875–885.
- Fabrick J, Oppert C, Lorenzen MD, Morris K, Oppert B, Jurat-Fuentes JL. 2009. A Novel *Tenebrio molitor* Cadherin Is a Functional Receptor for *Bacillus thuringiensis* Cry3Aa Toxin. *J Biol Chem.* 284(27):18401–18410.
- Flanagan MD, Whitehall SK, Morgan BA, 2013. An Atg10-like E2 enzyme is essential for cell cycle progression but not autophagy in *Schizosaccharomyces pombe*. *Cell Cycle* 12(2): 271–277.
- Gai Z, Zhang X, Islam M, Wang X, Li A, Yang Y, Li Y, Peng J, Hong H, Liu K. 2013. Characterization of atg8 in lepidopteran insect cells. *Arch. Insect Biochem. Physiol.* 00(0): 1–21.
- Hanada T, Satomi Y, Takao T, Ohsumi Y. 2009. The amino-terminal region of Atg3 is essential for association with phosphatidylethanolamine in Atg8 lipidation. *FEBS Letters* 583:1078–1083.
- Hershko A, Ciechanover A. 1998. The ubiquitin system. *Annu. Rev. Biochem.* 67: 425–479.
- Hoffman M, Chiang ML. 1996. Isolation of Degradation-Deficient Mutants Defective in the Targeting of Fructose-1,6-bisphosphatase into the Vacuole for Degradation in *Saccharomyces cerevisiae*. *Genetics.* 143(4):1555–1566.
- Hu Z, Zhang J, Zhang Q. 2011. Expression pattern and functions of autophagy-related gene atg5 in zebrafish organogenesis. *Autophagy.* 7(12): 1514–1527.

- Jones DT, Taylor WR, Thornton JM. (1992). The rapid generation of mutation data matrices from protein sequences. *Comp. Applic. Biosc.* 8:275-282.
- Joyce SA, Gahan CGM. 2010. Molecular pathogenesis of *Listeria monocytogenes* in the alternative model host *Galleria mellonella*. *Microbiology.* 156:3456–3468.
- Juhasz G, Csikos G, Sinka R, Erdelyi M, Sass M. (2003). The *Drosophila* homolog of Aut1 is essential for autophagy and development. *FEBS Lett.* 543:154-158.
- Kawano S, Umemiya-Shirafuji R, Boldbaatar D, Matsuoka K, Tanaka T, Fujisaki K. 2011. Cloning and characterization of the autophagy-related gene 6 from the hard tick, *Haemaphysalis longicornis*. *Parasitol. Res.* 109:1341–1349.
- Khoa DB, Takeda, M. 2012. Expression of autophagy 8 (Atg8) and its role in the midgut and other organs of the greater wax moth, *Galleria mellonella*, during metamorphic remodeling and under starvation. *Insect Molecul. Biol.* 21(5):473–487.
- Lam GY, Czuczman MA, Higgins DE, Brumell JH. 2012. Chapter 2 – Interactions of *Listeria monocytogenes* with the Autophagy System of Host Cells. *Adv. Immunol.* 113: 7–18.
- Larkin MA, Blackshields G, Brown NP, Chenna R, McGettigan PA, McWilliam H, Valentin F, Wallace IM, Wilm A, Lopez R, Thompson JD, Gibson TJ, Higgins DG. (2007) Clustal W and Clustal X version 2.0. *Bioinformatics* 23: 2947-2948.
- Liu K, Tang Q, Fu C, Peng J, Yang H, Li Y, Hong H. 2007. Influence of glucose starvation on the pathway of death in insect cell line SI: apoptosis follows autophagy. *Cytotechnology.* 54: 97–105.

- Mizushima N, Yamamoto A, Hatano M, Kobayashi Y, Kabeya Y, Suzuki K, Tokuhiya T, Ohsumi Y, Yoshimori T. 2001. Dissection of Autophagosome Formation using Apg5-deficient Mouse Embryonic Stem Cells. *J. Cell Biol.* 152: 657-68.
- Morishita H, Eguchi S, Kimura H, Sasaki J, Sakamaki Y, Robinson ML, Sasaki T, Mizushima N. 2013. Deletion of Autophagy-related 5 (Atg5) and Pik3c3 Genes in the Lens Causes Cataract Independent of Programmed Organelle Degradation. *J. Biol. Chem.* 288(16): 11436–11447.
- Nakamoto M, Moy RH, Xu J, Bambina S, Yasunaga A, Shelly SS, Gold B, Cherry S. 2012. Virus Recognition by Toll-7 Activates Antiviral Autophagy in *Drosophila*. *Immunity* 36:658–667.
- Pradeep AN, Anitha J, Awasthi AK, Babu, MA, Geetha MN, Arun HK, Chandrashekhar S, Rao GC, Vijayaprakash NB. (2013) Activation of autophagic programmed cell death and innate immune gene expression reveals immuno-competence of integumental epithelium in *Bombyx mori* infected by a dipteran parasitoid. *Cell Tissue Res.* 352(2): 371-85.
- Scott SV, Hefner-Gravink A, Morano A, Noda T, Ohsumi Y, Klionsky DJ. 1996. Cytoplasm-to-vacuole targeting and autophagy employ the same machinery to deliver proteins to the yeast vacuole. *Proc. Natl. Acad. Sci. USA.* 93:12304–12308.
- Scott SV, Guan J, Hutchins MU, Kim J, Klionsky DJ. 2001. Cvt19 Is a Receptor for the Cytoplasm-to-Vacuole Targeting Pathway. *Mol Cell.* 7(6):1131–1141.

- Shelly S, Lukinova N, Bambina S, Berman A, Cherry S. (2009). Autophagy is an essential component of *Drosophila* immunity against vesicular stomatitis virus. *Immunity*. 30(4):588-598 .
- Shieh PB, Hu SC, Bobb K, Timmusk T, Ghosh A. 1998. Identification of a signaling pathway involved in calcium regulation of BDNF expression. *Neuron* 20: 727–740.
- Tamura K, Peterson D, Peterson N, Stecher G, Nei M, Kumar S. 2011. MEGA5: Molecular Evolutionary Genetics Analysis using Maximum Likelihood, Evolutionary Distance, and Maximum Parsimony Methods. *Molecular Biology and Evolution* 28: 2731-2739.
- Tian L, Ma L, Guo E, Deng X, Ma S, Xia Q, Cao Y, Li S. 2013. 20-hydroxyecdysone upregulates Atg genes to induce autophagy in the *Bombyx* fat body. *Autophagy* 9(8): 1172-87.
- Wang CW, Klionsky DJ. 2003. The molecular mechanism of autophagy. *Mol. Med.* 9: 65-76.
- Wei W, Gai Z, Ai H, Wu W, Yang Y, Peng J, Hong H, Li Y, Liu K. 2012. Baculovirus Infection Triggers a Shift from Amino Acid Starvation-Induced Autophagy to Apoptosis. *PLoS ONE* 7(5): e37457.
- Wu W, Wei W, Ablimit M, Ma Y, Fu T, Liu K, Peng J, Li Y, Hong H. 2011. Responses of two insect cell lines to starvation: Autophagy prevents them from undergoing apoptosis and necrosis, respectively. *J. Insect Physiol.* 57: 723–734.

- Yamada Y, Suzuki NN, Hanada T, Ichimura Y, Kumeta H, Fujioka Y, Ohsumi Y, Inagaki F, 2007. The Crystal Structure of Atg3, an Autophagy related Ubiquitin Carrier Protein (E2) Enzyme that Mediates Atg8 Lipidation. *J. BIOL. CHEM.* 282(11): 8036–8043.
- Yang YP, Liang ZQ, Gu ZL, QIN ZH. 2005. Molecular mechanisms and regulation of autophagy. *Act. Phamacol. Sin.* 26(12): 1421-1434.
- Yano T, Mita S, Ohmori H, Oshima Y, Fujimoto Y, Ueda R, Takada H, Goldman WE, Fukase K, Silverman N, Kurata S. 2008. Autophagic control of listeria through intracellular innate immune recognition in drosophila. *Nat. Immunol.* 9(8): 908-916.
- Zhang X, Hu, ZY, Li WF, Li QR, Deng XJ, Yang WY, Cao Y, Zhou CZ. 2009. Systematic cloning and analysis of autophagy-related genes from the silkworm *Bombyx mori*. *BMC Mol.Biol.* 10:50.

Chapter 3. Molecular cloning and characterization of autophagy-related gene *ATG8* in *Listeria*-invaded hemocytes of *Tenebrio molitor*

3.1 Abstract

Macroautophagy (hereinafter called autophagy) is a highly regulated process used by eukaryotic cells to digest portions of the cytoplasm leading to nutrients recycling, remodeling and disposal of unwanted cytoplasmic constituents. Currently 36 autophagy-related gene (*ATG*) homologues have been characterized in yeast and higher eukaryotes including insects. In the present study, we identified and functionally characterized the immune function of *ATG8* homologue in a coleopteran insect, *Tenebrio molitor* (*TmATG8*). The cDNA of *TmATG8* comprises of an ORF of 363 bp encoding a protein of 120 amino acid residues. *TmATG8* transcripts are detected in all the developmental stages analyzed. *TmAtg8* contains a highly conserved C-terminal glycine residue (G116) and shows high amino acid sequence identity (98%) to its *Tribolium castaneum* homologue, *TcAtg8*. Loss of function of *TmATG8* by RNAi led to a significant increase in mortality of *T. molitor* larvae against *Listeria monocytogenes*. Unlike *dsEGFP*-treated control larvae, *TmATG8*-silenced larvae failed to turn-on autophagy in hemocytes after *L. monocytogenes* injection. These data suggest that *TmATG8* play a role in mediating autophagy-based clearance of *Listeria* in *T. molitor*.

3.2 Introduction

Autophagy is a cellular process by which the cell degrades unnecessary and/or dysfunctional cellular components by the action of lysosomes. The autophagy mechanism is conserved from yeast to higher eukaryotes and is implicated in various house-keeping functions such as organelle turnover, growth, aging, cell death, and mobilization of amino acids upon starvation (Melendez et al., 2003; Levine and Klionsky, 2004; Rusten et al., 2004). Through a subtype of autophagy termed xenophagy, invasive intracellular bacteria can be targeted and engulfed into autophagosomes for their eventual degradation in autolysosomes (Levin, 2005; Deretic, 2011; Knodler and Celli, 2011; Yuk et al., 2012). Eukaryotic cells can deploy xenophagy to restrict the rapid multiplication of internalized extracellular pathogens such as group A *Streptococcus* (GAS) (Nakagawa, et al., 2004; Yamaguchi, et al., 2009; Sakurai, et al., 2010) or typical intracellular pathogen such as *Francisella tularensis* (Checroun et al., 2006) and *Listeria monocytogenes* (Py et al., 2007; Yano et al., 2008).

The molecular mechanism of autophagy was discovered during genetic screens in yeast that led to identification of autophagy-related (*ATG*) genes. To date, 36 *ATG* genes have been identified in yeast and orthologues of these genes are continuously being discovered in various organisms across the Eukaryota. A subset of *ATG* genes involved in the formation of autophagosome is referred to as the “core autophagy machinery”, and is conserved in all subtypes of autophagy (Xie and Klionsky, 2007). The core autophagy machinery comprises of genes placed into three major functional categories namely (i) the Atg9 cycling system which includes Atg9, the Atg1 kinase complex (Atg1 and Atg13), Atg2, and Atg18; (ii) the phosphatidylinositol 3-OH kinase (PI(3)K) complex which includes Vps34, Vps15, Atg6 (Vps30), and Atg14, and (iii) the ubiquitin-like protein (Ubl) system, which includes Atg8-PE complex, the Atg8 modifying protease, (Atg4), the Atg12-Atg5-Atg16 complex, the activating

enzyme (Atg7), and two analogues of ubiquitin-conjugating enzymes (Atg10 and Atg3) (Xie and Klionsky, 2007).

Atg8 is an ubiquitin-like protein involved in controlling the expansion of the phagophore during autophagosome formation, such that the amount of Atg8 available determines the size of the autophagosome formed (Xie et al., 2008). The fact that Atg8 remains localized to the autophagosome has made this protein a reliable marker for the induction and progression of autophagy (Nakatogawa et al., 2007). *ATG8* genes have been characterized in various insect species including *Galleria mellonella* (Khoa and Takeda, 2012), *Bombyx mori* (Hu et al., 2010), *Aedes aegypti* (Bryant and Raikhel, 2011), and *Spodoptera litura* (Zhang et al. 2014). However, no work has reported the identification and characterization of Atg8 in the coleopteran insect, *Tenebrio molitor* (*TmATG8*). We identified a *TmATG8* homologue through RNASeq approach, cloned, and subsequently characterized its function using RNA interference (RNAi) and immunofluorescence targeting. We show that the disruption of the autophagy pathway via RNAi-mediated silencing of *TmATG8* makes *T. molitor* larvae more susceptible to infections caused by an intracellular pathogen, *Listeria monocytogenes*.

3.3 Materials and Methods

3.3.1 Insect collection and Maintenance

T. molitor larvae procured from College of Pharmacy, Pusan National University, Busan, South Korea were reared in an environmental chamber at $26 \pm 1^\circ\text{C}$ with $60 \pm 5\%$ relative humidity and a 16:8 h light: dark cycle. The larvae were fed on autoclaved artificial diet composed of 200 g wheat bran (Milworm house, Busan, Korea); 20 g bean powder (Donggran food, Daejeon, Korea); 10 g brewer's yeast (Beer Yeast Korea Inc., HNH Seoul, Korea); 0.15 g chloramphenicol (Duchefa Biochemie, Haarlem, Netherlands); 1.1 g sorbic acid (Sigma Aldrich, Louis, USA), and 1.1 ml propionic acid (Sigma Aldrich, Louis, USA) mixed in 440 ml of distilled water.

3.3.2 Full-length cDNA Cloning and Sequencing

Partial cDNA sequence of *TmATG8* was obtained from *T. molitor* whole larva RNAseq database annotated for the identification and characterization of immunity-related genes. The full-length cDNA sequence was obtained by performing 5'- and 3'- rapid amplification of cDNA ends -polymerase chain reaction (RACE-PCR) using SMARTer™ RACE cDNA amplification kit (Clontech Laboratories, CA, USA) according to manufacturer's instructions. Total RNA was used as template to synthesize RACE-ready cDNA. Gene-specific primers (Table-1) for *TmATG8* were designed based on the partial cDNA sequence and, subsequently the first and nested PCR reactions were conducted using the RACE-ready cDNA under the following conditions: initial denaturation at 94°C for 3 min followed by 28 cycles of denaturation at 94°C for 30 s, annealing at 60°C for 30 s, extension at 72°C for 1 min and a final extension at 72°C for 10 min. The nested PCR products were resolved on 1 % agarose gel at 100 V for 20 min, extracted and gel-purified by using AccuPrep Gel purification kit (Bioneer Company, Daejeon,

Korea). The purified DNA fragments were subsequently cloned into TOPO TA cloning vector (Invitrogen Corporation, Carlsbad, CA) and transformed into competent *E. coli* DH5 α cells. The transformed DH5 α cells were sub-cultured overnight and plasmids carrying the target gene products were recovered and sequenced. The TmATG8 full-length cDNA sequence has been registered in GenBank under accession number KM676434.

Table 3-1: Primers used in this study

Primer name	Direction	Sequence (5'-3')*
Oligo(dT)adaptor	R	GGCCACGCGTCGACTAGTACT17
M13-F	F	GTAAAACGACGGCCAG
M13-R	R	CAGGAAACAGCTATGAC
<i>TmL27a</i>	F	TCATCCTGAAGGCAAAGCTCCAGT
<i>TmL27a</i>	R	AGGTTGGTTAGGCAGGCACCTTTA
<i>TmATG8</i> qPCR	F	AAGATCCGCCGAAAGTATCC
<i>TmATG8</i> qPCR	R	AACTGGCCGACTGTCAAATC
<i>TmATG8</i> dsRNA		<u>TAATACGACTCACTATAGGGTTTCGAGAAGAGGAAGTCGA</u>
<i>TmATG8</i> dsRNA	R	<u>TAATACGACTCACTATAGGGTGGTAGAGCGAGCCCATTGTA</u>
<i>TmATG8</i> sqPCR	F	ATGAAATTTCAATATAAAGAGGAGCACCC
<i>TmATG8</i> sqPCR	R	TTAGAGCTCATCACCACCATAGAC
<i>TmATG8</i> - ExPCR	F	GGGGAATTCATGAAATTTCAATATAAAGAGGAGCAC CCTTTCGAG
<i>TmATG8</i> -Ex- PCR	R	GGGCAAGCTTGGTTAGAGCTCATCACCACCATAGACG TTCTCATC
<i>TmATG8</i> 3'RACE GSP1	F	GTTATTCCCCCAACATCCGCTAC
<i>TmATG8</i> 3'RACE (nested)	F	GAACGTCTATGGTGGTGATGAGC
<i>TmATG8</i> 5'RACE GSP1	R	CAGAAAGTAGAACTGGCCGACT
<i>TmATG8</i> 5'RACE (nested)	R	CCATGTACTCTGCGTTGATACC

T7 polymerase recognition sequences are underlined

EcoR1 and HindIII restriction sites sequences are in bold

F = Forward, R = Reverse

* Sequences are read from 5' to 3' end

3.3.3 *In Silico* characterization of TmATG8

The cDNA and deduced amino acid sequence of *TmATG8* were analyzed using InterProScan at the European Bioinformatics Institute (EBI) (<http://www.ebi.ac.uk/Tools/pfa/iprscan/>) and Basic Local Alignment Search Tool (BLAST) algorithm at the National Center for Biotechnology Information (NCBI) (<http://blast.ncbi.nlm.nih.gov/>). Specific protein domains for TmAtg8 were highlighted by the InterProScan during the analysis. Amino acid sequence of TmAtg8 homologs were obtained by performing a search using tBLASTn on GenBank (<http://www.ncbi.nlm.nih.gov>). The accession numbers of TmAtg8 homologs used in the present study have been shown in Table-2.

Multiple sequence alignment and percentage identity analysis of TmAtg8 with its homologs were performed using ClustalX2 (Larkin et al., 2007) and MEGA5 (Tamura et al., 2011) programs respectively. Subsequently the MEGA5 program was used to construct a phylogenetic tree using maximum likelihood (ML) method based on the JTT matrix-based model (Jones et al., 1992).

Table 3-2: Accession numbers of Atg8 amino acid sequences from various organisms used to generate the phylogenetic tree, percentage distance and identity matrices

	Species name	Abbreviations	Accession numbers
1	<i>Tenebrio molitor</i>	TmAtg8	KM676434
2	<i>Drosophila melanogaster</i>	DmAtg8	NP_727447.1
3	<i>Apis mellifera</i>	AmAtg8	XP_001120069.1
4	<i>Homo sapiens</i>	HsAtg8	NP_009209.1
5	<i>Mus musculus</i>	MmAtg8	EDL12513.1
6	<i>Danio rerio</i>	DrAtg8	AAH56701.1
7	<i>Anopheles gambiae</i>	AgAtg8	XP_312238.3
8	<i>Aedes aegypti</i>	AaAtg8	AAW21996.1
9	<i>Riptortus pedestris</i>	RpAtg8	BAN20392.1
10	<i>Helicoverpa armigera</i>	HaAtg8	AFK91514.1
11	<i>Bombyx mori</i>	BmAtg8	NP_001040244.1
12	<i>Tribolium castaneum</i>	TcAtg8	XP_973073.1
13	<i>Caenorhabditis elegans</i>	CeAtg8	C32D5.9

3.3.4 Developmental and Tissue-specific Expression Pattern of *TmATG8*

Total RNA was extracted from various developmental stages of *T. molitor*, including the late-instar larvae (LIL), pupal day 1-7 (P1-P7) and adult day 1 and 2 (A1 and A2). For analysis of tissue-specific expression pattern of ATG8 in *T. molitor*, total RNA was extracted from various tissues of the larval stages which included gut, hemocytes, integument, Malpighian tubules, and fat body, as well as the ovaries and testes of the adult stage using SV Total RNA isolation system (Promega Corporation, Madison, WI) according to manufacturer's instructions. cDNAs corresponding to each stage of growth and/or sampled tissue was synthesized using AccuPowerR RT Pre-Mix kit (Bioneer Company, Daejeon, Korea). Quantitative PCR (qPCR) reactions were performed in an Exicycler™ 96 real-time quantitative thermal block (Bioneer Company, Daejeon, Korea) using gene specific primers (Table 1) set to an initial denaturation of 95 °C for 20 s, followed by 45 cycles of denaturation at 95 °C for 5 s and annealing at 60 °C for 20 s. The $2^{-\Delta\Delta C_t}$ method (Livak and Schmittgen, 2001) was employed to analyze the expression levels of *TmATG8*. The reactions were performed in triplicate and represented as the mean \pm SE ($n = 3$) of three biological replicates. *T. molitor* ribosomal protein L27a (TmL27a) was used as an internal control to normalize differences in concentration of templates between samples.

3.3.5 dsRNA synthesis and injections

TmATG8 cDNA template was amplified by semi-quantitative PCR using gene-specific primers (product size; 297 bp) flanked with T7 promoter sequence on their respective 5' ends. The primer information for dsRNA synthesis has been shown in Table 1. The PCR reaction was carried out under the following conditions: initial denaturation at 94°C for 3 min followed by 28 cycles of denaturation at 94°C for 30 s, annealing at 53°C for 30 s, extension at 72°C for 1 min and a final extension at 72°C for 10 min. The PCR products were purified using the AccuPrep

PCR purification kit (Bioneer Company, Daejeon, South Korea) and subsequently used to synthesize the dsRNA with an Ampliscribe™ T7-Flash™ transcription kit (Epicentre Biotechnologies, Madison, WI, USA) according to manufacturer's instructions. After synthesis, dsRNA was purified and precipitated using 5M ammonium acetate and checked for its integrity by running 1% agarose gel and quantification using Epoch spectrophotometer (BioTek instruments Inc, Winooski, VT, USA). As a control, dsRNA for *T. molitor* enhanced green fluorescent protein (*dsTmEGFP*) was synthesized and stored at -20°C until injected into *T. molitor* larvae.

The synthesized *dsTmATG8* was dissolved in injection buffer (0.1 mM sodium phosphate, 2.5 mM potassium chloride, pH 7.2) (Fabrick et al., 2009) to a final concentration of 0.5 µg/µl. Injection of dsRNA (1 µg/µl) into the 2nd or 3rd visible sternite of last-instar larvae (*n* = 50) was performed using disposable needles mounted onto a micro-applicator (Picospritzer III micro dispense system, Parker Hannifin, Hollis, NH, USA). Another set of last-instar larvae (*n* = 50) were injected with equal amount of *dsEGFP* dissolved in the injection buffer and acted as a negative control. Injected animals were maintained on artificial diet under standard rearing conditions until the extraction of total RNA. *TmATG8* knockdown was evaluated five days post injection of dsRNA. Total RNA isolation and subsequent cDNA synthesis was conducted as described above. The experiment was repeated at least three times to confirm the silencing of *TmATG8* transcripts.

3.3.6 Bacterial Injections and Bioassay studies

Listeria monocytogenes strain ATCC 7644 was grown in Brain-heart infusion (BHI) medium (Difco, Sparks, MD, USA) at 37°C. For infection studies, a single colony was picked from BHI agar plate using a sterile wire loop and inoculated into 5 ml of fresh BHI broth in 15

ml round-bottomed culture tube. The tube was incubated overnight under aerobic conditions in an orbital shaker at 200 rpm and 37°C. The overnight culture was washed thrice in phosphate-buffer saline (PBS), re-suspended and serially diluted in 0.9% saline to achieve desired concentrations as determined by measurements at OD₆₀₀. Each dilution was plated on BHI agar and incubated at 37°C for 16 h prior to colony counting.

For bioassay studies, dsRNA (1 µg/larva) of *TmATG8* or *EGFP* was injected into the hemocoel of larvae at the 2nd or 3rd visible sternite as described above. Five days post-injection of dsRNA, knockdown levels were confirmed by qPCR. The larvae in both *TmATG8* and *EGFP* groups (n = 30 each) were challenged with 2 µl (~10⁶ cells/larva) of diluted cultures of *L. monocytogenes*. The challenged larvae were maintained at 26 °C while the numbers of dead larvae were recorded on a daily basis for 6 days. The rate of survival was compared between the *TmATG8* silenced and the *EGFP* control groups. The results represent an average of three biological replications. Statistical analysis was conducted using the Wilcoxon-Mann-Whitney test (Yano et al., 2008) and the cumulative survival rates are considered significant ($P < 0.05$).

3.3.7 Expression of *TmATG8* in *E.coli*

The full-length ORF of *TmATG8* was sub-cloned into TOPO-TA cloning vector as described in section 2.2 above. The insert was subsequently amplified using gene specific primers which contained *EcoRI* and *HindIII* restriction sites (Table 1) to facilitate directional cloning of the PCR product into pET28a(+) expression vector (Novagen, Germany). The PCR product was resolved in 1% agarose gel electrophoresis and purified using gel purification kit (Bioneer, Korea). The DNA was then sub-cloned into *EcoRI-HindIII* digested pET28a(+) expression vector, transformed into competent DH5α cells, spread-plated onto LB agar plates containing Kanamycin (50mg/ml) and X-gal (40mg/ml) and incubated at 37°C overnight.

Positive transformant colonies were sub-cultured for 16 h and plasmids carrying the target gene product were recovered and sequenced.

After confirming the sequence, plasmids carrying the *TmATG8* full ORF were transformed into *E. coli* BL21 cells, spread-plated onto Kanamycin-containing LB agar plates and incubated overnight at 37°C. Selected BL21 colonies were sub-cultured in Kanamycin-containing LB broth and, the expression of the recombinant TmAtg8 (rTmAtg8) protein was induced by addition of IPTG to a final concentration of 0.25mM.

3.3.8 Sodium dodecyl sulphate-Polyacrylamide gel electrophoresis (SDS-PAGE) and Western blot analysis

T. molitor larvae were surface-sterilized by rinsing in 70% ethanol and subsequently anaesthetized on ice for 10 to 15 min. Using sterile scissors proleg was cut and the outflowing hemolymph was collected directly into a tube containing modified hemolymph collection solution (Stoepler et al., 2012), the latter constituted of 70% Grace's insect medium, 10% bovine serum albumin, and 20% anticoagulant Buffer (98 mM NaOH, 186 mM NaCl, 1.7 mM EDTA, and 41 mM citric acid, pH 4.5). For collection of hemocytes, the hemolymph was centrifuged at 200 g at 4 °C for 5 min. The sedimented hemocytes were washed twice in the collection solution and re-suspended into protein extraction solution (Pro-Prep™ iNtRON Biotechnology, Seongnam, Korea) to extract the proteins. The hemolymph proteins were denatured by boiling in 2x *Laemmli* protein loading buffer at 100 °C for 5 min, allowed to cool to room temperature and loaded onto a 16% SDS-PAGE gel for electrophoresis at 100 V for 90 min.

The SDS-PAGE separated proteins were blotted onto Immobilon-P (Millipore, Billerica, MA, USA) membrane at 100 V for 70 min at 4°C. Subsequent to blotting, the membrane was

dissolved in 1mM levamisole in Tris-buffered saline (TBS) (10 mM Tris, 150 mM NaCl, pH 7.5) for 10 min, following which the membrane was blocked in 5% non-fat dry milk in TBST (TBS supplemented with 0.01% Tween 20) for 1 h at room temperature. The membrane was incubated with anti-TmAtg8 antibody (raised in rabbit against amino acid sequences FQYKEEHPFEKRKSC of TmAtg8 (Yong In Frontier Co Ltd., Seoul, Korea)) diluted at 1: 3000 in 5% non-fat dry milk in TBST for 1 h at room temperature. After three washes of 5 min each, the membrane was incubated in goat anti-rabbit IgG (h+l) alkaline phosphatase conjugated antibody (Bethyl Laboratories, Inc., TX USA) diluted at a ratio of 1: 5000 in 5% non-fat dry milk in TBST for 1 h at room temperature. The membrane was washed three times for 5 min each. The bands so obtained were visualized by treating the membrane with Sigmafast™ BCIP/NBT alkaline phosphatase substrate solution (Sigma Aldrich Co., St. Louis, Missouri, USA).

3.3.9 Immunofluorescence staining and confocal microscopic analysis

Hemocytes from *Listeria*-infected or non-infected larvae ($n = 50$) were collected as described above. For live cell autophagy detection, the hemocytes were incubated with an autophagosomal probe, Cyto-ID green detection reagent (Enzo life Sciences Inc., NY, USA) in assay buffer for 30 min at 37°C. Subsequently, the cells were washed twice with assay buffer, applied to glass slides and left for 30 min at room temperature to allow for hemocytes adhesion to slides. Slides were stained for 20 min with TO-PRO-3 iodide to visualize the nuclei. Following three additional washes with assay buffer, slides were mounted with an aqueous mounting medium (Dako North America Inc., CA, USA) and covered for immediate observation under an FV500 laser-scanning confocal microscope (Olympus). For Cyto ID/Lysotracker red co-staining, Lysotracker was added (to a final concentration of 25 nM) to the cells incubated

with Cyto-ID for 15 min and left to co-stain for additional 15 min at 37 °C (Oeste et al., 2013). Co-stained cells were processed as described above and visualized immediately afterwards.

To visualize *Listeria* inside the *Tenebrio* hemocytes, hemocytes were collected from infected larvae as described above, washed twice in PBS and applied to glass slides. Following incubation at room temperature for 30 min, slides were rinsed twice with PBS and fixed for 20 min with ice-cold 4% paraformaldehyde in PBS. After fixation, slides were washed three times with PBS, permeabilized using 0.2% Triton-X100 in PBS for 15 min, washed three times, and blocked with 1% BSA in PBS for 1 h at room temperature. Subsequently, the slides were incubated with anti-*Listeria monocytogenes* polyclonal antibody (Ab35132; Abcam, Cambridge, UK), diluted at 1: 300 in 1% BSA in PBS for 1.5 h at room temperature. Slides were washed three times in PBS and incubated with fluorescein rhodamine-conjugated goat anti-rabbit IgG antibody Alexa flour 546, diluted at 1: 300 in 1% BSA in PBS for 1 h at room temperature. After washing 3 times in PBS, slides were stained with TO-PRO-3 iodide (Invitrogen) for 30 min, processed and observed under FV500 laser-scanning confocal microscope (Olympus) as described above.

3.4 Results

3.4.1 cDNA characterization and phylogenetic analysis of TmATG8

The full-length *TmATG8* cDNA (accession number: KM676434) was obtained from the partial sequence screened from the *T. molitor* RNAseq database. The full length cDNA of *TmATG8* contains an open reading frame (ORF) of 363 bp encoding a protein of 120 amino acid residues (Fig. 3-1). The 5'- and 3'- untranslated regions (UTR) of *TmATG8* were of 141 and 369 bp, respectively. The poly (A) signal (AATAA) was found 9 bp upstream of the poly (A) tail. Signal peptide was not predicted for TmAtg8 protein. An analysis of TmAtg8 deduced amino acid sequence reveals a characteristic microtubule-associated proteins 1a/1b light chain 3-related domain (Fig. 3-1).

Multiple alignment of TmAtg8 with its orthologs indicates high degree of conservation of Atg8 amino acid sequence within insects (Fig. 3-2). Furthermore, TmAtg8 is phylogenetically closer to Atg8 of another coleopteran beetle, *Tribolium castaneum* (TcAtg8) (Fig. 3-3). TmAtg8 share highest sequence identity (98%) with TcAtg8 followed by those with *Homo sapiens* (94%), *Mus musculus* (94%), *Riptortus pedestris* (94%), *Helicoverpa armigera* (94%), and *Bombyx mori* (94%) (Fig. 3-4). The distance matrix shows that TmAtg8 is placed at a distance of 0 from TcAtg8 compared to distances of 0.05 and 0.11 from *Drosophila melanogaster* and *Apis mellifera*, respectively (Fig. 3-4).

>TmAtg8

```

AAG CAG TGG TAT CAA CGC AGA
GTA CAT GGG GCA TTC GAT TGG TTG TTT TGT GTC ACA ACA AGC AGA AGT GAG AAA ACT GAG
CAA ACG TAC TGA ACC CAT CGC ATT GAT TCC CTA AAT TCT GGT GTA ATA TAT CAA AAA ACA

ATG AAA TTT CAA TAT AAA GAG GAG CAC CCT TTC GAG AAG AGG AAG TCC GAG GGT GAG AAG   60
M K F Q Y K E E H P F E K R K S E G E K   20

ATC CGC CGA AAG TAT CCC GAC AGA GTG CCA GTG ATC GTC GAA AAG GCC CCC AGA GCT CGA   120
I R R K Y P D R V P V I V E K A P R A R   40

ATC GGT GAC TTA GAC AAG AAA AAG TAT CTA GTC CCG TCA GAT TTG ACA GTC GGC CAG TTC   180
I G D L D K K K Y L V P S D L T V G Q F   60

TAC TTT CTG ATC AGG AAG AGG ATC CAC TTG AGG CCC GAG GAT GCC CTA TTT TTC TTT GTA   240
Y F L I R K R I H L R P E D A L F F F V   80

AAT AAT GTT ATT CCC CCA ACA TCC GCT ACA ATG GGC TCG CTC TAC CAG GAA CAT CAT GAG   300
N N V I P P T S A T M G S L Y Q E H H E   100

GAG GAC TTT TTC TTA TAC ATT GCT TAT TCT GAT GAG AAC GTC TAT GGT GGT GAT GAG CTC   360
E D F F L Y I A Y S D E N V Y G G D E L   120

TAA   363
*   120

TTA ATG AAA CAA GTG ATT GAT TTT TTT ATA GAT ATC TGA TTC AAT AAA GCA CCG GTA AAA
CAT AAA AGT TAC ATT TAT TTT ATA TTT TTG GAT TGT CAT TTG CTG CTG ACT TAA TGT GAT
AGT TGT ATA GCT ATG TTA TTG TGT TTT TTT TTT TTA ATT ATG TAA ACA TTT ATT TTG TTA
GGG TAT CGC GAA AGA GAT TTT GAG TTT GTT TTT CAG ACA CTG GAA AGA GAT TAA TTT CGT
CAT AAA TTT TAT ATT TGA TAT CAA ATT TCT GAT GAA GTC ACT GAA GTA TTA GAC TAG ATC
TAT AAC ATA ATG TAG TTA TAA AAA TAA AAA CGT TCC GAA AAA AAA AAA AAA AAA AAA AAA
AAA AAA AAA

```

Figure 3-1: Nucleotide and deduced amino acid sequence for *TmATG8*

Domains were analyzed by interproscan program (<http://www.ebi.ac.uk/Tools/pfa/iprscan/>).

Predicted microtubule-associated proteins 1a/1b light chain 3-related domain is highlighted.

Underline indicates the polyadenylation signal.

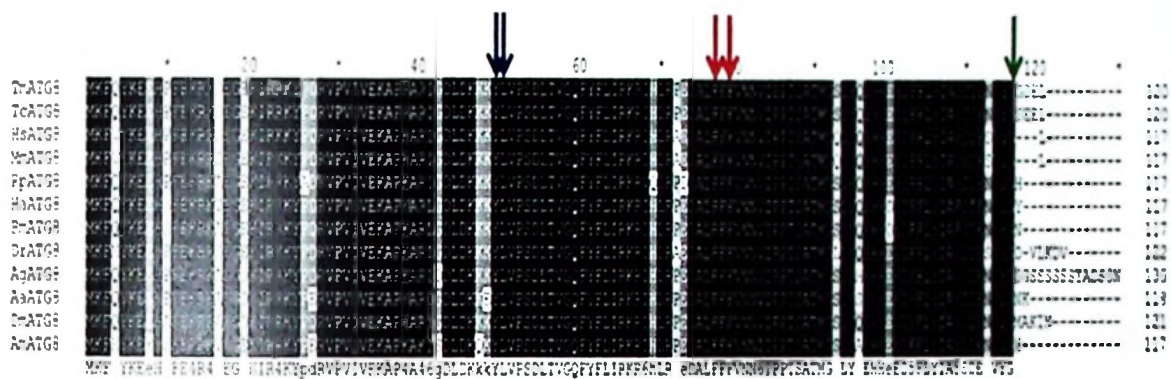


Figure 3-2: Multiple alignment of TmAtg8 with orthologs from other insects.

The conserved C-terminal glycine residue (G116) which would be exposed after Atg4-mediated cleavage of terminal arginine residue (green arrow), Phe77 and Phe79 which form part of Atg4 recognition site (red arrows) and Tyr49 and Leu50 important for Atg7 and Atg3 as E1 and E2-like enzyme activity on Atg8 (blue arrows) are shown. Amino acid sequences used for the alignments have been presented in Table 3-2.

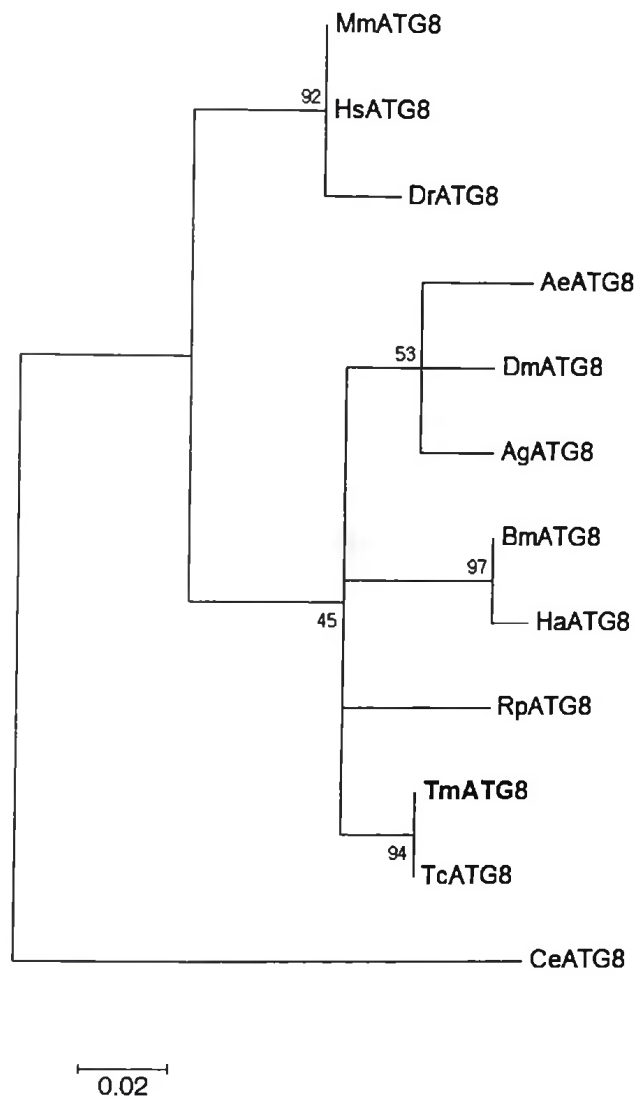


Figure 3-3: Molecular phylogenetic analysis of Atg8 sequences by Maximum Likelihood method.

The evolutionary history was inferred by using the Maximum Likelihood method based on the JTT matrix-based model. TcAtg8 presented the phylogenetically closest counterpart of TmAtg8. The accession numbers of all sequences of insect species used to create the trees are enlisted in Table 3-2.

	TmATG8	TcATG8	HsATG8	MmATG8	RpATG8	HaATG8	BmATG8	DrATG8	AgATG8	AaATG8	DmATG8	AmATG8	
TmATG8		98	94	94	94	94	94	92	92	92	92	89	Identity (%)
TcATG8	0		94	94	94	94	94	92	93	92	92	89	
HsATG8	0.06	0.06		100	91	91	91	93	90	90	91	86	
MmATG8	0.06	0.06	0		91	91	91	93	90	90	91	86	
RpATG8	0.05	0.05	0.1	0.1		91	92	90	92	91	92	87	
HaATG8	0.05	0.05	0.1	0.1	0.08		98	90	91	91	92	88	
BmATG8	0.05	0.05	0.1	0.1	0.07	0.01		90	92	92	93	88	
DrATG8	0.06	0.06	0.02	0.02	0.1	0.1	0.1		86	89	89	85	
AgATG8	0.05	0.05	0.1	0.1	0.07	0.08	0.07	0.1		95	93	88	
AaATG8	0.06	0.06	0.11	0.11	0.08	0.09	0.08	0.11	0.04		94	88	
DmATG8	0.05	0.05	0.08	0.08	0.07	0.07	0.06	0.08	0.04	0.04		87	
AmATG8	0.11	0.11	0.15	0.15	0.14	0.12	0.12	0.15	0.12	0.12	0.13		
	Distance (%)												

Figure 3-4: Estimates of evolutionary divergence between sequences.

Sequences of all insect species used in the analysis are presented in Table 3-2. TmAtg8 shared the highest percentage (98%) identity with its orthologue in *T. castaneum*, TcAtg8. The % identity results are highly supported by the % distance results which put TmAtg8 at 0% from its *T. castaneum* counterpart, TcAtg8.

3.4.2 Developmental and tissue-specific expression patterns of TmATG8 mRNAs

The expression levels of *TmATG8* transcripts were analyzed by quantitative real-time PCR (Fig. 3-5). The transcripts of *TmATG8* were detected in all developmental stages and tissues examined. In adult insect, hemocytes and ovaries show lower TmATG8 transcript level (Fig. 3-5Ai), whereas in the larva hemocytes show lower transcript levels (Fig. 3-5Aii). Although the *TmATG8* transcripts were found in all the developmental stages tested, higher transcript levels were observed in the early and late pupal stages (Fig. 3-5B).

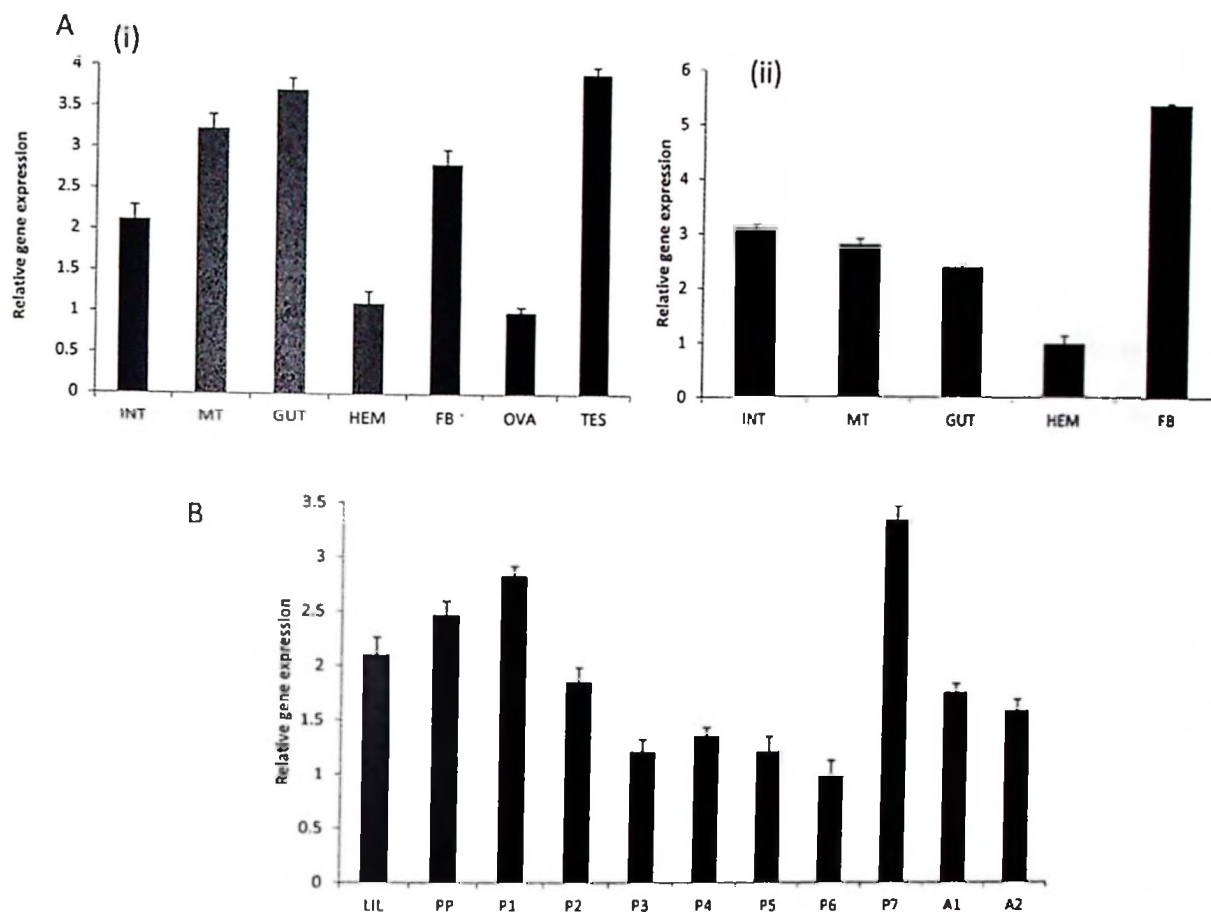


Figure 3-5: Spatial and developmental expression patterns of *TmATG8* in adults and larvae.

(A): Relative gene expression levels in various tissues of the adult (i) and larva (ii). (B): Relative gene expression levels at various developmental stages spanning from late-instar larvae through the pupal to early adult stages. INT, MT, FB, HEM, OVA and TES represent integument, Malpighian tubules, fat body, hemocytes, ovaries and testes, respectively. LIL, PP, P1-P7 and A1 and A2 represent late-instar larvae, pharate pupa, pupa day 1-7 and adult day 1 and day 2, respectively. Data are shown as the mean \pm standard deviation ($n = 3$).

3.4.3 Characterization of TmAtg8 polyclonal antibody

Under normal non-autophagic conditions, Atg8 exists in an unconjugated form (Atg8-I). but upon starvation or microbial infections, most of Atg8 is lipidated by conjugation with phosphatidylethanolamine (PE) to form Atg8-PE conjugate (Atg8-II) and subsequently recruited to the developing phagophore (Nair et al., 2011). To detect the Atg8-I and Atg8-II forms in *T. molitor*, we designed and generated a peptide-based anti-TmAtg8 polyclonal antibody. The specificity of anti-TmAtg8 antibody was validated by its ability to detect recombinant TmAtg8 protein (rTmAtg8) as well as endogenous TmAtg8 in protein extracts from whole insects (Fig. 3-6). Furthermore, anti-TmAtg8 was able to track the second band (TmAtg8-II) potentially resulting from infection-induced autophagy in hemocytes after 12 h and 24 h. Infection of *T. molitor* late-instar larvae with 10^6 CFU of either *E.coli* or *L. monocytogenes* appeared to induce autophagy in hemocytes with little or no autophagy observed in the fat body (Fig. 3-7). Autophagic signals based on the intensity of the second band (TmAtg8-II) appeared to be more pronounced in larvae infected with *L. monocytogenes* than those infected with *E.coli*.

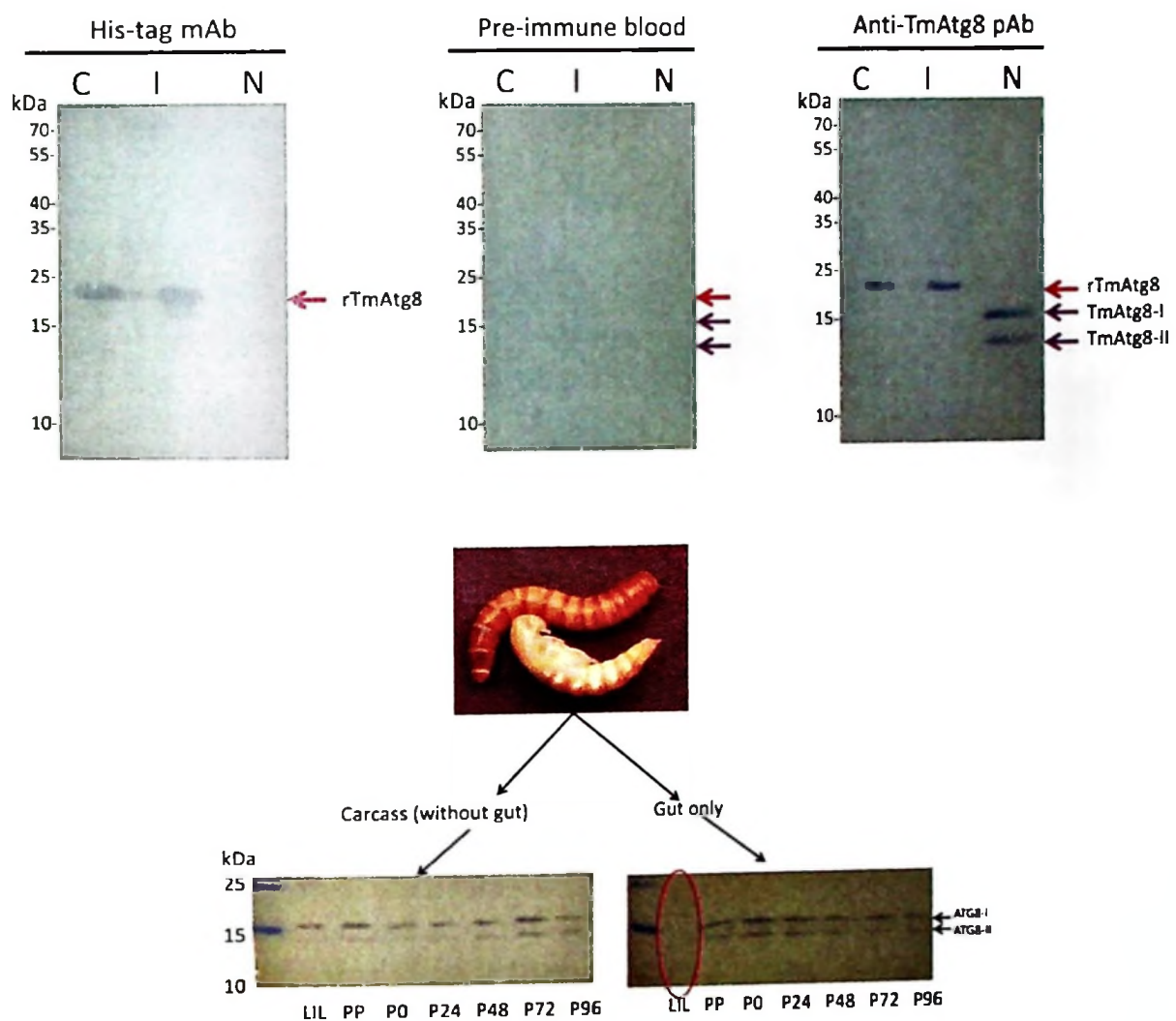


Figure 3-6: Characterization of anti-TmAtg8 polyclonal antibody.

Upper: Detection of recombinant (rTmAtg8) and native TmAtg8 proteins by western blotting. His-tag monoclonal antibody was used to specifically detect the rTmAtg8. Anti-TmAtg8 antibody detected both rTmAtg8 (red arrow) and the native TmAtg8-I and TmAtg8-II (purple arrows). Pre-immune blood was used as a negative control. C = Un-induced bacterial lysate, I = IPTG-induced bacterial lysate, N = Whole-body *T. molitor* larvae protein extracts.

Lower: Detection of TmAtg8-I and TmAtg8-II resulting from developmentally-induced autophagy in *T. molitor*. LIL = Late-instar larvae, PP = Pharate pupae, P0, P24, P48, P72, P96 = Pupa at 0, 24, 48, 72, 96 h post-pupation, respectively.

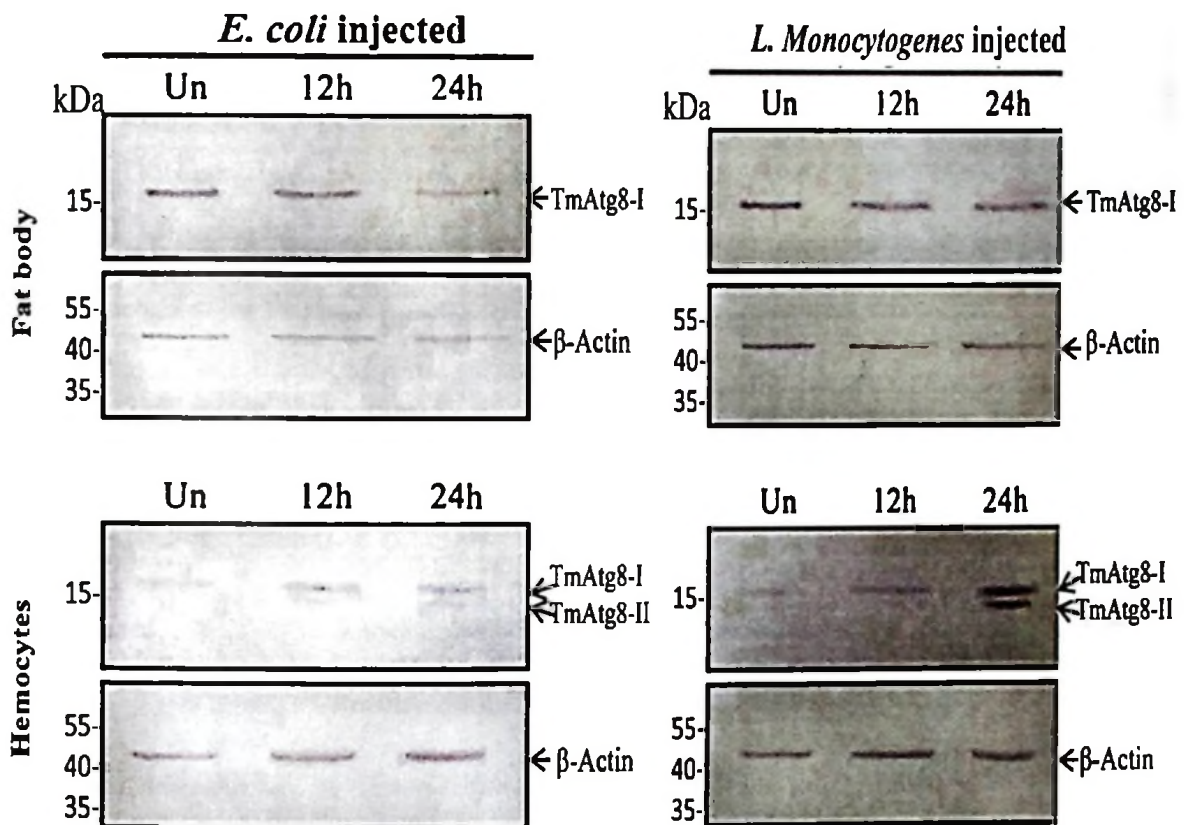


Figure 3-7: Induction patterns of autophagy detected by Western blot analysis with anti-TmAtg8 antibody after injection of *E. coli* and *L. monocytogenes*.

After injection of 10^6 cells of *E. coli* and *L. monocytogenes* into *T. molitor* late-instar larva, fat body and hemocytes were collected and autophagy signals were detected by Western blot analysis with anti-TmAtg8 antibody. β -actin mAb was used as loading control. These results suggest that the autophagy is more pronounced in *Listeria*-infected hemocytes than that of *E. coli*-infected hemocytes. Little or no autophagy occurred in fat body from both *Listeria*- and *E. coli*-infected insects.

3.4.4 *TmATG8* gene silencing results in high mortality of *Tenebrio* larvae against infection by *Listeria monocytogenes*

To functionally characterize *TmATG8*, we knocked down its gene expression by RNAi and monitored its influence on the ability of *T. molitor* larvae to resist infections by an intracellular pathogen, *Listeria monocytogenes*. The nearly 70% down-regulation of the *TmATG8* transcripts (Fig. 3-8A) were corroborated by western blot results at a protein level where the target protein band was reduced to undetectable levels in the ds*TmATG8*-injected larvae compared to the control ds*EGFP*-injected larvae (Fig. 3-8B).

Under *TmATG8* knockdown conditions, inoculation of *L. monocytogenes* at concentration of 10^6 CFU/larva resulted in significant ($P < 0.05$) reduction in survival of *TmATG8* RNAi larvae compared to ds*EGFP*-injected control or 0.9% saline-injected larvae (Fig. 3-9A, B). No difference in mortality was observed between the controls and the *TmATG8*-depleted larvae in the first three days post-*Listeria* challenge, but mortality was pronounced in the *TmATG8*-depleted larvae from day 4 onwards. The 0.9% saline and ds*EGFP*-injected insects showed similar survival abilities against the pathogen (Fig. 3-9A, B).

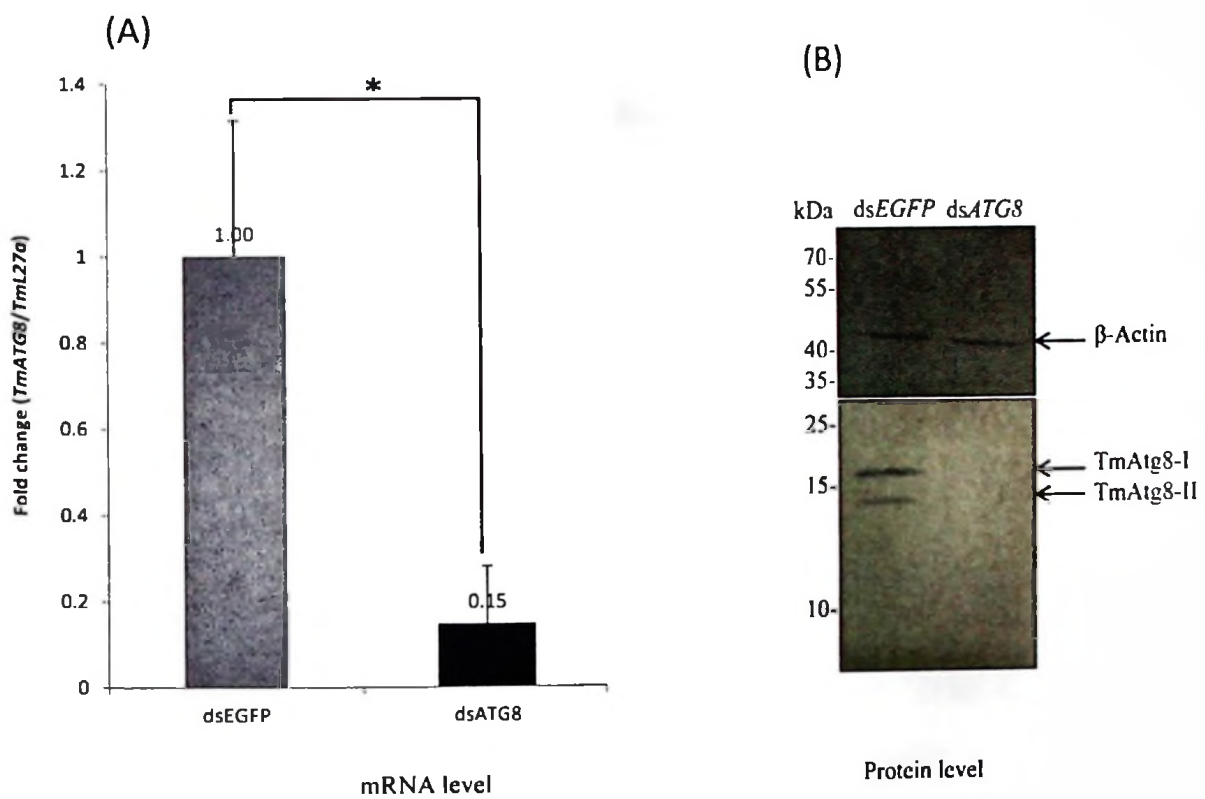


Figure 3-8: Knockdown of *TmATG8* by RNA interference.

(A) Expression levels of *TmATG8* transcripts 5 days post-dsRNA injection were analyzed by real time PCR. “*” indicates significant ($p < 0.05$) difference between control treatments. (B) Western blot results showing the disappearance of TmAtg8 protein bands after *dsTmATG8* injection into *Tenebrio* larvae. Data are shown as mean \pm standard deviation ($n = 3$).

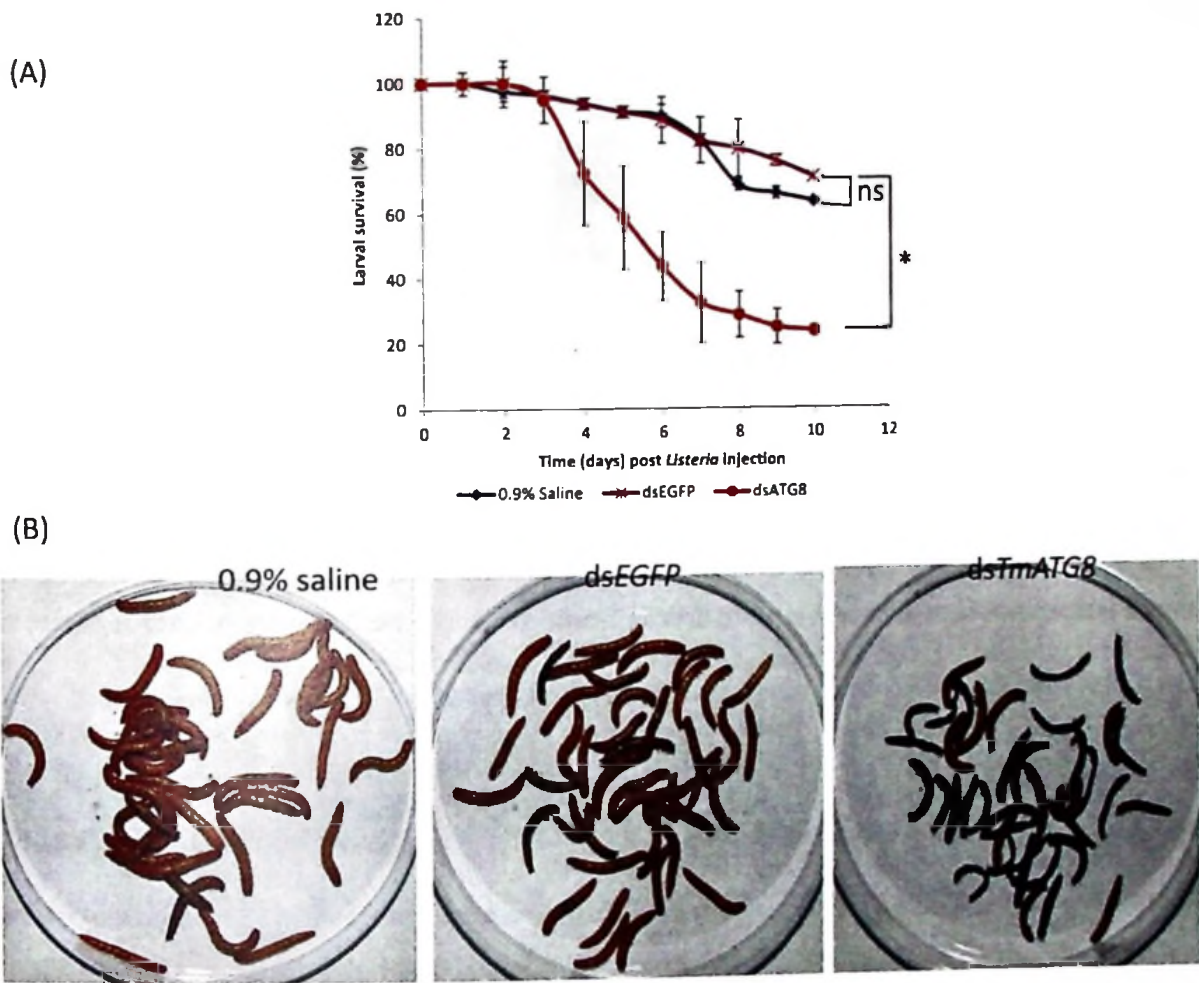


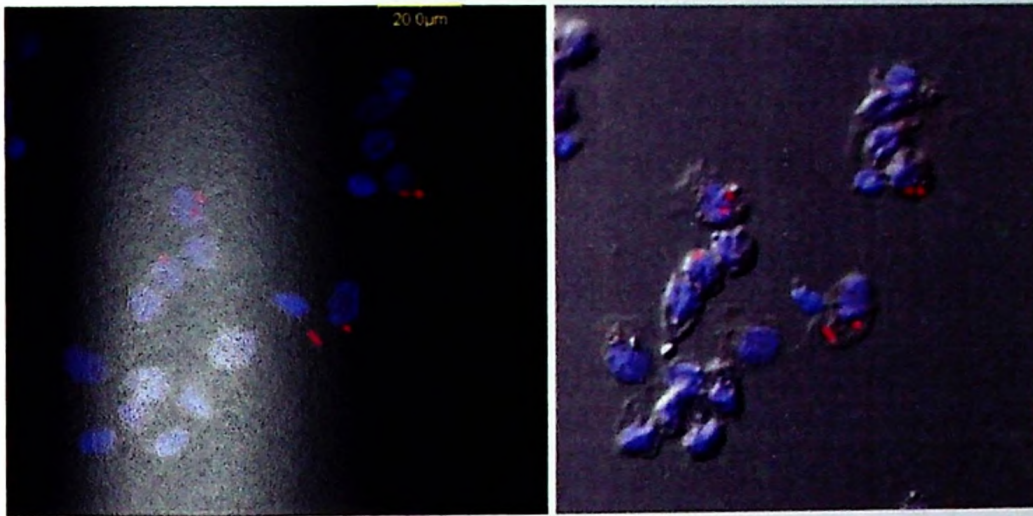
Figure 3-9: Survival of *Tenebrio* larvae against *L. monocytogenes* infection.

(A). Larval survival curves over time following infection with *L. monocytogenes*. Bacteria-induced mortality of larvae that had been previously treated with ds*TmATG8* (1 μ g/insect) were compared to those treated with 0.9% saline or ds*EGFP* as positive controls. (B). Pictorial presentation of the treated larvae under investigation. The ds*TmATG8*-treated larvae showed high mortality and melanization phenotypes compared to control larvae. “*” indicate significant difference ($p < 0.05$), ns = not significant. Data are shown as mean \pm standard deviation ($n = 3$).

3.4.5 *TmATG8* gene silencing causes failure of *T. molitor* larvae to turn-on autophagic response to invading *Listeria* in hemocytes

In order to confirm the requirement of autophagy in counteracting against *L. monocytogenes* infection, we tracked the bacterial infection of hemocytes and the status of the autophagy signal in presence or absence of TmAtg8 using a combination of RNAi and immunostaining techniques. Results show that *L. monocytogenes* can invade hemocytes within 1 h of their inoculation into the hemocoel of *Tenebrio* larvae by microinjection (Fig. 3-10). However, the autophagy signal was not detected in hemocytes until about 6 h post-infection. The intensity of the autophagosome-specific probe, Cyto-ID green dye and the endo-lysosomal probe, LysoTracker Red DND-99 increased with increasing time of exposure to the pathogen. Furthermore, most but not all signals of the two probes co-localized as indicated by the merged image (Fig. 3-10). These results suggest that the host requires duration of at least 6 h to form the autophagosome (xenophagosome) after infection.

Silencing of *TmATG8* transcripts resulted in inhibition of autophagy in hemocytes following *Listeria* infection. While a strong autophagic signal was detectable in control hemocytes (hemocytes from dsEGFP-injected larvae), no signal was detectable in the *TmATG8* RNAi group (Fig. 3-11).



Blue: TO-PRO-3 stained hemocyte nuclei
 Red: *Listeria* cells

X400 magnification

Time (h)	DICT image	Cyto-ID	Lysotracker Red	Merge (Cyto-ID/LTR)	<i>Listeria</i> pAb
1					
3					
6					
9					
12					

Figure 3-10: Time-course autophagy staining in hemocytes.

Top: Enlarged photo to show *Listeria* in hemocytes. Bottom: Co-staining of *Listeria*-infected *Tenebrio* hemocytes with one autophagosome probe, the Cyto-ID green detection reagent and a lysosomal dye, Lysotracker Red DND 99.

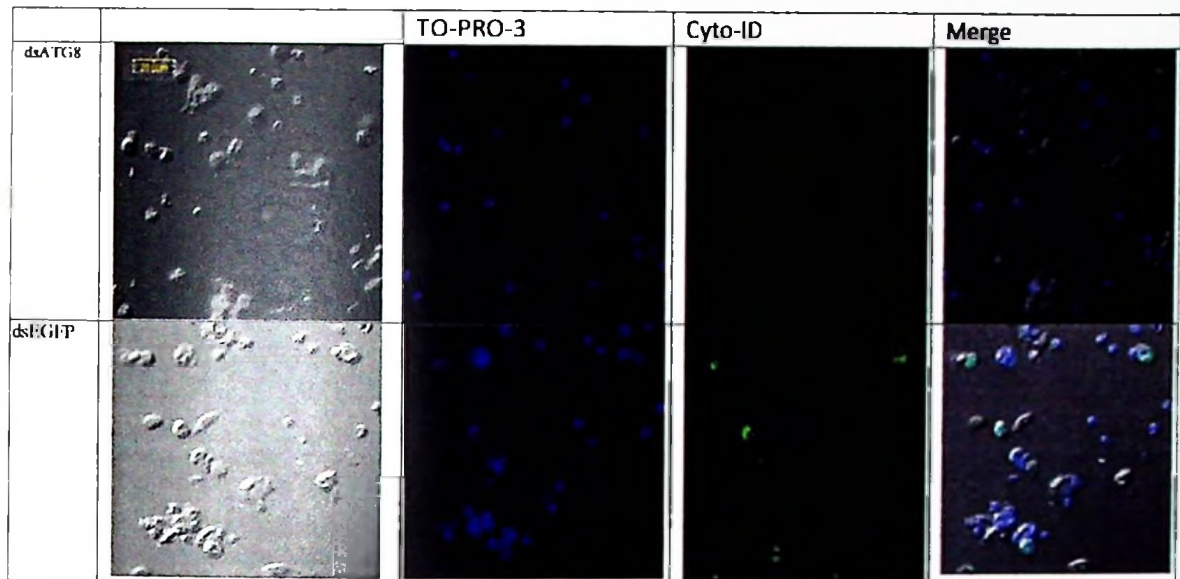


Figure 3-11: Tracking *Listeria*-induced autophagy using Cyto-ID green detection reagent in hemocytes isolated from ds*TmATG8*-treated *T. molitor* larvae.

Late-instar larvae were microinjected with ds*TmATG8* or ds*EGFP* (1µg/insect). 5 days post dsRNA injection, larvae were challenged with 10⁶ CFU/Larva of *L. monocytogenes* for 12 h prior to hemocytes isolation and live-cell staining as described in materials and methods.

3.5 Discussion

Atg8 is an accepted marker of autophagy in a diverse list of organisms and is utilized to probe autophagic processes in eukaryotes. In order to delineate the autophagic process in the coleopteran insect, *T. molitor* we screened and identified homologs of ATG genes from the annotated RNASeq database. A partial sequence from the *T. molitor* RNASeq database was screened and identified to be ATG8 (*TmATG8*). We further cloned and functionally characterized *TmATG8* in the context of *L. monocytogenes*-triggered autophagy in *T. molitor*.

The first conclusive evidence for characterization of *TmATG8* at the sequence level was the identification of microtubule-associated proteins 1a/1b light chain 3-related domain. Multiple alignment of TmAtg8 with other Atg8 homologues from various organisms shows the highly conserved C-terminal glycine residue. As reported earlier, the conserved C-terminal glycine residue gets exposed following removal of a terminal arginine residue due to the proteolytic activity of Atg4 (Nakatogawa et al., 2007). With the exposed glycine residue, TmAtg8 could get conjugated to PE by the coordinated enzymatic activities of Atg7 and Atg3 (as E1- and E2-ubiquitin-like enzymes), respectively (Ichimura et al., 2000; Amar et al., 2006; Nakatogawa et al., 2007).

The observation that *TmATG8* mRNA transcripts are expressed in all the insect tissues including the fat body, hemocytes, gut, Malpighian tubules, integument, ovaries, and testes suggest that autophagy is a routine cell remodeling process occurring in various tissues and thus is important during growth and development, nutrient recycling upon starvation and clearance of invading pathogens (Scott et al., 2004; Berry and Baehrecke, 2007; Denton et al., 2009; Nezis et al., 2009; Khoa and Takeda, 2012; Tian et al., 2013). Our study also shows the ubiquitous presence of *ATG8* mRNA transcripts in all developmental stages of *T. molitor*, suggesting marked autophagy during growth of the insect.

To understand the role of autophagic processes in eliminating an intracellular pathogen, *L. monocytogenes* in *T. molitor*, we expressed the TmATG8 gene in *E. coli* system and purified rTmAtg8. We also generated a peptide-based polyclonal antibody against the TmAtg8 protein. The antibody was able to specifically recognize rTmAtg8 and the endogenous TmAtg8 from the whole-body protein extracts of late-instar *T. molitor* larvae. In the current study, western blotting did not detect autophagy in fat body of *T. molitor* larvae following microbial infection. This potentially differential regulation of autophagy in hemocytes and fat body of *T. molitor* is intriguing. It may be that xenophagy is a preferred defence strategy against invading pathogens in hemocytes of *T. molitor* larvae.

Using RNAi, we silenced the mRNA transcripts of *TmATG8* and its consequent protein levels, and subsequently challenged the *T. molitor* larvae with *L. monocytogenes*. The reduced survival ability of *TmATG8*-depleted larvae against *L. monocytogenes* infection suggests that autophagy play a major role in mediating resistance against *L. monocytogenes* infections in *T. molitor* larvae. Furthermore, an increase in autophagic signals over-time after the larval exposure to *Listeria* infection provides compelling evidence that *T. molitor* depends, at least partly, on autophagy to clear infections by *L. monocytogenes* in the hemocytes. The inability of *TmATG8*-depleted larvae to turn-on the autophagy machinery against invading *Listeria* indicates that *TmATG8* is indispensable during an autophagic response against *L. monocytogenes*. This is conforms to reports on the arrest of autophagic activity in the fat body of *Aedes aegypti* after silencing of *ATG8* transcripts either alone or in combination with *ATG1* (Bryant and Raikhel, 2011).

3.6 Conclusions

In this report, we identified and characterized the requirement of *ATG8* in autophagic clearance of *L. monocytogenes* in *T. molitor*. This is significant as we could establish the pathogenicity of *L. monocytogenes* in *T. molitor* system for the first time. We are now focusing on the functional roles of *TmATG8* in starvation-induced and developmentally triggered autophagy in *T. molitor*.

3.7 References

- Amar, N., Lustig, G., Ichimura, Y., Ohsumi, Y. and Elazar, Z. (2006). Two newly identified sites in the ubiquitin-like protein Atg8 are essential for autophagy. *EMBO Rep.* 7, 635–642.
- Berry, D.L., and Baehrecke, E.H. (2007). Growth arrest and autophagy are required for salivary gland cell degradation in *Drosophila*. *Cell* 131, 1137–1148.
- Bryant, B. and Raikhel, A.S. (2011). Programmed autophagy in the fat body of *Aedes aegypti* is required to maintain egg maturation cycles. *PLoS ONE* 6(11): e25502. doi:10.1371/journal.pone.0025502
- Checroun, C., Wehrly, T.D., Fischer, E.R., Hayes, S.F., and Celli, J. (2006). Autophagy-mediated reentry of *Francisella tularensis* into the endocytic compartment after cytoplasmic replication. *Proc. Natl. Acad. Sci. USA* 103, 14578–14583.
- Denton, D., Shrivage, B., Simin, R., Mills, K., Berry, D.L., Baehrecke, E.H., and Kumar, S. (2009). Autophagy, not apoptosis, is essential for midgut cell death in *Drosophila*. *Curr. Biol.* 19, 1741–1746.
- Deretic, V. (2011). Autophagy in immunity and cell-autonomous defense against intracellular microbes. *Immunol. Rev.* 240, 92-104.
- Fabrick, J., Oppert, C., Lorenzen, M.D., Morris, K., Oppert, B. and Jurat-Fuentes, J.L. (2009). A novel *Tenebrio molitor* cadherin is a functional receptor for *Bacillus thuringiensis* Cry3Aa toxin. *J. Biol. Chem.* 284, 18401–18410.

- Hu, C., Zhang, X., Teng, Y-B., Hu, H-X. and Li, W-F. (2010). Structure of autophagy-related protein Atg8 from the silkworm *Bombyx mori* Acta Cryst. F66, 787–790.
- Ichimura, Y., Kirisako, T., Takao, T., Satomi, Y., Shimonishi, Y., Ishihara, N., Mizushima, M., Tanida, I., Kominami, E., Ohsumi, M., Noda, T. and Ohsumi, Y. (2000). A ubiquitin-like system mediates protein lipidation. Nature 408, 488–492.
- Juhasz, G., Csikos, G., Sinka, R., Erdelyi, M. and Sass, M. (2003). The *Drosophila* homolog of Aut1 is essential for autophagy and development. FEBS Lett. 543, 154–158.
- Khoa, B.D. and Takeda, M. (2012). Expression of Autophagy 8 (Atg8) and its role in the midgut and other organs of the greater wax moth, *Galleria mellonella*, during metamorphic remodelling and under starvation. Insect Mol Biol. 21, 473-487.
- Knodler, L.A. and Celli, J. (2011). Eating the strangers within: host control of intracellular bacteria via xenophagy. Cell Microbiol. 13, 1319-1327.
- Larkin, M.A., Blackshields, G., Brown, N.P., Chenna, R., McGettigan, P.A., McWilliam, H., Valentin, F., Wallace, I.M., Wilm, A., Lopez, R., Thompson, J.D., Gibson, T.J. and Higgins, D.G. (2007). Clustal W and Clustal X version 2.0. Bioinformatics 23, 2947-2948.
- Levine, B. and Klionsky, J. (2004). Development by self-digestion: Molecular mechanisms and biological functions of autophagy. Dev. Cell 6, 463–477.
- Levine, B. (2005). Eating oneself and uninvited guests: autophagy-related pathways in cellular defense. Cell 120, 159–162.

- Livak, K.J. and Schmittgen, D. (2001). Analysis of relative gene expression data using real-time quantitative PCR and the $2^{-\Delta\Delta C_t}$ method. *Methods* 25, 402-408.
- Melendez, A., Tallozy, Z., Seaman, M., Eskelinen, E.L., Hall, D.H. and Levine, B. (2003). Autophagy genes are essential for dauer development and life-span extension in *C. elegans*. *Science* 301, 1387–1391.
- Nair, U., Thumm, M., Klionsky, D.J. and Krick, R. (2011). GFP-Atg8 protease protection as a tool to monitor autophagosome biogenesis. *Autophagy* (12), 1546-1550.
- Nakagawa, I., Amano, A., Mizushima, N., Yamamoto, A., Yamaguchi, H., Kamimoto, T., Nara, A., Funao, J., Nakata, M., Tsuda, K., Hamada, S. and Yoshimori, T. (2004). Autophagy defends cells against invading Group A *Streptococcus*. *Science* 306, 1037-1040.
- Nakatogawa, H., Ichimura, Y. and Ohsumi, Y. (2007). Atg8, a ubiquitin-like protein required for autophagosome formation mediates membrane tethering and hemifusion. *Cell* 130, 165–178.
- Nezis, I.P., Lamark, T., Velentzas, A.D., Rusten, T.E., Bjorkoy, G., Johansen, T., Papassideri, I.S., Stravopodis, D.J., Margaritis, L.H., Stenmark, H. and Brech, A. (2009). Cell death during *Drosophila melanogaster* early oogenesis is mediated through autophagy. *Autophagy* 5, 298–302.
- Oeste, C. L., Seco, E., Patton, W.F., Boya, P. and Pe´rez-Sala, D. (2013). Interactions between autophagic and endo-lysosomal markers in endothelial cells. *Histochem. Cell Biol.* 139, 659–670.

- Py, B.F., Lipinski, M.M. and Yuan, J. (2007). Autophagy limits *Listeria monocytogenes* intracellular growth in the early phase of primary infection. *Autophagy* 3, 117–125.
- Rusten, T.E., Lindmo, K., Juha'sz, G., Sass, M., Seglen, P.O., Brech, A. and Stenmark, H. (2004). Programmed autophagy in the *Drosophila* fat body is induced by ecdysone through regulation of the pi3k pathway. *Dev. Cell.* 7, 179–192.
- Sakurai, A., Maruyama, F., Funao, J., Nozawa, T., Aikawa, C., Okahashi, N., Shintani, S., Hamada, S., Ooshima, T. and Nakagawa, I. (2010). Specific behavior of intracellular *Streptococcus pyogenes* that has undergone autophagic degradation is associated with bacterial streptolysin O and host small G proteins Rab5 and Rab7. *J. Biol. Chem.* 285, 22666-22675.
- Scott, R.C., Schuldiner, O. and Neufeld, T.P. (2004). Role and regulation of starvation-induced autophagy in the *Drosophila* fat body. *Dev. Cell.* 7, 167–178.
- Stoepler, T.M., Castillo, J.C., Lill, J.T. and Eleftherianos, I. (2012). A simple protocol for extracting hemocytes from wild caterpillars. *J. Vis. Exp.* 69:e4173. doi: 10.3791/4173.
- Tamura, K., Petersen, D., Petersen, N., Stecher, G., Nei, M. and Kumar, S. (2011). MEGA5: Molecular evolutionary genetics analysis using maximum likelihood, evolutionary distance and maximum parsimony methods. *Mol. Biol. Evol.* doi:10.1093/molbev/msr121.

- Tian, L., Ma, L., Guo, E., Deng, X., Ma, S., Xia, Q., Cao, Y. and Li, S. (2013). 20-hydroxyecdysone upregulates Atg genes to induce autophagy in the *Bombyx* fat body. *Autophagy* 9, 1172-1187.
- Tindwa, H., Jo, Y.H., Patnaik, B.B., Noh, M.Y., Kim, D.H., Kim, I., Han, Y.S., Lee, Y.S., Lee, B.L. and Kim, N.J. (2014). Depletion of autophagy-related genes atg3 and atg5 in *Tenebrio molitor* leads to decreased survivability against an intracellular pathogen, *Listeria monocytogenes*. *Arch. Insect Biochem. Physiol.* doi: 10.1002/arch.21212.
- Xie, Z., and Klionsky, D.J. (2007). Autophagosome formation: core machinery and adaptations. *Nat. Cell. Biol.* 9, 1102-1109.
- Xie, Z., Nair, U., and Klionsky, D.J. (2008). Atg8 controls phagophore expansion during autophagosome formation. *Mol. Biol. Cell.* 19, 3290–3298.
- Yamaguchi, H., Nakagawa, I., Yamamoto, A., Amano, A., Noda, T. and Yoshimori, T. (2009). An initial step of GAS-containing autophagosome-like vacuoles formation requires Rab7. *PLoS Pathog.* 5(11): e1000670. doi:10.1371/journal.ppat.1000670.
- Yano, T., Mita, S., Ohmori, H., Oshima, Y., Fujimoto, Y., Ueda, R., Takada, H., Goldman, W.E., Fukase, K., Silverman, N. and Kurata, S. (2008). Autophagic control of listeria through intracellular innate immune recognition in *Drosophila*. *Nat. Immunol.* 9, 908-916.
- Yuk, J-M., Yoshimori, T. and Jo, E-K. (2012). Autophagy and bacterial infectious diseases. *Exp. Mol. Med.* 44, 99-108.

Zhang, X., Lu, H., Ai, H., Peng, R., Yang, Y., Li, A., Hong, H., Peng, J. and Liu, K. (2014).
Distribution, cleavage and lipidation of Atg8 fusion proteins in *Spodoptera litura* SI-HP
Cells. PLoS ONE 9(5): e96059. doi:10.1371/journal.pone.0096059.

Chapter 4. Cloning, characterization and effect of *TmPGRP-LE* gene silencing on survival of *Tenebrio molitor* against *Listeria monocytogenes* infection

4.1 Abstract

Peptidoglycan recognition proteins (PGRPs) are a family of innate immune molecules that recognize bacterial peptidoglycan. PGRP-LE, a member of the PGRP family, selectively binds to diaminopimelic acid (DAP)-type peptidoglycan to activate both the immune deficiency (Imd) and proPhenoloxidase (proPO) pathways in insects. A PGRP-LE-dependent induction of autophagy to control *Listeria monocytogenes* has also been reported. We identified and partially characterized a *PGRP-LE* homologue, from *Tenebrio molitor* and analyzed its functional role in the survival of the insect against infection by a DAP-type PGN containing intracellular pathogen, *L. monocytogenes*. The cDNA is comprised of an open reading frame (ORF) of 990 bp and encodes a protein of 329 residues. *TmPGRP-LE* contains one PGRP domain, but lacks critical residues for amidase activity. Quantitative RT-PCR analysis indicated a broad constitutive expression of the *TmPGRP-LE* transcripts at various stages of development spanning from larva to adult. RNAi-mediated knockdown of the *TmPGRP-LE* transcript, followed by a challenge with *L. monocytogenes*, resulted in a significant reduction in survival rate of the larvae, suggesting a putative role of *TmPGRP-LE* in sensing and control of *L. monocytogenes* infection in *T. molitor*. These results implicate *TmPGRP-LE* as a defense protein necessary for survival of *T. molitor* against infection by *L. monocytogenes*.

4.2 Introduction

Innate immunity serves as a major line of defense in insects and recognizes, modulates and signals effector functions against invading pathogens. The first important step in innate immunity is the recognition of pathogen-associated molecular patterns (PAMPs), which are exclusively found in microbes as dangerous, non-self entities. This role is accomplished through the activity of various molecular families capable of sensing the presence of invading microbial pathogens in either hemolymph or various immune cells (hemocytes, fat cells, gut epithelial cells) of host organisms (Yano and Kurata, 2011). Such molecular families, collectively called pattern recognition receptors (PRRs), include the toll-like receptors in mammals, and β -1,3-glucan recognition proteins (β GRPs), Gram-negative binding proteins (GNBPs) and peptidoglycan recognition proteins (PGRPs) in insects and other invertebrates.

Peptidoglycan (PGN), a PAMP in the cell walls of both Gram-positive and Gram-negative bacteria, consists of *N*-acetylglucosamine and *N*-acetylmuramic acid in β -1,4 linkages, cross-linked by short peptide stems composed of alternating L- and D-amino acids (Schleifer and Stackerbrandt, 1983). The PGRP family of PRRs is an integral component of host innate immune response as its members are required for the recognition of PGNs and for subsequent activation of antimicrobial peptides (AMPs) (Dziarski and Gupta, 2006). PGRPs were first characterized in the moths, *Bombyx mori* and *Trichoplusia ni* (Yoshida et al., 1996; Kang, et al., 1998), and have since been identified in insects, mollusks, echinoderms and vertebrates (Dziarski and Gupta, 2006b; Ni et al., 2007), but not in plants and nematodes. In insects, up to 19 different PGRPs have so far been identified (Dziarski and Gupta, 2006). In *Drosophila*, members of the PGRP family have been found in the hemolymph and on the surface and/or inside immune competent cells (Lemaitre et al., 2007; Yano et al., 2008). Some of these

members have been classified as catalytic PGRPs, including PGRP-SC1a, SC1b and PGRP-LB, which cleave PGN between *N*-acetylmuramic acid of the backbone and L-alanine in the stem peptide (Kim et al., 2003; Mellroth et al., 2003). Others are the non-catalytic forms including PGRP-SA, PGRP-LE, PGRP-LC and PGRP-SD and constitute the majority of known PGRPs. These can bind to PGNs leading to the activation of the Toll and Imd signal transduction pathways. These pathways eventually control the production AMPs through either nuclear factor kappa-light-chain-enhancer of activated B cell (NF- κ B) or Relish transcription factors (Yano et al., 2008).

Although most PGRPs function as extracellular microbial sensors, PGRP-LE has been shown to play a role in intracellular bacterial recognition in addition to its extracellular roles (Takehana et al., 2002). Yano et al. (2008) demonstrated that DmPGRP-LE is responsible for recognition of an intracellular DAP-type PGN containing the bacterium, *Listeria monocytogenes* and subsequently inducing autophagy to inhibit the pathogen's growth in the cytosol of *Drosophila* immune cells. PGRP-LE is known to be present in both the hemolymph and inside immune cells and specifically binds to the *meso*-diaminopimelic acid (DAP)-type PGN. In the hemolymph, PGRP-LE preferentially activates Imd signaling pathway in a non-cell autonomous manner and depends mainly on the activity of another member of the family, PGRP-LC (Mellroth et al., 2003). Such a synergistic action of PGRP-LE and PGRP-LC has been reported in *Drosophila*, wherein the single mutants (*PGRP-LE*¹¹² and *PGRP-LC*⁷⁴⁵⁴) showed complete resistance but the double mutants (*PGRP-LE*¹¹²/*PGRP-LC*⁷⁴⁵⁴) were found susceptible against *E. coli*. Also, while *PGRP-LC* mutant *Drosophila* flies had highly reduced expression of AMPs after infection with *E. coli* and other Gram-negative bacteria such as *Erwinia carotovora*, *PGRP-LE* mutants showed normal expression of transcripts (Takehana et al., 2004).

In the mealworm beetle, *Tenebrio molitor* (Coleoptera: Tenebrionidae), roles of individual PGRP family members, such as PGRP-SA and PGRP-SC2 have been reported (Park et al., 2007; Yu et al., 2010). TmPGRP-SA acts by binding to Lys-type PGN leading to the recruitment of GGBP1 and modular serine proteases to form a complex which acts as an initial activator triggering serine protease cascades in the Toll and proPO pathways in response to infections (Park et al., 2007). Similarly, TmPGRP-SC was confirmed to be specifically induced by injection of monomeric DAP-type and polymeric DAP- and Lys-type PGN into *Tenebrio* larvae. Moreover, TmPGRP-SC2 showed strong *N*-acetylmuramic-L-alanine amidase activity against DAP-type PGN and only a weak activity against Lys-type PGN (Yu et al., 2010). In this study, we identified and partially characterized a *TmPGRP-LE* homologue in *T. molitor*. We performed RNAi to study the functions of *TmPGRP-LE* in the host's ability to control and survive against *L. monocytogenes* infection.

4.3 Materials and methods

4.3.1 Insect collection and maintenance

T. molitor larvae were procured from College of Pharmacy, Pusan National University, Busan, South Korea and maintained on wheat bran meal in an environmental chamber at 26 ± 1 °C with $60\% \pm 5\%$ relative humidity and a 16:8 h light and dark cycle. Only late-instar larvae were used for all experiments unless otherwise stated. To ensure uniformity in size, the larvae were separated according to their physical sizes using a set of laboratory test sieves (Pascall Eng. Co. Ltd, Crawley, Sussex, UK).

4.3.2 Chemicals

All chemicals used for the experiments were of analytical grade, obtained from Sigma Chemical Co. (St. Louis, MO, USA) unless otherwise mentioned in the text.

4.3.3 Bacterial strains and media

L. monocytogenes strain ATCC 7644 used in the study was directly procured from the American Type Culture Collection (ATCC) and the *E. coli* ATCC 25922 strain was a kind gift from Prof. Oh, S.-J., Division of Animal Science, Chonnam National University, Gwangju, South Korea. The media used for the multiplication and colony forming unit (CFU) determination of bacteria were (i) Luria Bertani (LB) [Tryptone 10 g, Yeast extract 5 g, Sodium chloride 10 g (pH, 7.0) per liter] and (ii) Brain-heart infusion (BHI) for *E. coli* and *L. monocytogenes*, respectively.

4.3.4 Construction of full-length enriched cDNA library of *T. molitor* larvae

Total RNA from *T. molitor* larvae ($n = 200$) was isolated by TRIzol reagent (Molecular Research Centre, Inc., Cincinnati, OH, USA) after homogenization using TissueLyser (Qiagen, Valencia, CA, USA) and subsequently mRNA was purified using Absolutely mRNA

Purification Kit (Stratagene, Santa Clara, CA, USA). The cDNA library was synthesized using Express cDNA Synthesis Kit (Stratagene, Santa Clara, CA, USA). The cDNAs of more than 500 bp in length were ligated into pBK-CMV vector (Agilent Technologies, Inc., Santa Clara, CA, USA) and packaged using the ZAP expression cDNA Gigapack[®] III Gold cloning kit (Stratagene, Santa Clara, CA, USA) according to manufacturer's instructions. cDNA library clones (~2000) were cultured in Terrific broth (TB) medium containing kanamycin (50 mg/mL) at 37 °C for 15 h. Plasmid DNAs extracted from the selected colonies were sequenced by ABI 3730 XL capillary sequencer (Applied Biosystems, Foster City, CA, USA). Clones corresponding to the partial sequence of *PGRP-LE* (*TmPGRP-LE*) were identified, by conducting BLASTX with Swissprot analysis (EMBL-EBI, Hinxton, Cambridge, UK). By using the plasmid DNA as templates, full-length sequencing was performed by a clone-by-clone primer walking method using a Model 3730 XL sequence analyzer (Applied Biosystems, Foster City, CA, USA). Sequencing reaction was performed using the BigDye Terminator version 3.1 cycle sequencing kit (Applied Biosystems, Foster City, CA, USA). Sequences were assembled using the Phrap program (University of Washington, Seattle, WA, USA) (Ewing et al., 1998). Based on the assembled sequences, primers corresponding to the terminal sequences were designed using Primer3 (version 0.4.0, Whitehead Institute, Cambridge, MA, USA) (Untergrasser et al., 2012). The primer walking procedure was repeated until poly (A) tail region for the sequence was identified. The full-length sequences were finished by trimming the vector-derived sequences from both ends using the cross match program. The consensus full-length cDNA sequence of *TmPGRP-LE* obtained from 200 *T. molitor* larvae has been registered with the European Nucleotide Archive-European Bioinformatics Institute (ENA-EBI, Hinxton, Cambridge, UK) with the accession number HF935084.

4.3.5 *TmPGRP-LE* sequence analysis

The cDNA and deduced amino acid sequence of *TmPGRP-LE* was analyzed using UltraEdit-32 Professional Text/HEX editor (version 12.00, IDM Computer Solutions Inc., Hamilton, OH, USA) software package and deduced amino acid sequence was predicted by Open Reading Frame finder at National Centre for Biotechnology Information (NCBI) (<http://www.ncbi.nlm.nih.gov/gorf/gorf.html/>) and the Expert Protein Analysis System (Swiss Institute of Bioinformatics, Lausanne, Switzerland) at ExPASy bioinformatics resource portal (<http://www.expasy.org/>). The conserved protein domains were identified by using the Simple Modular Architecture Research Tool (SMART) (version 4.0, EMBL, Heidelberg, Germany). Multiple sequence analysis and percentage identity matrix of the conserved amidase/PGRP domains in the PGRP-LE homologue from *T. molitor* was done in comparison with other representative PGRP-LEs from insects using Clustal X (version 2.0.12, University of Strasbourg, Strasbourg, France) (Park et al., 2007). Protein sequences of PGRPs of representative insect groups were extracted from the GenBank repository at NCBI and have been presented in Table 4-1. The prediction of the putative signal peptide sequence was done at the Signal 4.0 server (www.cbs.dtu.dk). The protein sequence analysis tools used in the study for the prediction of theoretical M_w and isoelectric point (pI) was done at (<http://expasy.org>). ProtParam (<http://web.expasy.org/protscale/>) at ExPASy bioinformatics resource portal was used to compute the various physical and chemical parameters of the deduced protein sequence. PeptideCutter (http://web.expasy.org/peptide_cutter/) at ExPASy bioinformatics resource portal was used to predict the potential proteases cleavage sites in the sequence. ProtScale at ExPASy bioinformatics resource portal was used to compute and represent the profile produced by amino acid scale on the protein. The prediction of *N*-glycosylation sites was confirmed at NetNGlyc 1.0 server ([Technical University of Denmark, Lyngby, Denmark](http://www.cbs.dtu.dk)). Post-translational

modifications such as *N*-acetylation, *O*-glycosylation, phosphorylation and kinase-specific phosphorylation were predicted with the aid of NetAcet 1.0, NetOGlyc, NetPhos 2.0 and NetPhosK 1.0 server, respectively, (Technical University of Denmark, Lyngby, Denmark). The potential coding region was predicted using FGENESH (Softberry, Inc., Mount Kisco, NY, USA) (Solovyev et al., 2006). ORF and protein statistics were inferred by the EditSeq tool of Lasergene 9.0 software (DNASTAR Inc., Madison, WI, USA). The software was also used to study the codon usage, base composition in the ORF and predicted structural class of the protein.

4.3.6 Phylogenetic analysis

Prior to phylogenetic analysis, Clustal X software (version 2.012, University of Strasbourg, Strasbourg, France) was used to perform multiple sequence alignment of the conserved amidase/PGRP domains from the deduced amino acid sequence of PGRP-LE homologue in *T. molitor* in comparison with related conserved domain sequences of PGRPs in other representative insects. MEGA 5.0 (Tamura et al., 2011) software (The Biodesign Institute, Tempe, AZ, USA) was used to construct the consensus phylogenetic tree using the UPGMA method (Sneath, et al., 1973). The evolutionary distances for the representative sequences were computed using the Poisson correction and are in the units of the number of amino acid substitutions per site. The bootstrap values were estimated by 5000 replications.

Table 4-1: Accession numbers of PGRPs from various insect species used to generate the phylogenetic tree, percentage distance and identity matrices

Species name	Abbreviations	Accession numbers
<i>Tenebrio molitor</i>	TmPGRP-LE	HF935084
<i>Tribolium castaneum</i>	TcPGRP-LE	XP_968926.1
<i>Drosophila melanogaster</i>	DmPGRP-LEa	NP_573078.1
<i>Armigeres subalbatus</i>	AsPGRP-LE	AEX31482.1
<i>Camponotus floridanus</i>	CfPGRP-LE	EFN63542.1
<i>Aedes aegypti</i>	AaPGRP-LC	XP_001656352.1
<i>Culex quinquefasciatus</i>	CqPGRP-LC	XP_001842237.1
<i>Bombus terrestris</i>	BtPGRP-LC	XP_003396511.1
<i>Apis florea</i>	AfPGRP-LC	XP_003693124.1
<i>Bombus impatiens</i>	BiPGRP-SC2	XP_003396511.1
<i>Nasonia vitripennis</i>	NvPGRP-SC2	XP_001603488.1
<i>Apis florea</i>	AfPGRP-SC2	XP_003694493.1
<i>Culex quinquefasciatus</i>	CqPGRP-SB2	XP_001849091.1
<i>Aedes aegypti</i>	AaPGRP-SB2	XP_001654275.1
<i>Bombus terrestris</i>	BtPGRP-LB	XP_003400160.1
<i>Bombus impatiens</i>	BiPGRP-LB	XP_003493260.1
<i>Apis florea</i>	AfPGRP-LB	XP_003694545.1
<i>Apis mellifera</i>	AmPGRP-S2	NP_001157188.1
<i>Apis dorsata</i>	AdPGRP-S2	ACT66892.1
<i>Phlebotomus papatasi</i>	PpPGRP	ABV60369.1

4.3.7 Secondary Structure Prediction and Modeling

Secondary structure predictions of the conserved PGRP domain were performed using the consensus prediction program available at PSIPRED protein structure prediction server 2.6 (Bloomsbury Centre for Bioinformatics, London, UK) (Buchan et al., 2013). The generated consensus led to three possible states for each residue (“H”: alpha helix, “E”: Extended strand and “C”: Coil). The accuracy of prediction may reach a score of 80.7%. Three-dimensional structures were modeled using SWISS-MODEL, a fully automated protein structure homology modeling server (<http://swissmodel.expasy.org>) (Arnold et al., 2000) and TmPGRP-LE in complex with tracheal cytotoxin (monomeric DAP-type PGN) (PDB code: 2cb3) was used as the template. Model quality was evaluated by Anolea and QMEAN (Benkert, et al., 2011). The structure of the model was visualized by using PyMol molecular graphics system (version 1.5, Schrodinger, Cambridge, MA, USA).

4.3.8 Developmental- and Tissue-specific Expression Pattern of *TmPGRP-LE*

For the expression patterns of *TmPGRP-LE*, total RNA was isolated from the whole body ($n = 5$) at various stages of development in *T. molitor*, namely, late-instar larva (LIL), pharate pupa (PP), pupa day 1 to 7 (P1–P7) and adult day 1 and 2 (A1 and A2) using SV Total RNA isolation system (Promega Corporation, Madison, WI, USA) by following manufacturer’s instructions. Total RNA was also isolated from various tissues including gut, fat body, hemocytes, integument and Malpighian tubules of the larvae and ovaries and testes of the adults. Using total RNA, cDNA corresponding to each stage of growth and/or tissue sampled was synthesized using AccuPowerR RT PreMix kit (Bioneer, Daejeon, Korea) according to manufacturer’s instructions. cDNAs were used as templates for the quantitative PCR (qPCR) reactions performed on an Exicycler™ 96 real-time quantitative thermal block (Bioneer, Korea) using gene-specific primers (Table 4-2) at an initial denaturation of 95 °C for 20 s, followed by

45 cycles of denaturation at 95 °C for 5 s and annealing at 60 °C for 20 s. The $2^{-\Delta\Delta C_t}$ method was employed to analyze the expression levels of *TmPGRP-LE*. *TmL27a* was used as an internal control to normalize differences in concentration of templates between samples (Bustin, et al., 2011; mouillet et al., 1999).

Table 4-2: Primers sequences used in the current study.

Primer name	Primer direction	Sequence (5'-3')*
Oligo (dT) adaptor	R	GGCCACGCGTCGACTAGTACT17
M13-F	F	GTAAAACGACGGCCAG
M13-R	R	CAGGAAACAGCTATGAC
<i>RpL27a</i>	F	TCATCCTGAAGGCAAAGCTCCAGT
<i>RpL27a</i>	R	AGGTTGGTTAGGCAGGCACCTTTA
<i>TmPGRP-LE</i> qPCR	F	CTTCGCTTGCGGAATGGCAGATTA
<i>TmPGRP-LE</i> qPCR	R	AACACACGCTCAAATCCTTTCCCG
<i>TmPGRP-LE</i> dsRNA	F	TAATACGACTCACTATAGGGAGAGGCAACGTAAATAAGGACGG
<i>TmPGRP-LE</i> dsRNA	R	TAATACGACTCACTATAGGGAGAGTAGGCGATATCGTTCCACTTC

* Sequences are read from 5' to 3' end.

T7 polymerase recognition sequence is indicated in bold

F = Forward, R = Reverse.

4.3.9 RNA interference of *TmPGRP-LE*

The PCR product containing a *TmPGRP-LE* gene fragment was used to generate a template for *in vitro* transcription using gene-specific primers tailed with a T7 promoter sequence (Table 4-1). The dsRNA for *TmPGRP-LE* was synthesized using the Ampliscribe™ T7-Flash™ transcription kit (Epicentre Biotechnologies, Madison, WI, USA) according to manufacturer's instructions. ds*PGRP-LE* was purified by ammonium acetate precipitation and its integrity was checked by running on 1% agarose gel for 20 min at 100 V and quantified using NanoDrop spectrophotometer (Thermo Scientific, Wilmington, DE, USA). dsRNA for a gene encoding enhanced green fluorescent protein (*EGFP*) was also synthesized to serve as negative control. dsRNAs were stored at -20 °C until injected into *T. molitor* larvae. Cohorts of *T. molitor* larvae were injected with ds*PGRP-LE* or ds*EGFP* dissolved in injection buffer (0.1 mM sodium phosphate, 2.5 mM potassium chloride, pH 7.2) to a final amount of 1 µg/insect. Injections were done using a disposable needle mounted into a micro-applicator (Picospiritzer III micro dispense system, Parker Hannifin, Hollis, NH, USA) to which the pressure was carefully adjusted so that the contents could be safely released into the hemocoel of the larvae. dsRNAs were injected at the 2nd or 3rd visible sternite from the posterior end of the larvae chilled on ice and handled in a dorsal-ventral position. Animals surviving the injection process were reared on diet under standard rearing conditions until the extraction of total RNA.

To evaluate *TmPGRP-LE* gene silencing, total RNA was isolated five days post-injection of dsRNAs and subsequent cDNA synthesis was conducted as described above. cDNA was used as a template for semi-quantitative PCR amplification of the partial gene product using the gene-specific primers (Table 4-1). The PCR cycles were performed as follows: initial denaturation at 94 °C for 3 min followed by 28 cycles of denaturation at 94 °C for 30 s, annealing at 55 °C for 30 s, extension at 72 °C for 60 s and a final extension at 72 °C for 10 min

in a PTC-200 thermal cycler (MJ Research, GMI, Ramsey, MN, USA). Quantitative real-time PCR was performed on Exicycler™ 96 real-time quantitative thermal block (Bioneer, Korea) as previously described above. Data was analyzed by Student's *t*-test and differences of $p < 0.05$ were considered significant.

4.3.10 Bacterial injections and bioassays

The bacterial cultures were grown aerobically in LB broth (for *E. coli*) and BHI broth (for *L. monocytogenes*) in an orbital shaker at 200 revolutions per minute (rpm) and 37 °C. The overnight grown cultures were washed thrice, re-suspended in sterile distilled water and serially diluted in 0.9% saline to achieve desired concentrations as determined by measurements at OD₆₀₀. The OD₆₀₀ values were confirmed by aseptically spread-plating the serially diluted samples on LB and BHI agar plates for *E. coli* and *L. monocytogenes*, respectively. The plates were incubated at 37 °C for 16 h prior to colony counting.

To investigate the survival ability of *TmPGRP-LE*-depleted larvae against *Listeria* infection, larvae were injected with either *dsEGFP* or *dsPGRP-LE* as described above. Five days post-injection of dsRNA, larvae were challenged with 2 µL (~1000 CFU/Larva) of the diluted *Listeria* cultures. Treated larvae were incubated at 26 °C and the number of dead larvae was recorded on a daily basis for six days post injection. Rates of survival were compared between the *dsTmPGRP-LE*- and *dsEGFP*-treated groups. *E. coli*, which like *L. monocytogenes* is a DAP-type PGN-containing bacterium but (unlike *L. monocytogenes*) cannot survive in phagocytic cells, was included in the survival study to enable us to clearly establish the intracellular roles of *TmPGRP-LE* on *Tenebrio* immunity.

4.3.11 Statistical Analysis

Analysis of the qPCR data was done according to the $2^{-\Delta\Delta Ct}$ method, where $\Delta\Delta Ct$ is equal to ΔCt (treated sample) – ΔCt (control) (Schmittgen et al., 2008). Data from insect survival study was analyzed by the Wilcoxon-Mann Whitney test (Statistical Analysis Software, Cary, NC, USA). For the cumulative survival rates (%), a p -value < 0.05 was considered significant.

4.4 Results and Discussion

4.4.1 Characterization of *TmPGRP-LE* full-length cDNA

A single expressed sequence tag (EST) homologous to known and fully characterized PGRPs of other organisms was identified from the sequencing of random clones of *T. molitor* cDNA library. Re-sequencing of the identified EST yielded a full-length sequence comprised of 1248 nucleotides (Figure 4-1). The *TmPGRP-LE* open reading frame (ORF) is comprised of 990 nucleotides encoding a protein of 329 amino acids with a predicted molecular weight of 37.3 kDa. The 5'- and 3' UTR regions comprised of 119 and 72 bp, respectively. No signal peptide was predicted suggesting its existence in the cytoplasm, where it acts as an intracellular receptor for DAP-type PGN (Mellroth et al., 2003). Intriguingly, the extracellular roles of PGRP-LE upstream of and in coordination with PGRP-LC to recognize PGN and activate the Imd pathway have been reported (Takehana et al., 2004; Kaneko et al., 2006). However, the lack of signal peptide in *TmPGRP-LE* is consistent with the observation that other long-form members of the family such as PGRP-LA, LC and LD possess no signal peptides (Gosh et al., 2011; Bao et al., 2013) despite being transmembrane proteins. Furthermore, PGRP-LB, which is not a transmembrane protein, is reported to lack a signal peptide (Bao et al., 2013).

The putative glycosylation sites in *TmPGRP-LE* were predicted at position N39 and N135 with glycosylation potential of 0.689 and 0.604, respectively. Putative phosphorylation sites in deduced amino acid sequence of *TmPGRP-LE* were predicted to be serine at positions 10, 36, 41, 47, 54, 172, 183, 185, 208, 225 and 296, threonine at position 58 and tyrosine at position 49, 102, 126, 170, 189, 227 and 285 (Blom et al., 2004). The prediction for *N*-acetylation was positive, as there was a serine at position 3 in the amino acid sequence of *TmPGRP-LE*. The theoretical pI of the protein was 5.97 (charge at pH 7.0 = -5.099), and the molecular mass was 37.3kDa as predicted by Protean software analysis program of Lasergene

suite. Apart from the above, the compositional analysis of TmPGRP-LE included 33 strongly basic (10.0%), 39 strongly acidic (11.9%), 100 hydrophobic (30.4%) and 106 polar (32.2%) amino acid residues with the charged residue count of 104 (31.6%) (Nishikawa et al., 1986). TmPGRP-LE also showed a highly charged *N*-terminal domain connected to the PGRP domain. The computed extinction coefficient of the protein was $46,130 \text{ M}^{-1}\cdot\text{cm}^{-1}$, in case all the cysteines in the sequence form cystines and $45,380 \text{ M}^{-1}\cdot\text{cm}^{-1}$, in case all the cysteines get reduced. These computational values may be considered reliable as TmPGRP-LE contains tryptophan residues. Normally, proteins without tryptophan residues can form a 10% error in the extinction coefficient predictions. The instability index for the protein was 38.65, which classified the protein as stable, whereas the aliphatic index was 83.83. Also, the general average of hydropathicity (GRAVY) plot, calculated as the sum of hydropathy values of all amino acid residues in the sequence, was -0.416 , suggesting its elevated hydrophilic properties (Kyte and Doolittle, 1982).

To understand the homology of the gene product from *T. molitor* genome, we conducted BLAST analysis with the deduced amino acid sequence (results not shown). The sequences found were used to search for additional members of the PGRP gene family. TmPGRP-LE sequence showed highest similarity of 65% with that of its close relative, *Tribolium castaneum* PGRP-LE (TcPGRP-LE), followed with a low homology of about 38% with unrelated companion, *Armigeres subalbatus* PGRP-LE (AsPGRP-LE).

Furthermore, the analysis included the majority of known PGRP homologues and their isoforms from *D. melanogaster*, grouped into two major classes of short (including PGRP-SA, SB1 and SB2, SC1A and SC1B, SC2 and SD) and long (PGRP-LA, LB, LC, LD, LE and LF) forms. The classes of PGRP homologues, their distribution and diversification within the *Drosophila* genome have been reported (Werner et al., 2000). TmPGRP-LE showed a homology

of about 36% with *D. melanogaster* PGRP-LE-A and PGRP-LE-B isoforms (DmPGRP-LE-A and DmPGRP-LE-B), as well as DmPGRP-LB (isoforms A, B, E and F), and a homology of about 33% with DmPGRP-LF and other DmPGRP-LB isoforms such as A, C and D. The amino acid sequence homology of TmPGRP-LE with shorter forms of *Drosophila* PGRPs was in the range of 30%–34% with maximum relatedness to DmPGRP-SB2. The multiple sequence alignment and percentage identity analysis showed a significant variability in the number and pattern of *N*-terminal amino acids within the PGRPs characterized from insects thus far. This reflects the categorization of the family into PGRP-S, that are usually small (about 20 kDa) and predominantly secreted extracellular proteins, intermediate forms (PGRP-I) that are 40–45 kDa transmembrane proteins and PGRP-Ls up to 90 kDa, which may be intracellular, transmembrane, or extracellular proteins (Dziarski and Gupta, 2006).

We further dissected the TmPGRP-LE sequence by the identification of PGRP domain signature sequence using the SMART analysis program (Figure 4-2A). As expected, the highly conserved PGRP domain spanning from amino acid residue 148 to 293 (E-value 4.95×10^{-59}), was found overlapping with the predicted amidase domain spanning from amino acid number 162 to 299 (E-value 2.97×10^{-11}) at the *C*-terminus. All PGRPs share a highly conserved PGRP domain (approximately 160 amino acids on their *C*-termini) with similarities to the zinc-dependent *N*-acetylmuramoyl-L-alanine amidase of bacteriophage T7 lysozyme (Bao et al., 2013; Gelius et al., 2003; Liu et al., 2001; Mellroth et al., 2003; Wang et al., 2003). Therefore, we found it appropriate to discuss the predicted PGRP domain of TmPGRP-LE in comparison with similar sequences from other representative insects. In order to predict the catalytic and specific PGN recognition residues in TmPGRP-LE, we conducted analysis of the 129 amino acid residues in the PGRP domain (from amino acid 173 to 293). For the same, we made a comparison of the domain with similar domains of PGRP-LE families in insects by amino acid

sequence alignment, percentage identity matrix, and phylogenetic tree analysis. The alignment of PGRP domain of TmPGRP-LE was used to examine the amino acid residues that form the Zn²⁺ binding site, responsible for catalytic (amidase) mode of action (Figure 4-2B). Structural studies have highlighted that the zinc-binding activities in PGRPs are primarily coordinated with the help of two histidines in the overlapping domain and a cysteine in the binding groove of PGRP domain. Although the residues are strictly conserved in PGRPs (especially in fish and humans), the non-catalytic PGRPs lack the potentiality of binding to Zn²⁺.

In the case of TmPGRP-LE, the lack of a histidine and a cysteine at position 8 and 126 in the amidase/PGRP domains may be relevant in explaining its non-catalytic (non-amidase) activity on PGN (Mellroth et al, 2006). The position of amino acid 297 is always associated with a cysteine with amidase activity in PGRPs and most often is occupied by serine in PGRPs devoid of amidase activity. *T. castaneum* PGRP-LB (TcPGRP-LB) and PGRP-SB (TcPGRP-SB) also contain key residues for an amidase activity (Zou et al., 2007). Similarly, in humans, PGLYRP-2 possesses *N*-acetylmuramoyl-L-alanine amidase activity while PGLYRP-1, PGLYRP-3 and PGLYRP-4 do not (Liu et al., 2001; Wang et al., 2003).

Catalytic residues related to amidase activity have been reported in *Crassostrea gigas* PGRP (CgPGRP) proteins (Zhang et al., 2013) and *Sciaenops ocellatus* PGRP homologues (Li et al., 2012). The three residues (39G, 40W, 61R) involved in PGN recognition (Swaminathan et al., 2006) are highly conserved with a certain degree of mutation, indicating their critical function and also the evolutionary pressure to serve in the capacity of PGN recognition. It has to be noted here that, PGN structures from different bacteria present a remarkable set of variability in their peptide stems, with certain degree of cross-linking adding to variability. PGN recognition sites are thus expected to vary accordingly. In TmPGRP-LE, and its close counterpart TcPGRP-LE, the substitution (39G to K) may indicate that affinity and/or specificity to PGN might differ from other members of the family.

ATTCGGCCATTACGGCCGGGGATTCCGTCACGTGACGTTCTTAACAAAGTGCAATGTGG	
TTGCACTAAGTCGTTCTATGCTCTCCAGTTTTCGGGCAAATGTACTAACTAGAAACCAATG	
ATGGAAAGTGACGCAACAAGACTTAGTGCCGTTTGTAAAGTAAATAACTGTGGCAACGTA	60
M E S D A T R L S A V C K V N N C G N V	20
AATAAGGACGGAACGATTGAAATGATCAATCAGTGCAGAAAATCACTGGACAATTGTAGT	120
N K D G T I E M I N Q C R K S L D N C S	40
TTGGGTGATGATTGTTTCGTTGTACGAGGATAGAATAAGTGCAGAAAGCGACACTTGATAGG	180
L G D D C S L Y E D R I S A E A T L D R	60
TTTGATGAGGGCAAATGGTTTTGGAAAACGAGAATGTCTGTATGACGAATAAAATGTGTT	240
F D E G K M V L E N E N V C M T N K I V	80
GGGAAGAATAATAACGACATGCTCATTTTTGACAACATAATGAATAAGAAGCCCAACCAC	300
G K N N N D M L I F D N I M N K K P N H	100
TACAAAAACATTGAGTTTACCAATCCCAAAATGTTTATATCGGCGACGTAACCCACATA	360
Y K N I Q I Y Q S Q N V H I G D V T H I	120
AACGGCCCAATTTACATAAACCAATTAACCCCAACGATAAATCAAACCATCAGATCAAC	420
N G P I Y I N Q L T P T I N Q T I T I N	140
ACAAACACACGCTCAAATCCTTTCCCGATAGTTGATCGCCGGACGTGGCTAGCACAAACC	480
T N T R S N P F P I V D R R T W L A Q P	160
CCCCTAGACCCCGAAGACGTGAAATATTTCTCATCACCTCGCAAGTTCGTAATAATCTGC	540
P L D P E D V K Y F S S P R K F V I I C	180
CATTCGCAAGCGAAGAGGCCTACACCCAAACGGACAACAACACTGTTGGTTGCTGTGATT	600
H S A S E E A Y T Q T D N N L L V R L I	200
CAACAGTTCACGTCGAAAGTCGGAAGTGAACGATATCGCCTACAATTTTCTAGTGGGG	660
Q Q F H V E S R K W N D I A Y N F L V G	220
GCGGATTGCAGCATTACGAAGGGCGCGGATGGGATATCATCGGGGCTCACACCCCTCGAC	720
A D C S I Y E G R G W D I I G A H T L D	240
TACAACTCCATTTCGATAGGAATATGTTTCATTGGATGCTACATGAACAAATGCGCGCG	780
Y N S I S I G I C F I G C Y M N K L P P	260
CCCGGAGTGTGAAGATGGCGCAGGAGTTTATCAGATATGGGGTCAAGATAGGGGCCATT	840
P G V L K M A Q E F I R Y G V K I G A I	280
GCGGAGGATTATGTGCTTTTGGACATTGCCAGTGCAGGAGCAGCGAGAATCCGGGGAGG	900
A E D Y V L L G H C Q C R S S E N P G R	300
AAGTTGTTTGAAGAGATTCAGAAATGGGATCGGTGGGATGGGTCCATCAGCGTGGCAAT	960
K L F E E I Q K W D R W D G S I S V G N	320
CCGTCGCGGTTAAAGATTCAACACAGTTAA	990
P S P L K I Q H S *	330
CACACTCTCTAGAATCGATATTGATTTTTATTAACGTTTGATTTATGAGCAAATACAAG	
ACTTATTATTTTTAA	
AAAAAAAAAAAAAAAAAAAAA	

Figure 4-1: Nucleotide and deduced amino acid sequence of a homologue of PGRP-LE

from *T. molitor*.

The nucleotides and amino acids are numbered along the right margin beginning with the translation start (ATG) and ending with the stop codon (TAA) highlighted with an asterisk. The amidase and PGRP domains have been shaded and underlined, respectively. The predicted N-glycosylation sites have been shown in green boxes. The predicted serine, threonine and tyrosine phosphorylation targets are shown in blue boxes. The conserved zinc binding residues are encircled. The predicted PGN recognition residues are boxed.

4.4.2 Phylogenetic analysis of TmPGRP-LE

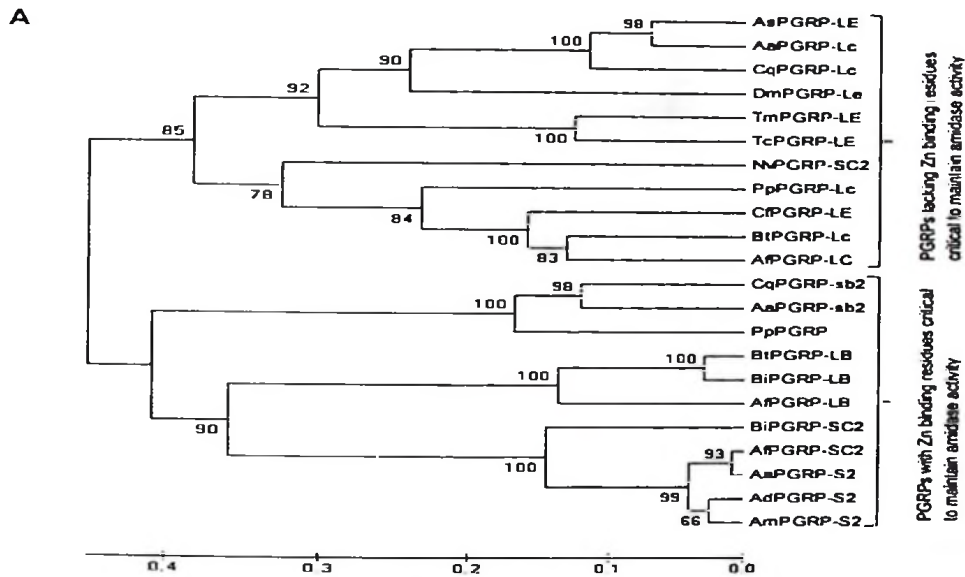
To deduce the phylogenetic relationship of TmPGRP-LE with PGRP domains of other representative members, we constructed a distance tree using the unweighted pair group method with arithmetic mean (UPGMA). The consensus of the tree was inferred from 5000 bootstrap replications, with most relationships found to be uncertain. This suggested that the PGRP family is highly diversified (Figure 4-3A) with two major groups identified based on the amidase activity. TmPGRP-LE was grouped in the PGRP class lacking Zn-binding residues and was placed together with TcPGRP-LE.

The separation of short and long forms of PGRPs reflects separated evolutionary histories with all the short *PGRP* genes derived from an ancestral pattern with two introns and subsequently losing out on one or both of introns during the course of evolution (Werner et al., 2000). The introns in long PGRPs do not correspond to introns of short genes as previously shown in *Drosophila* (Werner et al, 2000). However, PGRP-LB is an exception as it clusters with the short or the long forms depending on the sequences used for comparison.

Percentage identity matrix of the selected PGRP domains indicated greater levels of homology as compared to full-length cDNA (Figure 4-3B). The identities among the sequences increased appreciably due to the conserved status of the domains, and were about 80% with TcPGRP-LE and 55% with DmPGRP-LE-A. The homology of TmPGRP-LE with PGRPs from mosquitoes such as *Armigeres subalbatus* PGRP-LE (AsPGRP-LE), *Aedes aegypti* PGRP-LC (AaPGRP-LC) and *Culex quinquefasciatus* PGRP-LC (CqPGRP-LC) was in the range of 54%–57%. This conforms to the earlier report on beetle and mosquito *PGRP-LA* genes encoding two alternative splice forms and *PGRP-LA* and *-LC* genes placed next to each other in the same cluster (Zou et al., 2007).

4.4.3 Secondary Structure and Homology Modeling of TmPGRP-LE

The secondary structure prediction of TmPGRP-LE was done using PSIPRED software, and it indicated that TmPGRP-LE is composed of sheet, coil, and helical regions (Figure 4-4A). The low complexity in the *N*-terminal region is evident, as most of the structure takes the form of coils with interspersed sheet and helix regions. The tertiary structure of PGRP domain was constructed using *Drosophila* PGRP-LE in complex with tracheal cytotoxin as a template (PDB: 2cb3) (Figure 4-4B) (Lim et al., 2006). TmPGRP-LE PGRP domain model showed the presence of a central β -sheet with five β -strands and three α -helices. A previous report has suggested that amino acid residues subject to positive selection are basically located at the periphery of coils and α -helices rather than in central β -sheet or active center, a finding that is consistent with the insect PGRP family (Mendes et al., 2010).



B

	1	2	3	4	5	6	7	8	9	10	11	12	13	14	15	16	17	18	19	20	21	22	
1 TmPGRP-LE	100	90	57	54	57	55	51	50	50	43	46	46	43	47	45	45	42	47	46	47	47	47	47
2 TcPGRP-LE		100	57	57	60	58	50	50	50	43	53	47	47	45	49	49	43	50	49	49	50	50	50
3 AaPGRP-LE			100	60	83	85	56	56	55	47	52	40	39	42	44	44	44	47	45	47	47	47	45
4 AaPGRP-Lc				100	83	84	60	57	56	49	53	40	39	40	46	46	43	47	45	47	48	47	48
5 CqPGRP-Lc					100	82	66	54	54	52	54	39	40	40	45	45	41	47	45	48	48	48	48
6 DmPGRP-LE						100	49	50	48	44	51	42	41	41	43	43	43	44	43	45	46	46	46
7 BtPGRP-Lc							100	84	78	57	60	45	47	45	47	48	43	47	45	47	50	48	48
8 ApPGRP-Lc								100	80	57	60	48	46	50	51	51	47	48	47	48	51	50	50
9 CpPGRP-LE									100	54	60	46	49	47	47	44	44	50	48	50	52	51	51
10 NpPGRP-SC2										100	53	42	43	43	44	44	46	46	48	48	47	47	47
11 PpPGRP-Lc											100	47	46	45	48	47	44	50	48	50	52	53	53
12 CqPGRP-sb2												100	81	72	49	49	49	50	50	49	50	50	50
13 AaPGRP-sb2													100	71	50	50	49	50	50	49	50	50	50
14 PpPGRP														100	49	49	48	49	49	49	49	49	49
15 BtPGRP-LB															100	65	75	54	54	55	55	55	
16 BtPGRP-LB																100	75	54	54	55	55	55	
17 ApPGRP-LB																	100	52	52	53	53	53	
18 BtPGRP-SC2																		100	98	93	93	93	
19 AaPGRP-S2																			100	91	92	92	
20 AdPGRP-S2																				100	94	94	
21 AmPGRP-S2																					100	81	
22 BtPGRP-SC2																						100	

Figure 4-3: Molecular phylogenetic and percentage identity analysis of TmPGRP-LE.

(A) Phylogenetic analysis as performed by MEGA 5.0 software with representative PGRP gene family members. The percentage of replicate trees in which the associated taxa clustered together in bootstrap test (5000 replicates) is shown on interior branches. The abbreviations and accession numbers of the sequences used have been presented in Table 4-1.

(B) Percentage identity matrix of the representative species as inferred using ClustalX 1.83.

4.4.4 Developmental- and Tissue-specific Expression Patterns of *TmPGRP-LE*

We analyzed the expression patterns of *TmPGRP-LE* gene, during various developmental stages (late larval, pupal and adult stages) and tissues including the larval gut, fat body, hemocytes, integument, and malphigian tubules and adult ovaries and testes by quantitative PCR. The *TmPGRP-LE* transcript was constitutively expressed at all stages of growth analyzed with lowest transcript levels observed at pupal stage (day 5) (Figure 4-5). The *TmPGRP-LE* transcripts were also detected in all the tissues analyzed. Similar patterns of expression of PGRPs have been reported in *D. melanogaster* (Werner et al., 2000; Takehana et al., 2002) suggesting that long PGRPs, a sub-group to which *PGRP-LE* belongs, are constitutively expressed in insects with an exception of *PGRP-LB*, which is inducible upon immune challenge.

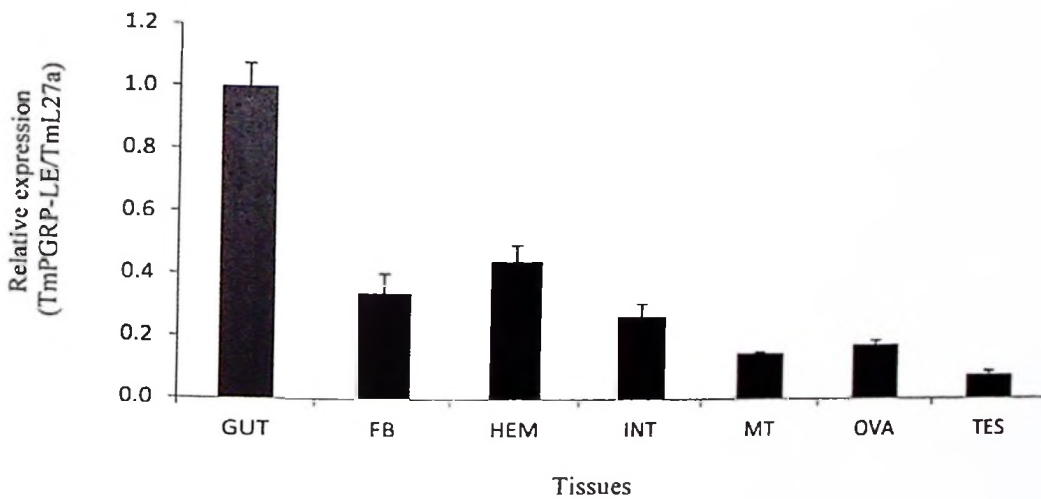
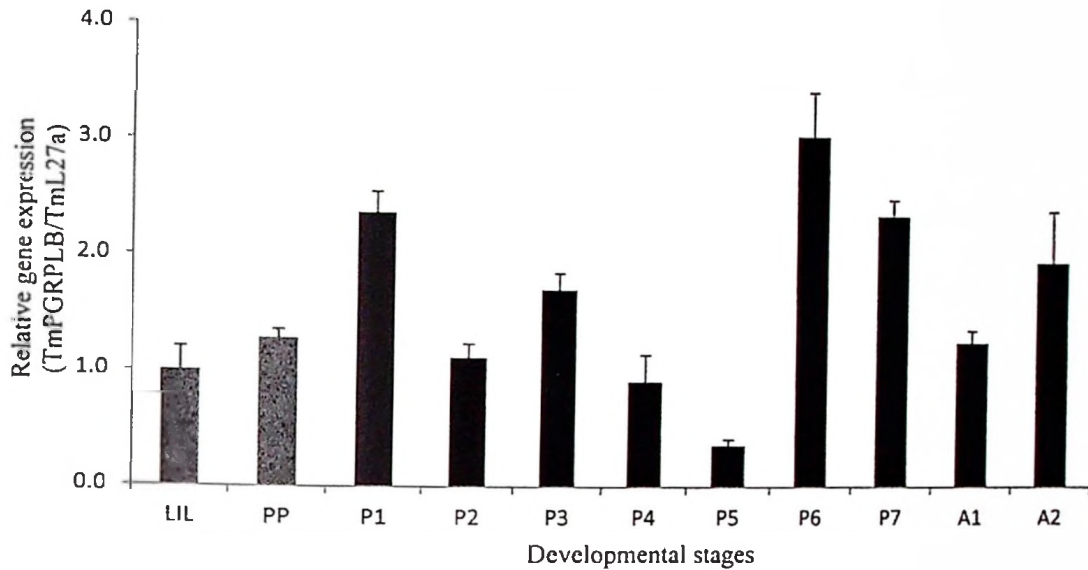


Figure 4-5: developmental and tissue-specific expression patterns of *TmPGRP-LE*.

Top: *TmPGRP-LE* transcripts at various developmental stages were quantified by real time PCR. LIL = Late-instar larva; P1-P7 = Pupa day 1 to pupa day7; A1, A2 = Adult day 1, and day 2, respectively. Bottom: Tissue-specific expression pattern of *TmPGRP-LE* as determined by real time PCR. GUT, FB, HEM, INT, MT, OVA and TES represent gut, fat body, hemocytes, integument and Malphigian tubules of larvae and ovaries and testes of the adults, respectively. Data are shown as mean \pm standard deviation (n = 3).

4.4.5 RNAi-mediated knockdown of *TmPGRP-LE* leads to reduced survival rate of *T. molitor* larvae infected with *L. monocytogenes*

PGRP-LE is known to recognize DAP-type PGN containing bacterial intruders into the host system and preferentially activate the Imd pathway. It was, therefore, hypothesized that down-regulation of *TmPGRP-LE* by RNAi would (i) impact the expression levels AMPs and (ii) compromise the host's ability to recognize and control intracellular *L. monocytogenes*. To this end, we first knocked down *TmPGRP-LE* transcripts by injecting ds*PGRP-LE* to Late-instar larvae (LIL) as described above. Following successful knockdown of *TmPGRP-LE* transcripts by RNAi (Figure 4-6A), the expression patterns of anti-microbial peptides (AMP) genes including *TmCecropin*, *TmColeoptericin*, *TmDefensin*, *TmLysozyme*, *TmTenecin 1*, *TmTenecin 2* and *TmTenecin 3* was monitored before and after challenge with DAP-type PGN-containing bacteria, *E. coli* and *L. monocytogenes*. The knockdown of *TmPGRP-LE* was unable to bring any significant change in the expression levels of the AMPs with or without bacterial challenge. This could be partly due to a redundancy between PGRP-LE and -LC in sensing DAP-type PGN and subsequent activation of Imd pathway. In *Drosophila*, *PGRP-LE¹¹²/PGRP-LC¹⁵⁴* double mutants were found to be more susceptible to *E. coli* infections than either of the mutants alone (Takehana et al., 2004). Furthermore, DmPGRP-LE has been shown to be dispensable *in vivo*, for systemic sensing of the monomeric form of PGN (the tracheal cytotoxin, TCT) and the activation of Imd pathway following infections by DAP-type PGN-containing bacteria such as *E. coli* and *Erwinia carotovora* 15 (Takehana et al., 2004; Neyen et al., 2012). Taken together, we believe that *TmPGRP-LE* plays an indispensable role in sensing the extracellular PGNs and that it may putatively activate Imd pathway upon infection by DAP-type peptidoglycan, more so under conditions where *PGRP-LC* expression remains unaltered.

The suggestions that the cytosolic recognition of the monomeric form of DAP-type PGN (TCT) by PGRP-LE, is neither dispensable nor PGRP-LC-dependent (Lemaitre and Hoffmann, 2007; Neyen et al., 2012) led us to hypothesize that TmPGRP-LE may play a role in the control of *L. monocytogenes* infection in the host, thus improving its survivability. To examine the effects of *TmPGRP-LE* RNAi on the ability of *T. molitor* L1L to survive *E. coli* and *L. monocytogenes* infections, we performed a larval survival assay by challenging *TmPGRP-LE* RNAi larvae with *E. coli* and *L. monocytogenes*. The survival data revealed a differential rate of survival between *dsPGRP-LE* and *dsEGFP*- injected larvae when challenged with *L. monocytogenes*. The *TmPGRP-LE* knockdown group showed a significantly reduced survival rate ($p < 0.05$) when compared with the control group (Figure 4-6B-i). This difference in survival rate was not observed when *E. coli* was inoculated (Figure 2-6B-ii). The survival curves for both the knockdown and control group were similar in the case of *E. coli* treatment. This indicates that neither groups showed superiority in the resistance against *E. coli* infections. The finding that *TmPGRP-LE* RNAi did not alter the survival of *T. molitor* larvae after *E. coli* challenge is in general agreement to a previous report (Wang and Beerntsen, 2013) in which *AsPGRP-LE* RNAi did not affect the survival rates of a mosquito *Armigeres sabalbatius*, after challenge by *E. coli* and *Micrococcus luteus*, despite the fact that the knockdown caused significant reductions in the transcription of two AMP genes, *Cecropin A* and *Defensin C1*. In *Drosophila*, intracellular PGRP-LE has been shown to be responsible for detecting the invading *L. monocytogenes* and subsequently inducing its autophagic control (Yano et al., 2008). Our data showed that *TmPGRP-LE* RNAi makes *T. molitor* very susceptible to *L. monocytogenes* infections, suggesting that TmPGRP-LE is also involved in the recognition and/or immune responses to DAP-type PGN containing bacteria.

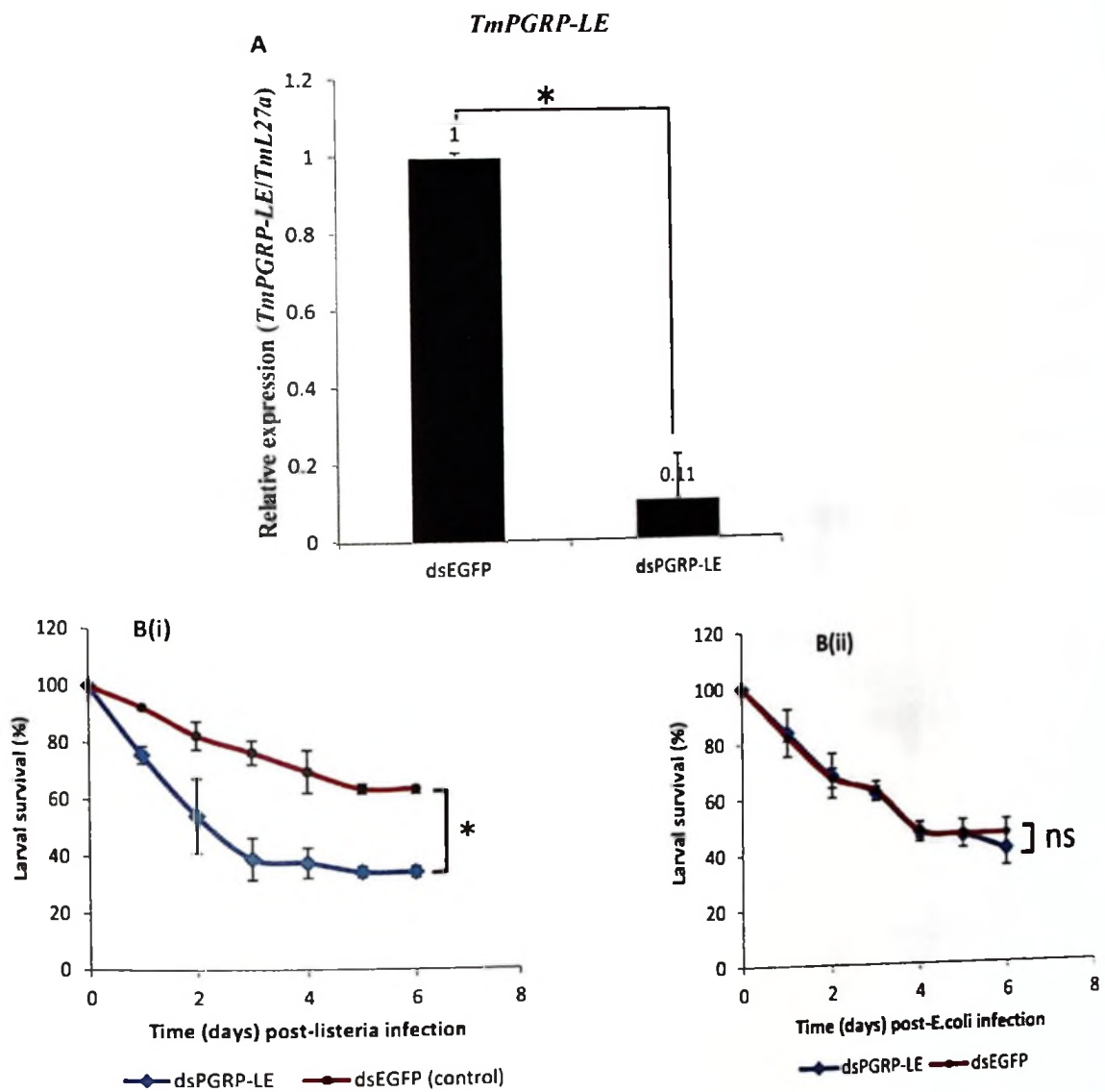


Figure 4-6: Effect of *TmPGRP-LE* knockdown on the survivability of *T. molitor* larvae

(A) *TmPGRP-LE* transcripts in the larvae of *T. molitor* after RNAi. dsEGFP-injected larvae were used as a negative control. (B) Survival pattern of *T. molitor* larvae following immune challenge by *L. monocytogenes*. *TmPGRP-LE* deficient larvae exhibited a significant reduction in survivability as compared to the control group (B-i). *E. coli* inoculation did not result in the differential survival pattern between ds*TmPGRP-LE*- and dsEGFP-treated larvae (B-ii). "*" indicates significant ($p < 0.05$) difference between means, ns = not significant difference. Data are shown as mean \pm standard deviation ($n = 3$).

4.5 Conclusion

In the present work, we have partially characterized a PGRP-LE homologue from a coleopteran beetle *T. molitor* and attempted to evaluate its role in the survival of *T. molitor* against *L. monocytogenes* by RNAi. Although *TmPGRP-LE* RNAi did not result in significant alteration of AMP expression with or without bacterial challenge, it still caused a significant reduction in the ability of the beetle to survive *L. monocytogenes* infections. The mechanism and/or signaling cascade, by which PGRP-LE helps to enhance the survivability of the host in response to *L. monocytogenes* infection, would be central to future investigations.

4.6 References

- Arnold, K., Bordoli, L, Kopp, J., Schwede, T. (2000). The SWISS-MODEL Workspace: A web-based environment for protein structure homology modelling. *Bioinformatics* 22, 195–201.
- Bao, Y.Y.; Qu, L.Y.; Zhao, D.; Chen, L.; Jin, H.Y.; Xu, L.M.; Cheng, J.A.; Zhang, C.X. (2013). The genome- and transcriptome-wide analysis of innate immunity in the brown planthopper, *Nilaparvata lugens*. *BMC Genomics* 14, 160.
- Benkert, P., Biasini, M., Schwede, T. (2011). Toward the estimation of the absolute quality of individual protein structure models. *Bioinformatics* 27, 343–350.
- Blom, N., Sicheritz-Ponten, T., Gupta, R., Gammeltoft, S., Brunak, S. (2004) Prediction of post-translational glycosylation and phosphorylation of proteins from the amino acid sequence. *Proteomics* 4, 1633–1649.
- Buchan, D.W.A., Minneci, F., Nugent, T.C.O., Bryson, K., Jones, D.T. (2013). Scalable web services for the PSIPRED protein analysis workbench. *Nucl. Acids Res.* 41, 340–348.
- Bustin, S.A., Benes, V., Garson, J.A., Hellems, J., Huggett, J., Kubista, M., Mueller, R., Nolan, T., Pfaffl, M.W., Shipley, G.L., *et al.* (2011). The MIQE guidelines: Minimum information for publication of quantitative real-time PCR experiments. *Clin. Chem.* 55, 611–622.
- Dobson, A.J., Johnston, P.R., Vilcinskas, A., Rolff, J. (2012). Identification of immunological expressed sequence tags in the mealworm beetle *Tenebrio molitor*. *J. Insect Physiol.* 58, 1556–1561.
- Dziarski, R. and Gupta, D. (2006). The peptidoglycan recognition proteins (PGRPs). *Genome Biol.* doi: 10.1186/gb-2006-7-8-232.

- Dziarski, R. and Gupta, D. (2006b). Mammalian PGRPs: Novel antibacterial proteins. *Cell. Microbiol.* 8, 1059–1069.
- Ewing, B. and Green, P. (1998). Base calling of automated sequencer traces using phred. II. Error probabilities. *Genome Res.* 8, 186–194.
- Expert Protein Analysis System (ExPASy) Bioinformatics Resource Portal. Available online: <http://www.expasy.org/> (accessed on 23 April 2013).
- Fabrick, J., Oppert, C., Lorenzen, M.D., Morris, K., Oppert, B., Jurat-Fuentes, J.L. (2009). A novel *Tenebrio molitor* cadherin is a functional receptor for *Bacillus thuringiensis* Cry3Aa toxin. *J. Biol. Chem.* 284, 18401–18410.
- Gelius, E., Persson, C., Karlsson, J., Steiner, H. (2003). A mammalian peptidoglycan recognition protein with *N*-acetylmuramoyl-L-alanine amidase activity. *Biochem. Biophys. Res. Commun.* 306, 988–994.
- Ghosh, J., Lun, C.M., Majeske, A.J., Sacchi, S., Schrankel, C.S., Smith, L.C. (2011). Invertebrate immune diversity. *Dev. Comp. Immunol.* 35, 959–974.
- Kaneko, T., Yano, T., Aggarwal, K., Lim, J.H., Ueda, K., Oshima, Y., Peach, C., Erturk-Hasdemir, D., Goldman, W.E., Oh, B.H., *et al.* (2006). PGRP-LC and PGRP-LE have essential yet distinct functions in the drosophila immune response to monomeric DAP-type peptidoglycan. *Nat. Immunol.* 7, 715–723.
- Kang, D., Liu, G., Lundstrom, A., Gelius, E., Steiner, H. (1998). A peptidoglycan recognition protein in innate immunity conserved from insects to humans. *Proc. Natl. Acad. Sci. USA* 95, 10078–10082.
- Kim, M.S., Byun, M., Oh, B.H. (2003). Crystal structure of peptidoglycan recognition protein LB from *Drosophila melanogaster*. *Nat. Immunol.* 4, 787–793.
- Kopp, J. and Schwede, T. (2006). The SWISS-MODEL Repository: New features and functionalities. *Nucl. Acids Res.* 34, D315–D318.

- Kyte, J. and Doolittle, R.F.(1982). A simple method for displaying the hydropathic character of a protein. *J. Mol. Biol.* 157, 105–132.
- Lemaitre, B. and Hoffmann, J.A. (2007). The host defense of *Drosophila melanogaster*. *Annu. Rev. Immunol.* 25, 697–743.
- Li, M.F., Zhang, M., Wang, C.L., Sun, L. (2012). A peptidoglycan recognition protein from *Sciaenops ocellatus* is a zinc amidase and a bactericide with a substrate range limited to Gram-positive bacteria. *Fish Shellfish Immunol.* 32, 322–330.
- Lim, J.H., Kim, M.S., Kim, H.E., Yano, T., Oshima, Y., Aggarwal, K., Goldman, W.E., Silverman, N., Kurata, S., Oh, B.H. (2006). Structural basis for recognition of diaminopimelic acid-type peptidoglycan by a subset of peptidoglycan recognition proteins. *J. Biol. Chem.* 281, 8286–8295.
- Liu, C., Xu, Z., Gupta, D., Dziarski, R. (2001). Peptidoglycan recognition proteins: A novel family of four human innate immunity pattern recognition molecules. *J. Biol. Chem.*, 276, 34686–34694.
- Mellroth, P. and Steiner, H. (2006). PGRP-SB1: An *N*-acetylmuramoyl L-alanine amidase with antibacterial activity. *Biochem. Biophys. Res. Commun.*, 350, 994–999.
- Mellroth, P., Karlsson, J., Steiner, H. (2003). Scavenger function for a *Drosophila* peptidoglycan recognition protein. *J. Biol. Chem.* 278, 7059–7064.
- Mendes, C., Felix, R., Sousa, A.M., Lamego, J., Charlwood, D, do Rosário, V.E., Pinto, J., Silveira, H. (2010). Molecular evolution of the three short PGRPs of the malaria vectors *Anopheles gambiae* and *Anopheles arabiensis* in East Africa. *BMC Evol. Biol.* doi:10.1186/1471-2148-10-9.
- Mouillet, J.F., Bousquet, F., Sedano, N., Alabouvette, J., Nicolai, M., Zelus, D., Laudet, V., Delachambre, J. (1999). Cloning and characterization of new orphan nuclear receptors

and their developmental profiles during *Tenebrio* metamorphosis. *Eur. J. Biochem.* 265, 972–981.

National Center for Biotechnology Information. Available online: <http://www.ncbi.nlm.nih.gov/gorf/gorf.html/> (accessed on 23 April 2013).

Neyen, C., Poidevin, M., Roussel, A., Lemaitre, B. (2012). Tissue- and ligand-specific sensing of gram-negative infection in *Drosophila* by PGRP-LC isoforms and PGRP-LE. *J. Immunol.* 189, 1886–1897.

Ni, D., Song, L., Wu, L., Chang, Y., Yu, Y., Qiu, L., Wang, L. (2007). Molecular cloning and mRNA expression of peptidoglycan recognition protein (PGRP) gene in bay scallop (*Argopecten irradians*, Lamarck 1819). *Dev. Comp. Immunol.* 31, 548–558.

Nishikawa, K. and Ooi, T. (1986). Radial locations of amino acid residues in a globular protein: Correlation with the sequence. *J. Biochem.* 100, 1043–1047.

Park, J.W., Kim, C.H., Kim, J.H., Je, B.R., Roh, K.B., Kim, S.J., Lee, H.H., Ryu, J.H., Lim, J.H., Oh, B.H., *et al.* (2007). Clustering of peptidoglycan recognition protein-SA is required for sensing lysine-type peptidoglycan in insects. *Proc. Natl. Acad. Sci. USA* 104, 6602–6607.

PeptideCutter Tool. Available online: http://web.expasy.org/peptide_cutter/ (accessed on 5 May 2013).

Petersen, T.N., Brunak, S., Heijne, G., Nielsen, H. (2011). Signal 4.0: Discriminating signal peptides from transmembrane regions. *Nat. Methods* 8, 785–786.

ProtParam Tool. Available online: <http://web.expasy.org/protscale/> (accessed on 23 April 2013).

ProtScale Tool. Available online: <http://web.expasy.org/protscale/> (accessed on 5 May 2013).

Roh, K.B., Kim, C.H., Lee, H., Kwon, H.M., Park, J.W., Ryu, J.H., Kurokawa, K., Ha, N.C., Lee, W.J., Lemaitre, B., *et al.* (2009). Proteolytic cascade for the activation of the insect

- toll pathway induced by the fungal cell wall component. *J. Biol. Chem.* 284, 19474–19481.
- Schleifer, K.H. and Stackerbrandt, E. (1983). Molecular systematics of prokaryotes. *Annu. Rev. Microbiol.* 37, 143–187.
- Schmittgen, T.D. and Livak, K.J. (2008). Analyzing real-time PCR data by the comparative C_T method. *Nat. Protoc.* 3, 1101–1108.
- Sneath, P.H.A. and Sokal, R.R. (1973). *Numerical Taxonomy*; W.H. Freeman: San Francisco, CA, USA, p. 115.
- Solovyev, V., Kosarev, P., Seledsov, I., Vorobyev, D. (2006). Automatic annotation of eukaryotic genes, pseudogenes and promoters. *Genome Biol.* 7, 1–10.
- Swaminathan, C.P., Brown, P.H., Roychowdhury, A., Wang, Q., Guan, R., Silverman, N., Goldman, W.E., Boons, G.J., Mariuzza, R.A. (2006). Dual strategies for peptidoglycan discrimination by peptidoglycan recognition proteins (PGRPs). *Proc. Natl. Acad. Sci. USA* 10, 684–689.
- Takehana, A., Katsuyama, T., Yano, T., Oshima, Y., Takada, H., Aigaki T., Kurata, S. (2012). Overexpression of a pattern-recognition receptor, peptidoglycan-recognition protein-LE, activates imd/relish-mediated antibacterial defense and the prophenoloxidase cascade in *Drosophila* larvae. *Proc. Natl. Acad. Sci. USA* 99, 13705–13710.
- Takehana, A., Yano, T., Mita, S., Kotani, A., Oshima, Y., Kurata, S. (2004). Peptidoglycan recognition protein (PGRP)-LE and PGRP-LC act synergistically in *Drosophila* immunity. *EMBO J.* 23, 4690–4700.
- Tamura, K., Petersen, D., Petersen, N., Stecher, G., Nei, M., Kumar, S. (2011). MEGA5: Molecular evolutionary genetics analysis using maximum likelihood, evolutionary distance and maximum parsimony methods. *Mol. Biol. Evol.* doi:10.1093/molbev/msr121.

- Untergrasser, A., Cutcutache, I., Koressaar, T., Ye, J., Faircloth, B.C., Remm, M., Rozen, S.G. (2012). Primer3—New capabilities and interfaces. *Nucl. Acids Res.* doi:10.1093/nar/gks596.
- Wang, S. and Beerntsen, B.T. (2013). Insights into the different functions of multiple peptidoglycan recognition proteins in the immune response against bacteria in the mosquito, *Armigeres subalbatus*. *Insect Biochem. Mol. Biol.*, 43, 533–543.
- Wang, Z.M., Li, X., Cocklin, R.R., Wang, M., Wang, M., Fukase, K., Inamura, S., Kusumoto, S., Gupta, D., Dziarski, R.(2003). Human peptidoglycan recognition protein-L is an *N*-Acetylmuramoyl-L-alanine amidase. *J. Biol. Chem.* 278, 49044–49052.
- Werner, T., Liu, G., Kang, D., Ekengren, S., Steiner, H., Hultmark, D. (2000). A family of peptidoglycan recognition proteins in the fruit fly, *Drosophila melanogaster*. *Proc. Natl. Acad. Sci. USA* 97, 13772–13777.
- Yano, T. and Kurata, S (2011). Intracellular recognition of pathogens and autophagy as an innate immune host defence. *J. Biochem.* 150, 143–149.
- Yano, T., Mita, S., Ohmori, H., Oshima, Y., Fujimoto, Y., Ueda, R., Takada, H.; Goldman, W.E., Fukase, K., Silverman, N.; *et al.* (2008). Autophagic control of *Listeria* through intracellular innate immune recognition in *Drosophila*. *Nat. Immunol.* 9, 908–916.
- Yoshida, H., Kinoshita, K., Ashida, M. (1996). Purification of a peptidoglycan recognition protein from hemolymph of the silkworm, *Bombyx mori*. *J. Biol. Chem.* 271, 13854–13860.
- Yu, Y., Park, J.W., Kwon, H.M., Hwang, H.O., Jang, I.H., Masuda, A., Kurokawa, K., Nakayama, H., Lee, W.J., Dohmae, N., *et al.* (2010). Diversity of innate immune recognition mechanism for bacterial polymeric meso-diaminopimelic acid-type peptidoglycan in insects. *J. Biol. Chem.* 285, 32937–32945.

Zhang, Y. and Yu, Z. (2013). The first evidence of positive selection in peptidoglycan recognition protein (PGRP) genes of *Crassostrea gigas*. *Fish Shellfish Immunol.* 34, 1352–1355.

Zou, Z., Evans, D.J., Lu, Z., Zhao, Z., Williams, M., Sumathipala, N., Hetru, C., Hultmark, D., Jiang, H. (2007). Comparative genomic analysis of the *Tribolium* immune system. *enome Biol.* 8, R177.

Chapter 5. Roles and immunological functions of *TmPGRP-LB* against a soil isolate

Pseudomonas geniculata-HT1

5.1 Abstract

Peptidoglycan recognition proteins (PGRPs) function as recognition molecules for the peptidoglycan (PGN) - a key cell wall component of virtually all bacteria. A subset of PGRPs has, in addition to the PGN-recognition function, an ability to cleave and destroy PGN and/or PGN-containing bacteria through amidase activity. PGRP-LB, one of several amidase-capable members of the PGRP family has been demonstrated to specifically recognise DAP-type PGN, thereby preventing over-activation of the IMD pathway upon infections Gram-negative bacteria. We have identified, cloned and partially characterized the immunological functions of a PGRP-LB homologue from *Tenebrio molitor* against a newly isolated Gram-negative bacterium *Pseudomonas geniculata* HT1 infection. *TmPGRP-LB* has an ORF of 597 bp encoding a protein with 198 amino acid residues and contains the conserved PGRP domain. *TmPGRP-LB* is closest to its ortholog TcPGRP-LB1 in *Tribolium castaneum* with which it shares the highest (71%) percentage identity. *TmPGRP-LB* transcripts were detected in all developmental stages examined spanning from the late-instar larva to adult day 1 and 2. *TmPGRP-LB* transcripts were also detected in all tissues examined including the gut, hemocytes, fat body, Malpighian tubules, integuments, ovaries and testes. Infection of *Tenebrio* larvae with HT1 resulted in increased expression of *TmPGRP-LB* but not other IMD pathway-related genes *TmPGRP-LC* and *TmPGRP-LE*. *TmPGRP-LB* loss of function by RNAi resulted in increased susceptibility of larvae to infections by Gram-negative bacteria HT1 and *E. coli* K12 but not Gram-positive bacteria *S. aureus* RN4220. Our results suggest that *TmPGRP-LB* plays a role in control of Gram-negative infections in *T. molitor*.

5.2 Introduction

Peptidoglycan recognition proteins (PGRPs) were first discovered in the haemolymph of a silkworm (*Bombyx mori*) as proteins that bind to bacterial peptidoglycan leading to activation of an antimicrobial host defence mechanism in insects called the prophenoloxidase cascade (Yoshida et al., 1996). Since then, PGRPs have been cloned and characterised from various organisms including insects, mollusks, echinoderms, and many vertebrates such as fish, birds, amphibians and mammals (Royet et al., 2011). Subsequent detailed research has revealed that PGRPs are a family of proteins that make up a distinct class of pattern recognition receptors (PPRs). PGRPs are a key component of immune response mechanisms in insects functioning upstream of the two major immune signal transduction pathways, Toll and Imd pathways.

PGRPs function as recognition molecules for the peptidoglycan (PGN) - a key cell wall component of virtually all bacteria. PGN is made of long glycan chains of alternating N-acetylglucosamine and N-acetylmuramic acid residues that are cross-linked to each other by short peptide bridges (Mengin-Lecreulx and Lemaitre, 2005). Two types of PGN exist in nature, distinguished by the type of amino acid residue found at the third position in the cross-linking peptide chain. While lysine-type PGN has a lysine on this position, the residue is replaced by a *meso*-diaminopimelic acid residue in DAP-type PGN. Astonishingly, most gram positive bacteria contain lysine-type PGN in their cell walls while all gram negative bacteria and a few gram positive bacilli such as *Listeria monocytogenes* contain, instead, DAP-type PGN on their cell walls.

PGRPs which share a conserved domain, of around 160 amino acids, with similarities to the bacteriophage T7 lysozyme, a zinc-dependent N-acetylmuramoyl- L-alanine amidase can be grouped into two subgroups, one with only recognition and the other with additional catalytic properties (Royet et al., 2005; Steiner, 2004). Structurally, PGRPs with the catalytic domain

have a zinc-dependent activity in the PGN binding groove to cleave the amide bond of PGN similar to the T7-lysozyme activity, but this crucial Zn residue is missing in the non-catalytic, recognition only PGRPs. (Royet et al., 2011). Both of these groups of PGRPs play crucial roles in immune defence in insects. The non-catalytic PGRPs play PGN recognition roles upstream of either the Toll or IMD pathways leading to eventual production of antimicrobial peptides (AMPs). At this capacity PGRPs are known to sufficiently discriminate between lysine-type and DAP-type PGN leading to selective activation of either the Toll pathway by the lysine-type PGN or the Imd pathway by the DAP-type PGN.

Studies in *Drosophila* led to the discovery of several predicted amidase PGRPs including PGRP-LB, PGRPS-C1A, PGRP-SC1B, PGRP-SC2, PGRP-SB1 and PGRP-SB2. Amidase activity has been demonstrated for PGRP-LB, PGRP-SC1B, and PGRP-SB1 and that the activity of at least two of them, PGRP-LB and PGRP-SB1 is required to down-regulate (or provide negative feedback mechanisms to) immune response pathways (Mellroth et al., 2003; Mellroth and Steiner, 2006; Zaidman-Re'my et al., 2006; Zaidman-Re'my et al., 2011). The Role of PGRP-LB, which specifically recognises DAP-type PGN, thereby itself being regulated by the IMD pathway has been clearly demonstrated (Zaidman-Remy et al., 2006; Paredes et al., 2011).

In the current study, we have identified, cloned and characterised the functions of a PGRP-LB homologue from *Tenebrio molitor* (*TmPGRP-LB*) by analyzing its interactions with a new soil bacterial isolate, the gram negative *Pseudomonas geniculata* HT1. Using RNAi, we showed that *TmPGRP-LB*, selectively reacts against infections by gram-negative bacteria *P. geniculata* and/or *E. coli* but not those of gram positive bacterium *Staphylococcus aureus*, and, that this interaction is influenced by the IMD pathway. We showed further that, *TmPGRP-LB*

RNAi insects are more susceptible to infections by *P. geniculata* HT1 or *E. coli* K12, than dsEGFP- injected control insects.

5.3 Materials and Methods

5.3.1 Insect rearing and Maintenance

Tenebrio larvae used in this study were reared under dark conditions in an environmental chamber at $26 \pm 1^\circ\text{C}$ and $60 \pm 5\%$ relative humidity. Unless otherwise specified, all animals were maintained on an autoclaved wheat bran meal with occasional supply of clean cabbage leaves to supply for their water requirements. Only larvae of about two weeks old with an average body length of 0.73 cm were used for all experiments.

5.3.2 Full-length PGRP-LB cDNA Cloning and Sequencing

Partial cDNA sequence of *TmPGRP-LB* was obtained from *T. molitor* expressed sequence tag (EST) and RNAseq databases whose annotation was conducted previously during the identification and characterization of immunity-related genes (unpublished data). To obtain the full-length cDNA sequence, 5'- and 3'- rapid amplification of cDNA ends (RACE)-polymerase chain reaction (PCR) was performed using SMARTer™ RACE cDNA amplification kit (Clontech laboratories, CA, USA) according to manufacturer's instructions. Briefly, total RNA was used as template to synthesize RACE-ready cDNA. Gene-specific primers for *TmPGRP-LB* (See Table 5.1 for primer details) were designed based on the partial sequence and the first and nested PCR reactions were conducted under the following conditions: initial denaturation at 94°C for 3min. followed by 28 cycles of denaturation at 94°C for 30 s, annealing at 60°C for 30 s, extension at 72°C for 1min and a final extension at 72°C for 10 min. The nested PCR products were resolved on 1% agarose gel at 100 V for 20 min, extracted and gel-purified by using AccuPrep Gel purification kit (Bioneer Company, Daejeon, Korea). The purified gene products were subsequently cloned into pEGM-T-Easy cloning vector and transformed into competent *E. coli* DH5a cells. The transformed DH5a cells were sub-cultured overnight and plasmids carrying the target gene products were recovered and sequenced.

Table 5-1: Primers used in this study

Primer name	Primer direction	Sequence (5'-3')*
Oligo (dT) adaptor	R	GGCCACGCGTCGACTAGTACT
<i>RpL27a</i>	F	TCATCCTGAAGGCAAAGCTCCAGT
<i>RpL27a</i>	R	AGGTTGGTTAGGCAGGCACCTTTA
<i>TmPGRP-LB</i> qPCR	F	CAAGGAATGATCCAGGAGGA
<i>TmPGRP-LB</i> qPCR	R	TCAGCGAAACTCCGAAAAGT
<i>TmPGRP-LB</i> sqPCR	F	ATGTCCGCATTGGTGTGACC
<i>TmPGRP-LB</i> sqPCR	R	TCAGGATTTGTGTTTGAAAAA
<i>TmPGRP-LB</i> dsRNA	F	TAATACGACTCACTATAGGGGATCATCCACCACAGCTAC
<i>TmPGRP-LB</i> dsRNA	R	TAATACGACTCACTATAGGGTTATCGTCTACGCCACTG

* Sequences are read from 5' to 3' end.

T7 polymerase recognition sequence is indicated in bold

F = Forward, R = Reverse.

5.3.3 *In Silico* characterization of *TmPGRP-LB*

The cDNA and deduced amino acid sequence of *TmPGRP-LB* were analyzed using InterProScan at EBI (<http://www.ebi.ac.uk/Tools/pfa/iprscan/>) and BLAST algorithm at NCBI (<http://blast.ncbi.nlm.nih.gov/>). Specific protein domains were highlighted by the InterProScan during the analysis. Amino acid sequence of *TmPGRP-LB* orthologues were obtained from GenBank (<http://www.ncbi.nlm.nih.gov>) and have been summarized in Table 5.2.

Multiple sequence alignment and percentage identity analysis were performed using ClustalX2 program (Larkin et al., 2007). MEGA5 (Tamura et al., 2011) program was used to calculate the corresponding percentage distances with ATG8 homologues from other insects. The maximum likelihood (ML) method based on the JTT matrix-based model (Jones et al., 1992) was used to generate a rooted phylogenetic tree using MEGA5 software.

Table 5-2: Accession numbers of PGRP-LB sequences from various insect species used to generate the phylogenetic tree, percentage distance and identity matrices

	Species name	Abbreviations	Accession numbers
1	<i>Tenebrio molitor</i>	TmPGRP-LB	
2	<i>Tribolium castaneum</i>	TcPGRP-LB1	EFA05744.1
3	<i>Drosophila melanogaster</i>	DmPGRP-LB-A	AAF54643.1
4	<i>Apis florea</i>	AmPGRP-LB1	XP_001121036.2
5	<i>Bombyx mori</i>	BmPGRP-LB1	XP_004929065.1
6	<i>Ceratitis capitata</i>	CcPGRP-LB	JAB96226.1
7	<i>Camponotus floridanus</i>	CfPGRP-LB	EFN73971.1
8	<i>Aedes aegypti</i>	AaPGRP	ABF18154.1
9	<i>Anopheles gambiae</i>	AgPGRP-LB	EGK97637.1
10	<i>Dendroctonus ponderosae</i>	DpPGRP-LB	ERL95020.1
11	<i>Glossina morsitans morsitans</i>	GmmPGRP-LB	ABC25064.1
12	<i>Galleria mellonella</i>	GmPGRP-LB	CAL36191.1
13	<i>Harpegnathos saltator</i>	HsPGRP-LB	EFN81746.1
14	<i>Musca domestica</i>	MdPGRP-LB	XP_005180889.1
15	<i>Manduca sexta</i>	MsPGRP2	ACX49764.1
16	<i>Nilaparvata lugens</i>	NlPGRP-LB	AGK40911.1
17	<i>Homo sapiens</i>	HsPGRP1	AAH96156.1

5.3.4 Developmental Expression Pattern of *TmPGRP-LB*

Total RNA was extracted from various developmental stages of *T. molitor*, including the last instar larvae (LIL), pupal day 1-7 (P1-P8) and adult day 1 and 2 (A1 and A2) using SV Total RNA isolation system (Promega Corporation, Madison, WI) according to manufacturer's instructions. The cDNA corresponding to each stage of growth sampled was synthesized using AccuPowerR RT Pre-Mix kit (Bioneer, Daejeon, Korea). The cDNAs were used as templates for quantitative PCR (qPCR) reactions performed on an Exicycler™ 96 real-time quantitative thermal block (Bioneer, Korea) using gene specific primers at an initial denaturation of 95°C for 20 s, followed by 45 cycles of denaturation at 95°C for 5 s and annealing at 60°C for 20 s. The $2^{-\Delta\Delta C_t}$ method was employed to analyze the expression of *TmPGRP-LB* transcripts. *TmRPL27a* was used as an internal control to normalize differences in concentration of templates between samples.

5.3.5 dsRNA Synthesis and injections

The open reading frame *TmPGRP-LB* sub-cloned into pEGM-T-Easy vector was used as a template for amplification and subsequent dsRNA synthesis. The template for target sequence was amplified by the semi-quantitative PCR using gene-specific primers tailed with T7 promoter sequence on their respective 5' ends (Table 1). The PCR products were purified using the AccuPrep PCR purification kit (Bioneer, Daejeon, South Korea) and used to synthesize the dsRNA with an Ampliscribe™ T7-Flash™ transcription kit (Epicentre Biotechnologies, Madison, WI, USA). ds*PGRP-LB* was purified by 5M ammonium acetate precipitation. dsENA for a gene encoding Enhanced green fluorescent protein (ds*EGFP*) were also synthesized in the same way. dsRNAs were stored at -20°C until injected into *T. molitor* larvae.

To inject *T. molitor* larvae with dsRNAs, ds*TmPGRP-LB* or ds*EGFP* were dissolved in injection buffer (0.1 mM sodium phosphate, 2.5 mM potassium chloride, pH 7.2) (Fabrick et al., 2009) to a final concentration of 3.5 µg/ul. Using disposable needles mounted onto a micro-applicator (Picospirtzer III micro dispense system, Parker Hannifin, Hollis, NH, USA), 3µl (~10.5µg) of ds*TmPGRP-LB* or ds*EGFP* solutions were injected per larvae held on a dorsal-ventral position at the 2nd or 3rd visible sternite. The *TmPGRP-LB* transcript knockdowns were checked and confirmed five days post injection of dsRNA by qPCR.

5.3.6 Isolation and identification of *Pseudomonas geniculata* HT1

Rhizosphere soils collected from rice fields in Suncheon, South Korea were serially diluted in 0.9% saline solution and inoculated on nutrient agar (Merck KGaA, Darmstadt, Germany) at 37°C for 16-24h. Clear isolated colonies were repeatedly sub-cultured to purity in the same medium. Several pure colonies were picked at random and sub-cultured in nutrient broth at 37°C on an orbital shaker at 180 rpm overnight. The overnight cultures were then serially diluted to the 10⁻⁵ dilution and injected to last instar larva of *Tenebrio molitor* at a rate of 1ul/larva. Injected larvae were maintained under standard rearing conditions and the number of deaths was monitored for 48h. Two isolates causing the highest mortality rate to *T. molitor* larvae were picked for further analysis. One of these was eventually selected and identified by using the 16S rRNA sequencing technique (Chun et al., 1995). The procedure for isolation and characterization of HT1 isolate is presented in Fig. 5-1.

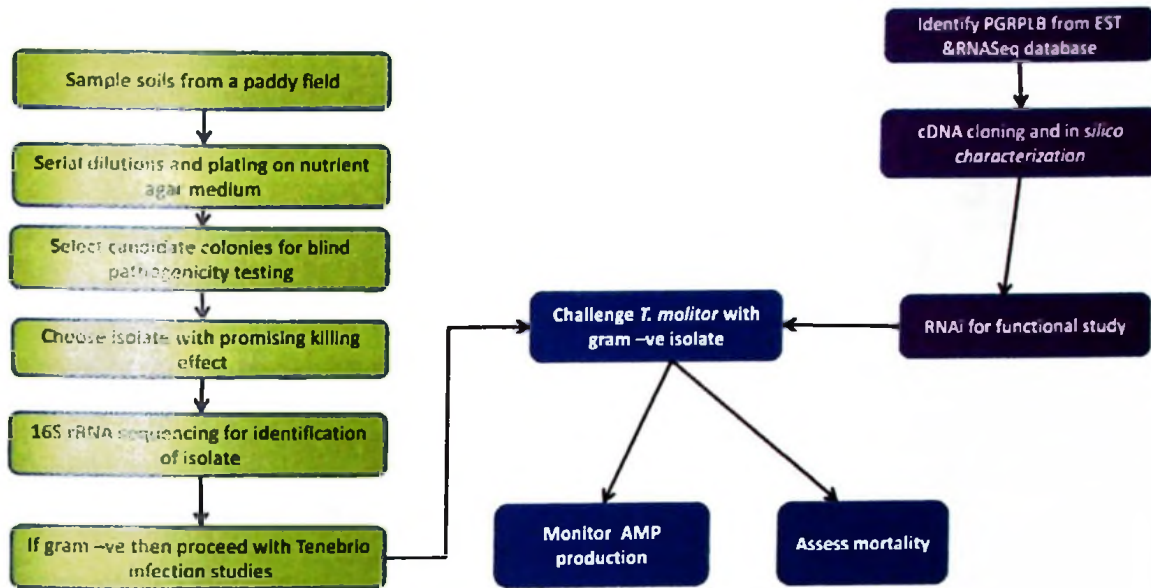


Figure 5-1: Schematic procedure on isolation and effect of *P. geniculata* on *Tenebrio* mortality

5.3.7 Bacterial Injections and Bioassays

Pseudomonas geniculata HT1 was cultured in Luria Bertani (LB) broth in a sterile, 14 mL round-bottomed, flask at 37°C overnight. The Overnight culture was washed three times in 0.9% saline, serially diluted to an equivalent of 10^6 CFU/ul based on spectrophotometer readings at OD₆₀₀. The OD₆₀₀ value was confirmed by aseptically spread-plating the serially diluted samples on LB agar plates. The plates were incubated at 37 °C for 16 h prior to colony counting. Only 1µl (10^6 CFU/larva) of this inoculum was injected dorso-laterally into the hemocoel of three weeks-old larvae using disposable syringes and needles mounted on a microapplicator (Picospiritzer III micro dispense system, Parker Hannifin, Hollis, NH, USA). The injected larvae were kept in an environmental chamber under standard rearing conditions and the number of dead larvae was recorded on a daily basis for six days post injection. Rates of survival were compared between the *TmPGRP-LB* silenced and *dsEGFP* injected (control) groups. *E. coli* K12 strain- a DAP-type PGN-containing bacterium and *S. aureus* which is a lysine-type PGN-containing bacterium were processed in the same manner and used for comparison to *P. geniculata* HT1-injected larvae.

5.4 Results and Discussion

5.4.1 Characterization of full-length *TmPGRP-LB* cDNA

The open reading frame (ORF) of *TmPGRP-LB* was identified from *T. molitor* RNAseq database. The ORF was subsequently confirmed by cloning and sequencing of *TmPGRP-LB* cDNA. The ORF of *TmPGRP-LB* encodes a protein of 198 amino acid residues (Fig. 5-2). Analysis of deduced amino acid sequence of *TmPGRP-LB* revealed the characteristically conserved PGRP domain (Fig. 5-2).

Multiple alignment of amino acid sequence of *TmPGRP-LB* with orthologous sequences revealed a highly conserved region (~ 155-160 amino acid residues) which putatively overlaps the PGRP domain (Fig. 5-3). Phylogenetic analysis revealed that *TmPGRP-LB* is closest to its *T. castaneum* counterpart *TcPGRP-LB1* (Fig. 5.4). *TmPGRP-LB* shares highest sequence identity (71%) with the *T. castaneum* (*TcPGRP-LB-1*) followed by those of a coleopteran, *Dendroctonus ponderosae* (61%) and dipteran insects, *Musca domestica* (61%), *Ceratitis capitata* (58%), and *Anopheles gambiae* (56%) (Fig. 5-5). These observations were validated by performing the distance matrix analysis. *TmPGRP-LB* was placed at a distance of 0.38 from *TcPGRP-LB1* compared to distances of 0.58, 0.61, 0.67 and 0.73 from *Dendroctonus ponderosae*, *Musca domestica*, *Ceratitis capitata* and *Anopheles gambiae*, respectively (Fig. 5-5). Like all PGRPs, the N-termini of PGRP-LB amino acid sequences are not conserved among insects. However, possession of a highly conserved PGRP domain, of around 160 amino acids, with little sequence similarities outside this domain (Werner et al., 2000; Liu et al., 2001; Chang et al., 2007), is a shared feature of all PGRPs, regardless of the host species.

ATG TCC GCA TTG GTG TTG ACC ACT CGC GAG GAA TGG AAC GCC CGC CCT CCA GTT CTG ATC	60
M S A L V L T T R E E W N A R P P V L I	20
GAA CCG ATG ACC AAC CCC GTC CCC TAC GTG ATC ATC CAC CAC AGC TAC ATC CCC CCG GCT	120
E P M T N P V P Y V I I H H S Y I P P A	40
TGT ACC ACC ACT GCC GAC TGC CTG GAC GCC ATG AGG AAG ATG CAG GAC ATG CAC CAG ATC	180
C T T T A D C L D A M R K M Q D M H Q I	60
ACC AAC GGA TGG AAC GAC ATT GGG TAC CAC TTC GCC GTG GGC GGC GAC GGA CAC GCT TAC	240
T N G W N D I G Y E F A V G G D G H A Y	80
GAG GGC AGG GGG TGG TCG AGA GTG GGG GCA CAC GCC CCC GGC TAC AAC AAC ATC AGC ATC	300
E G R G W S R V G A H A P G Y N N I S I	100
GGG ATC TGC GTG ATC GGC GAT TGG ACG CAG GAG TTG CCC CCC GAG TGG CAG CTG GAG GCC	360
G I C V I G D W T Q E L P P E W Q L E A	120
GTA CAT CAA CTC GTC GAG CAC GGA GTG GAG CAA GGA ATG ATC CAG GAG GAC TAC AAA CTG	420
V H Q L V E H G V E Q G M I Q E D Y K L	140
CTG GGA CAC AGG CAG GTC AGG GAT ACG GAG TGT CCA GGG GAC AGG CTC TTC AAC GAG ATA	480
L G H R Q V R D T E C P G D R L F N E I	160
ACC ACG TGG GAA CAC TTC AGC GAA ACT CCG AAA AGT ACC AAA GAA AAT AGC AAA GAA AGC	540
T T W E H F S E T P K S T K E N S K E S	180
GGC AAC GCC AGT GGC GTA GAC GAT AAT AAA CTT TTT TTT TTC AAA CAC AAA TCC TGA	597
G N A S G V D D N E L F F F K H K S *	198

Figure 5-2: Nucleotide and deduced amino acid sequence of a novel homologue of PGRP-

LB from *T. molitor*.

The open reading frame of TmPGRP-LB was cloned and sequenced. Boxed is PGRP-LB domain as identified by the inter-proscan.

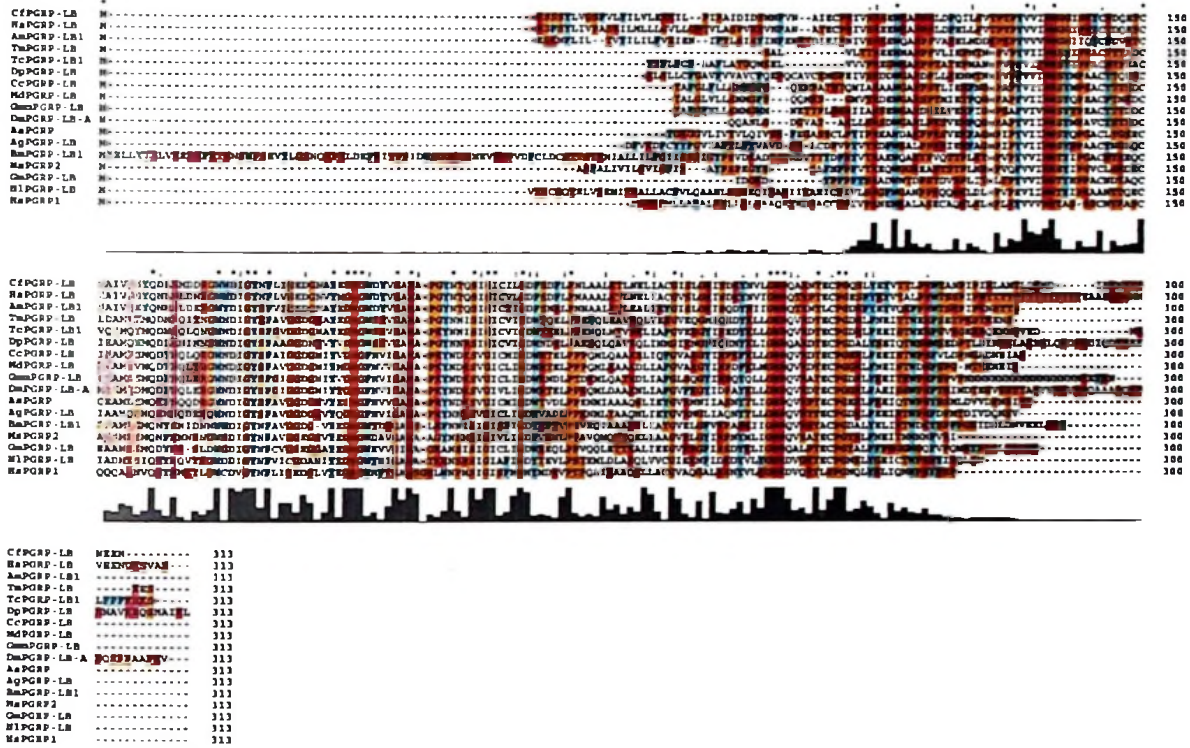


Figure 5-3: Multiple alignment of amino acid sequences of TmPGRP-LB homologues

Multiple alignment of amino acid sequences of PGRP-LB homologues from representative insects species. Sequences used were obtained from NCBI database and have been presented by accession numbers in Table 5-1.

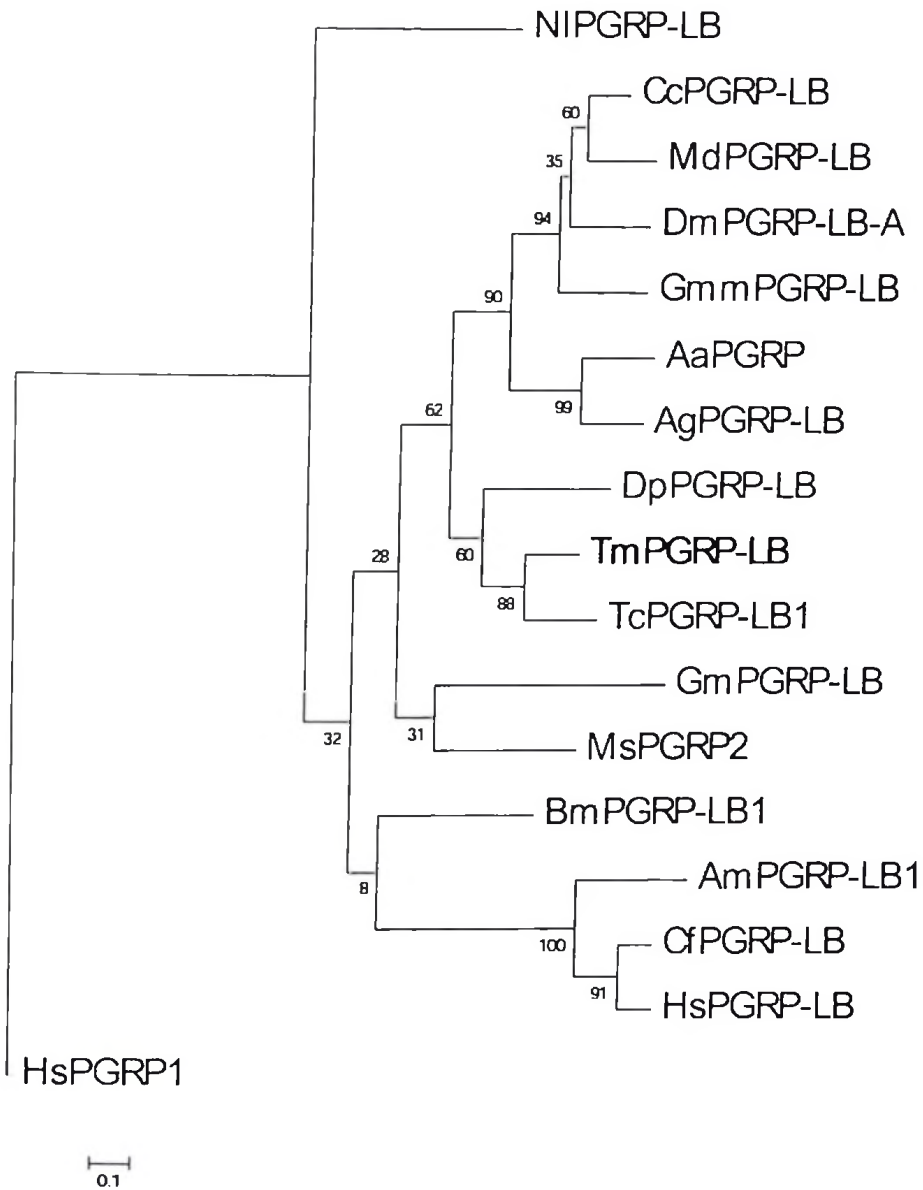


Figure 5-4: Molecular Phylogenetic analysis of TmPGRP-LB by Maximum Likelihood method

The evolutionary history was inferred by using the Maximum Likelihood method based on the JTT matrix-based model. TcPGRP-LB1 presented the phylogenetically closest counterpart of TmPGRP-LB. The accession numbers of all sequences used to create the trees are enlisted in Table 5-2.

	TmPGRP-LB	TcPGRP-LB1	DmPGRP-LB-A	AmPGRP-LB1	BmPGRP-LB1	CcPGRP-LB	CfPGRP-LB	AaPGRP	AgPGRP-LB	DpPGRP-LB	GmmPGRP-LB	GmPGRP-LB	HsPGRP-LB	MdPGRP-LB	MsPGRP2	NIPGRP-LB	HsPGRP1
TmPGRP-LB		71	53	44	50	58	44	55	57	61	55	49	43	61	52	47	36
TcPGRP-LB1	0.38		52	42	43	56	38	51	51	53	51	45	36	58	49	44	33
DmPGRP-LB-A	0.80	0.85		37	38	68	37	54	58	42	58	43	36	66	48	45	34
AmPGRP-LB1	1.09	1.24	1.38		35	37	63	36	38	39	41	38	59	37	36	34	33
BmPGRP-LB1	0.89	1.09	1.23	1.53		41	35	42	39	41	37	45	35	43	46	36	37
CcPGRP-LB	0.67	0.74	0.44	1.35	1.14		39	56	56	48	67	46	37	76	44	43	36
CfPGRP-LB	1.12	1.42	1.41	0.54	1.51	1.33		35	36	38	38	40	70	38	39	35	37
AaPGRP	0.75	0.85	0.75	1.40	1.19	0.72	1.46		65	47	53	43	40	55	46	42	36
AgPGRP-LB	0.73	0.85	0.68	1.31	1.30	0.72	1.45	0.47		46	52	44	36	54	44	39	31
DpPGRP-LB	0.58	0.79	1.14	1.28	1.20	0.91	1.30	0.95	1.02		44	41	37	50	43	39	32
GmmPGRP-LB	0.73	0.87	0.66	1.22	1.20	0.45	1.30	0.79	0.86	0.98		39	37	66	44	41	35
GmPGRP-LB	0.99	1.12	1.21	1.63	1.06	1.07	1.45	1.15	1.18	1.35	1.27		39	45	48	41	33
HsPGRP-LB	1.13	1.47	1.43	0.65	1.48	1.38	0.39	1.30	1.45	1.38	1.25	1.47		39	42	34	36
MdPGRP-LB	0.61	0.71	0.49	1.36	1.06	0.31	1.35	0.73	0.78	0.84	0.45	1.10	1.27		46	42	34
MsPGRP2	0.78	0.87	0.91	1.39	0.87	0.95	1.33	0.95	1.02	0.98	0.94	0.96	1.18	0.90		35	34
NIPGRP-LB	0.98	1.05	1.05	1.70	1.48	1.12	1.55	1.21	1.30	1.25	1.16	1.31	1.54	1.18	1.32		35
HsPGRP1	1.32	1.52	1.43	1.56	1.36	1.32	1.39	1.31	1.56	1.57	1.38	1.45	1.37	1.41	1.38	1.50	

% Identity

Distance

Figure 5-5: Percentage identity and distance analysis of TmPGRPLB with orthologs from other insects

Accession numbers of all sequences used in the analysis are presented in Table 5-2. TmPGRP-LB shared the highest percentage (71%) identity with its counterpart in *T. castaneum*, TcPGRP-LB1, followed by those of a coleopteran *Dendroctonus ponderosae* (61%) and a dipteran *Musca domestica* (61%). The % identity results are highly supported by the distance analysis results which put TmPGRP-LB at a lowest distance value of 0.38 from its *T. castaneum* counterpart, TcPGRP-LB1 compared to 0.58 and 0.61 from *Dendroctonus ponderosae* and *Musca domestica* respectively.

5.4.2 Developmental expression pattern of *TmPGRP-LB*

The developmental expression pattern of *TmPGRP-LB* was examined using quantitative PCR. *TmPGRP-LB* is expressed in all stage of development analyzed (Fig. 5.6). A gradual but persistent decrease of *TmPGRP-LB* transcript levels during the pupal stages was observed (Fig. 5.6).

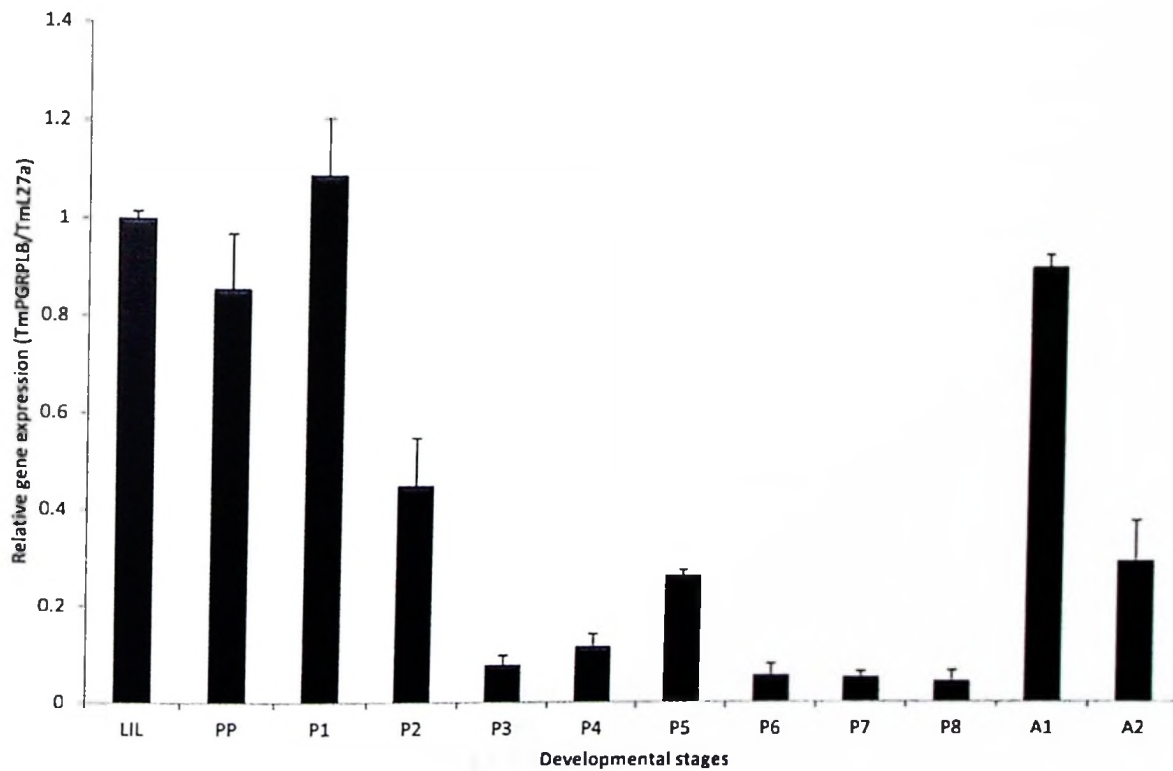


Figure 5-6: Developmental expression pattern of *TmPGRP-LB*.

TmPGRP-LB transcripts at various developmental stages were quantified by real time PCR. LIL = Late-instar larva; P1-P8 = Pupa day 1 to pupa day8; A1 and A2 = Adult day 1 and day 2, respectively. Data are shown as the mean \pm Standard deviation (n = 3).

5.4.3 *TmPGRP-LB* RNAi resulted in increased susceptibility of *Tenebrio* larvae to infection by a gram negative bacterium *P. geniculata* HT1.

We have isolated, identified and characterized the immunological effects of *Pseudomonas geniculata* designated as *Pseudomonas geniculata* HT1 on *Tenebrio molitor* immunity. HT1 is a Gram-negative, bacterial isolate from a rice rhizosphere soil whose 16S rRNA sequence information has been deposited in the European Nucleotide Archive with accession number LM653112. Preliminary infection studies revealed its ability to kill *Tenebrio* larvae at doses as low as 10^6 CFU/larva delivered into the hemocoel by microinjection (Fig. 5.7). Furthermore, injection of sub-lethal doses (300 CFU/insect) of HT1 to *T. molitor* larvae resulted in highly elevated expression of *TmPGRP-LB* transcript. In addition, HT1 induces, albeit to a lesser extent, the expression of *TmIMD* gene transcripts. Other IMD pathway-related PGRPs namely *TmPGRP-LC* and *TmPGRP-LE* showed an initial elevation of their respective transcript levels in the first 3 h post *P. geniculata* injection followed by decrease at later time points (Fig. 5.8).

Since HT1 is a Gram-negative bacterium, we speculated that, once delivered into the *T. molitor* hemocoel it might be confronted by the activity of DAP-type specific *TmPGRP-LB* among other immunological options. To evaluate our hypothesis, we knocked down *TmPGRP-LB* transcripts by injection of *dsPGRP-LB* and subsequently infected larvae with HT1. An additional DAP-type PGN-containing *E. coli* K12 and lysine-type PGN-containing *S. aureus* were included for comparison. As expected, *TmPGRP-LB* RNAi larvae were more susceptible, albeit not significantly, to infections by DAP-type containing bacteria HT1 and *E.coli* K12. However, compared to *dsEGFP*-injected control larvae, *TmPGRP-LB* RNAi larvae did not show increased susceptibility to infections by lysine-type PGN-containing bacterium *S. aureus* (Fig. 5.9). Disrupting the function of *PGRP-LB* either through mutation on the gene or RNAi-based

loss of function has been shown to negatively affect survival in *Drosophila* (Bosco-Drayon et al., 2012) probably due to over-activation of IMD pathway which happens in the absence of a proper function of *PGRPLB* (Bosco-Drayon et al., 2012; Zaidman-Remy et al., 2006).



Figure 5-7: Preliminary pesticidal tests of *Pseudomonas geniculata* HT1 on *T. molitor* larva. Late-instar larvae were injected with (10^6 CFU/larva) fresh culture of *P. geniculata* HT1 and incubated under standard rearing conditions for 24 h. Phenotypic changes were characterised by increasing melanization from the point of injection outwards.

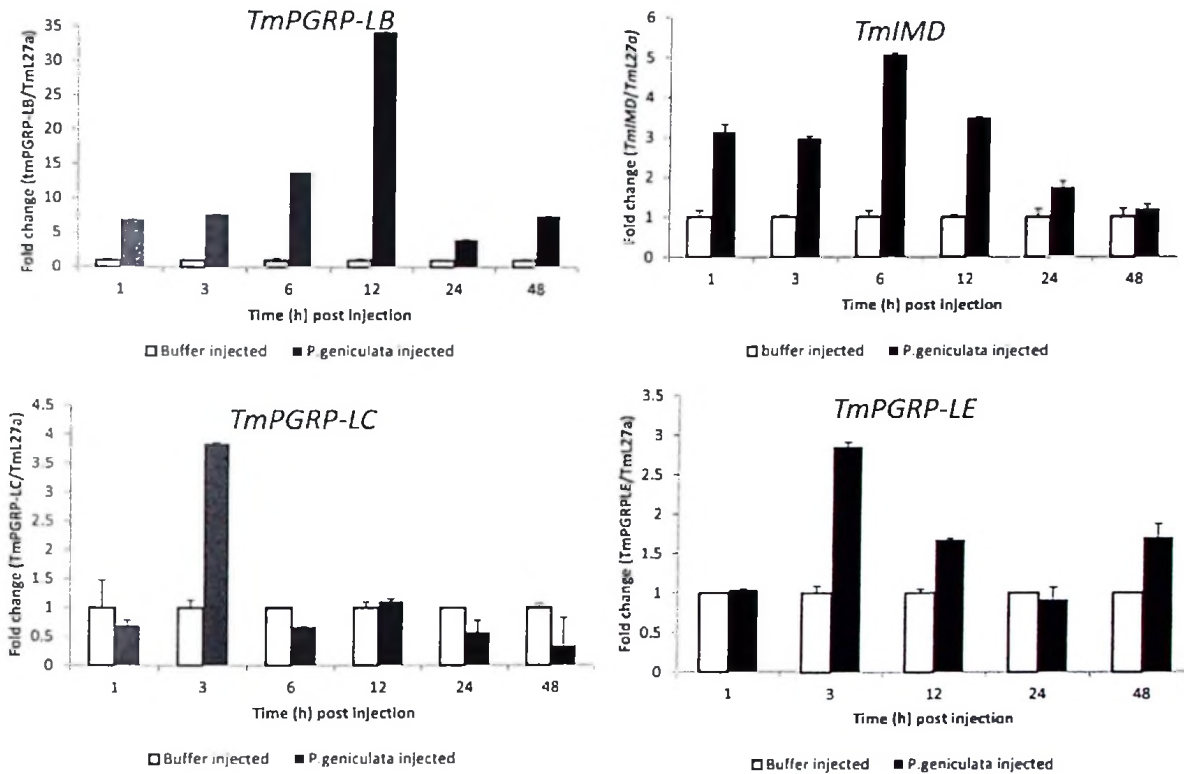


Figure 5-8: Expression patterns of extracellular IMD-pathway related genes after *P. geniculata* HT1 inoculation to *Tenebrio* larvae

P. geniculata induce elevated expression of *TmPGRP-LB* and *TmIMD* gene transcripts in a time-dependent manner. Induction of *TmPGRP-LC* and *TmPGRP-LE* transcripts was only evident in the first 3h post injection followed by a decrease to control levels at later time points.

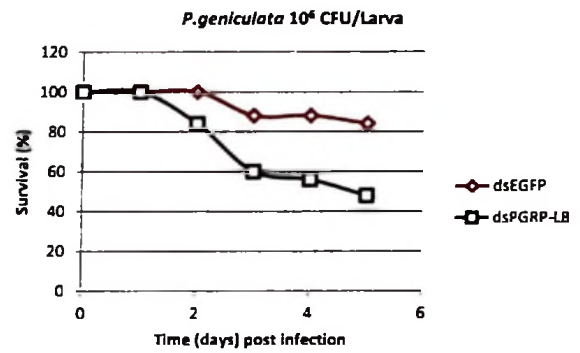
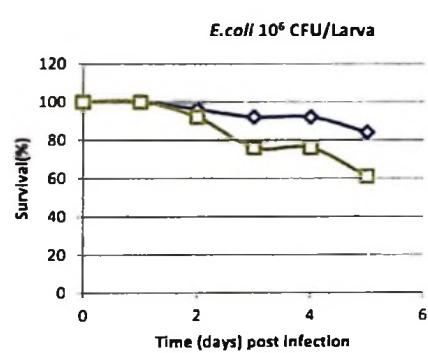
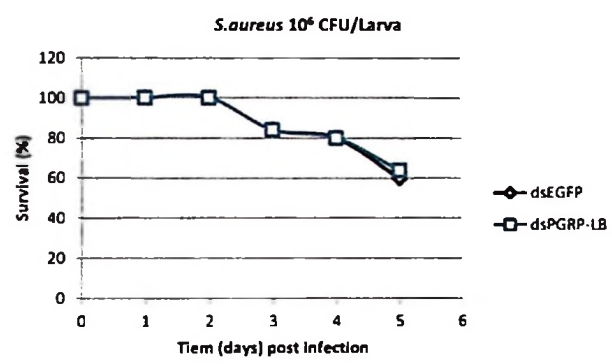
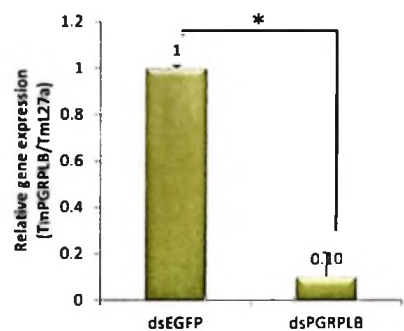


Figure 5-9: *Tenebrio* larval survival against DAP- and Lysine-type PGN containing bacteria.

Tenebrio larvae were treated with *dsPGRP-LB* or *dsEGFP*. Five days later, larvae (n = 30) were challenged with (10^6 CFU/insect) fresh cultures of *S. aureus*, *E. coli* or *P. geniculata* HT1 and the number of dead insects was recorded on a daily basis for 5 consecutive days.

5.5 References

1. Yoshida, H., Kinoshita, K. & Ashida, M. Purification of a peptidoglycan recognition protein from hemolymph of the silkworm, *Bombyx mori*. *J. Biol. Chem.* 271, 13854–13860.
2. Mengin-Lecreulx, D., and Lemaitre, B. (2005). Structure and metabolism of peptidoglycan and molecular requirements allowing its detection by the *Drosophila* innate immune system. *J. Endotoxin Res.* 11, 105–111.
3. Royet, J., Reichhart, J.M., and Hoffmann, J.A. (2005). Sensing and signaling during infection in *Drosophila*. *Curr. Opin. Immunol.* 17, 11–17.
4. Steiner, H. (2004). Peptidoglycan recognition proteins: on and off switches for innate immunity. *Immunol. Rev.* 198, 83–96.
5. Royet J., Gupta, D. and Dziarski, R. (2011). Peptidoglycan recognition proteins: modulators of the microbiome and inflammation. *Nat. Rev. Immunol.* 11: 837-351.
6. Mellroth, P., Karlsson, J., and Steiner, H. (2003). A scavenger function for a *Drosophila* peptidoglycan recognition protein. *J. Biol. Chem.* 278, 7059–7064.
7. Mellroth, P., and Steiner, H. (2006). PGRP-SB1: An N-acetylmuramoyl L-alanine amidase with antibacterial activity. *Biochem. Biophys. Res. Commun.* 350, 994–999.
8. Zaidman-Remy, A., Herve', M., Poidevin, M., Pili-Floury, S., Kim, M.S., Blanot, D., Oh, B.H., Ueda, R., Mengin-Lecreulx, D., and Lemaitre, B. (2006). The *Drosophila* amidase PGRP-LB modulates the immune response to bacterial infection. *Immunity* 24, 463–473.
9. Zaidman-Remy, A., Poidevin, M., Herve', M., Welchman, D.P., Paredes, J.C., Fahlander, C., Steiner, H., Mengin-Lecreulx, D., and Lemaitre, B. (2011). *Drosophila*

- immunity: Analysis of PGRP-SB1 expression, enzymatic activity and function. *PLoS ONE* 6, e17231.
10. Paredes, J.C., Welchman, D.P., Poidevin, M.I., and Lemaitre, B. (2011). Negative Regulation by Amidase PGRPs Shapes the *Drosophila* Antibacterial Response and Protects the Fly from Innocuous Infection. *Immunity* 35, 770–779.
 11. Chun, J. and M. Goodfellow. 1995. A phylogenetic analysis of the genus *Nocardia* with 16S rRNA gene sequences. *Int. J. Syst. Bacteriol.* 45: 240-245.
 12. Liu, C., Xu, Z., Gupta, D. and Dziarski, R. (2001). Peptidoglycan Recognition Proteins: A novel family of four human innate immunity pattern recognition molecules. *J. Biol. Chem.* 276 (37): 34686–34694.
 13. Chang, M.X., Nie, P. and Wei L.L. (2007). Short and long peptidoglycan recognition proteins (PGRPs) in zebrafish, with findings of multiple PGRP homologs in teleost fish. *Mol. Immunol.* 44 3005–3023.
 14. Werner, T., Liu, G., Kang, D., Ekengren, S., Steiner, H. and Hultmark, D. (2000). A family of peptidoglycan recognition proteins in the fruit fly *Drosophila melanogaster*. *Proc. Natl. acad. Sc.* 97 (25): 13772–13777.
 15. Bosco-Drayon, V. Poidevin, M., Boneca, I.G., Narbonne-Reveau, K., Royet, J. and Charroux, B. (2012). Peptidoglycan Sensing by the Receptor PGRP-LE in the *Drosophila* Gut Induces Immune Responses to Infectious Bacteria and Tolerance to Microbiota. *Cell Host & Microbe* 12: 153–165.

Listeria monocytogenes 와 *Pseudomonas geniculata* HT1
감염에 대한 갈색거저리의 *PGRP-LE*, *PGRP-LB* 그리고
autophagy-related genes *ATG3*, *5* 와 *8* 의 분자적 클로닝 및
기능 구명 연구

하미시 틴드와

응용생물학과

전남대학교 일반대학원

(지도 교수 한연수)

국문초록

최근까지 미생물 감염에 대한 갈색거저리(*Tenebrio molitor*)의 내재면역반응(innate immune response)이 연구되었다. 본 연구팀은 *TmATG3*, *TmATG5* 그리고 *TmATG8* 등의 오토파지 관련 유전자의 면역반응과 *TmPGRP-LE* 와 *TmPGRP-LB* 유전자의 기능을 밝히고자 하였다. 첫 번째 주제에서, 본 연구팀은 *TmATG3*, *TmATG5* 그리고 *TmATG8* 등 세가지 종류의 오토파지 관련 유전자를 밝혀냈으며, 세포 내 기생성균인 *Listeria monocytogenes* 균주의 감염에 대한 딱정벌레의 면역학적 기능을 구명하였다. *TmATG3* 와 *TmATG5* 유전자의 핵산 염기서열은 갈색거저리의 EST 와 RNAseq 데이터베이스로부터 밝혀냈다. *TmATG3* 와 *TmATG5* 유전자의 재조합 핵산 염기서열은 각각 320 아미노산

잔기를 암호화하는 963 bp 의 ORF 와 263 아미노산 잔기를 암호화하는 792 bp 의 ORF 를 포함하고 있다. *TmATG3* 와 *TmATG5* 전사체는 전체 발생과정 동안 발현되었으며, 주로 유충의 지방체와 혈구세포에서 발현되는 양상을 확인하였다. 분자계통학적 분석결과 *TmATG3* 와 *TmATG5* 의 아미노산 염기서열은 다양한 곤충의 유사 단백질의 아미노산 염기서열과 높은 유사성(58 - 95 %)을 가지고 있었으며, 거릿쌀도둑거저리(*Tribolium castaneum*)와 진화적으로 가장 유사함을 확인할 수 있었다. RNAi 에 의한 *TmATG3* 와 *TmATG5* 유전자의 발현 억제는 *L. monocytogenes* 감염에 대한 갈색거저리 유충의 생존 능력 감소를 야기하였다. dsEGFP 를 주사한 대조군과 비교하여, ds*TmATG3* 와 ds*TmATG5* 를 처리한 유충의 생존률이 *L. monocytogenes* 주사 후 6 일차에 급격히 감소되는 것을 확인할 수 있었다. 또한 본 연구팀은 오토파지의 중심유전자인 *TmATG8* 유전자의 면역학적 기능을 연구하였다. *TmATG8* 유전자의 재조합 핵산 염기서열은 120 아미노산 잔기를 암호화하는 363 bp 의 ORF 를 포함하고 있다. *TmATG8* 전사체 역시 전체 발생과정 동안 발현되는 것을 확인할 수 있었다. *TmAtg8* 아미노산 염기서열은 잘 보존된 C-말단의 글라이신(glycine) 잔기(G116)를 포함하고 있으며, 거릿쌀도둑거저리의 *Atg8* 아미노산 염기서열(*TcAtg8*)과 높은 유사성(98 %)을 가지고 있음을 확인할 수 있었다. *TmATG8* 유전자의 발현억제는 *L. monocytogenes* 감염에 대한 갈색거저리 유충의 급격한 사충률 증가를 야기하였다. 대조군인 dsEGFP 를 주사했을 경우와 대조적으로, *TmATG8* 유전자의 침묵은 *L. monocytogenes* 주사 후 혈구세포에서 오토파지를 유도시키지 못했다. 이러한 결과는 오토파지 관련 유전자인 *TmAtg3*, 5 그리고 8 이 갈색거저리 모델에서 오토파지에 기초한 리스테리아 균주의 제거에 중요한 기능을 한다는 것을 시사한다. 두 번째 주제에서, 갈색거저리의 *TmPGRP-LE* 와 *TmPGRP-LB* 유전자의 면역학적 기능연구를 수행하였다. 첫 번째로, DAP-type PGN 을 포함하는 *L. monocytogenes* 감염에 대한

갈색거저리의 *PGRP-LE* 유사체의 면역학적 기능을 연구하였다. *TmPGRP-LE* 유전자는 329 아미노산 잔기를 암호화하는 990 bp 의 ORF 로 구성되어 있었다. *TmPGRP-LE* 는 peptidoglycan recognition protein domain 을 가지고 있으나, amidase 활성에 중요한 아미노산 잔기가 결여되어 있었다. Real-time PCR 분석결과, *TmPGRP-LE* 전사체는 유충에서 성충까지의 발생과정에서 일정하게 발현되는 것을 확인할 수 있었다. *TmPGRP-LE* 전사체의 발현 억제는 *L. monocytogenes* 주사에 대한 갈색거저리 유충의 생존률 감소를 야기하였다. 이러한 결과는 *TmPGRP-LE* 가 잠재적으로 *L. monocytogenes* 균주를 인식하고 방제하는데 중요한 역할을 한다는 것을 시사한다. Amidase 활성을 갖는 PGRP family 의 하나인 PGRP-LB 는 DAP-type PGN 을 특이적으로 인식한다고 알려져 있다. 때문에 그람음성균의 감염에 대한 IMD pathway 의 과활성을 억제할 수 있다. 본 연구팀은 PGRP-LB 유사체를 갈색거저리로부터 밝혔으며, 본 연구실에서 새로 분리한 그람음성균인 *Pseudomonas geniculata* HT1 감염에 대한 면역학적 기능을 연구하였다. *TmPGRP-LB* 는 peptidoglycan recognition protein domain 을 포함하는 198 아미노산 잔기를 암호화하는 597 bp 의 ORF 를 가지고 있었다. *TmPGRP-LB* 는 거짓쌀도둑거저리의 PGRP-LB 유사체인 TcPGRP-LB1 와 TcPGRP-LB2 동형단백질과 가장 높은 유사성(73 %)을 가지고 있었다. *TmPGRP-LB* 전사체는 유충에서 성충까지의 발생과정에서 발현되는 것을 확인할 수 있었다. *TmPGRP-LB* 전사체의 조직특이적 발현양상을 확인한 결과, *TmPGRP-LB* 는 장, 혈구세포, 지방체, 말피기소관, 외피, 난소 및 정소를 포함하는 전체 조직에서 발현되고 있음을 알 수 있었다. *P. geniculata* HT1 을 갈색거저리에 주사하였을 때, *TmPGRP-LB* 유전자의 발현은 유도되었으나, IMD 신호전달 관련 유전자인 *TmPGRP-LC* 와 *TmPGRP-LE* 의 발현은 유도되지 않았다. *TmPGRP-LB* 의 발현억제는 그람음성균인 *P. geniculata* HT1 과 *E. coli* K12 감염에 대한 감수성의 증가를 야기하였으나, 그람

양성균인 *S. aureus* RN4220 감염에 대해서는 감수성에 영향을 주지 않았다. 이러한 결과는 *TmPGRP-LB* 가 갈색거저리에서 그람음성균 감염을 조절하는데 중요한 역할을 한다는 것을 시사한다. 본 연구를 통하여, 갈색거저리의 오토파지시스템과 IMD의 신호전달관련 유전자인 *PGRP-LE/-LB* 가 외부에서 침입한 병원균에 대한 내재면역에 중요한 역할을 하고 있다는 사실을 확인하였다.

Acknowledgements

This dissertation is a result of contributions from a long list of people both during the course of study and in preparing this final manuscript. I wish to record my appreciations for their assistance without which this work could have either been concluded at a quality much lower than its current form or impossible to achieve altogether.

My gratitude is first and foremost extended to my supervising professor, Yeon Soo Han, for his ineffable assistance all through my study period. He was highly forthcoming and his stylish mixture of guidance and constructive criticisms during experimentations has made it possible that this document carries its present form.

Sincere thanks are extended to members of my PhD defence committee, Profs. Iksoo Kim, Yasuyuki Arakane, In Seok Bang, Yong Seok Lee and Yeon Soo Han for their guidance and critical reviews of the manuscript. Heart-felt thanks are also extended to Prof. Hunseung Kang- the current chairperson of our department and to all academic members of staff in our department for their support and encouragement throughout my study period. For sure, I learnt a lot from each and every one of them.

All members of our laboratory deserve a place in my heart for their tireless day-to-day support. They were a reason for my renewed strength when things got too heavy to handle. Special thanks to Drs. Jo, Y.H, Patnaik, B.B, Oh, S.H, Noh, M.Y. and Kim, D.H. for their cordial support. Many thanks also go to Kim, S.H., Seo, G.W., Seong, J.H, Lee, H.J., Kim, S.G, Koo, B.W., Park, S.Y., Mun, S.G., Park, K.B., Park, C.H, and Hwang, J.H. to all of whom my heartfelt appreciations for their love and care are hereby sincerely registered.

Generally, many people had helped me in one way or another during the entire course of my PhD study. Although the list would be too long for their names to be individually written here, my thanks to them all are sincerely registered.

This PhD dissertation is dedicated to my wife, Nuru and my son, Abdulrahim.

Hamisi,

Gwangju, South Korea.

(December, 2014).

SPE
QH442
.2
T5

